Intelligent Control and Operation of Distribution System

Bhattarai, Bishnu Prasad

Publication date:
2015

Document Version
Publisher's PDF, also known as Version of record

INTELLIGENT CONTROL AND OPERATION OF DISTRIBUTION SYSTEM

by

Bishnu Prasad Bhattarai

AALBORG UNIVERSITY
DENMARK

A Dissertation Submitted to
the Faculty of Engineering and Science at Aalborg University
In Partial Fulfillment for the Degree of
Doctor of Philosophy in Electrical Engineering

August 2015
Aalborg University

Aalborg University
Department of Energy Technology
Pontoppidanstræde 101
Aalborg East, Dk-9220
Denmark

Printed in Denmark by Uniprint
First Edition: August 2015.

The professional software/tools used in this research:

DIgSILENT PowerFactory 15.0

MATLAB R2013a

Real Time Digital Simulator

OMNeT++

Python

THESIS DETAILS

Thesis title:	Intelligent Control and Operation of Distribution System
Ph.D. Student:	Bishnu Prasad Bhattarai
Supervisor(s):	Assoc. Prof. Birgitte Bak-Jensen
	Assoc. Prof. Jayakrishnan Radhakrishna Pillai
Ph.D. Committee:	Prof. Remos Teodorescu, Aalborg University (Chairman)
	Prof. Sami Rapo, Tampere University of Technology
	Assoc. Prof. Olof Samuelsson, Lund University
Moderator:	Prof. Calus Leth Bak, Aalborg University

Scientific Contributions:

J.1. **Bhattarai, B.P.**; Levesque, M.; Bak-Jensen, B.; Pillai, J. R.; Maier, M.; and Tipper, D., "Design and co-simulation of a hierarchical control architecture for demand response coordination", IEEE *Transactions on Power Delivery (To be submitted)***.**

J.2. **Bhattarai, B. P.**; Kouzelis, K.; Mendaza, I. D. D. C.; Bak-Jensen, B.; and Pillai, J. R., "Smart grid constraint violation management for balancing and regulating purposes," *IEEE Transactions on Smart Grid* (To be submitted).

J.3. **Bhattarai, B.P.**; Levesque, M.; Maier, M.; Bak-Jensen, B.; and Pillai, J. R., "Optimizing electric vehicle coordination over a heterogeneous mesh network in a scaled-down smart grid testbed," *IEEE Transactions on Smart Grid*, vol. 6, no. 2, pp. 784-794, Jan. 2015.

C.1. **Bhattarai, B. P.**; Bak-Jensen, B.; Mahat, P.; Pillai, J.R.; and Maier, M., "Hierarchical control architecture for demand response in smart grid scenario," *in Proc. IEEE PES Asia Pacific Power and Energy Engineering Conference (APPEEC)*, pp. 1-6, Dec. 2013.

C.2. **Bhattarai, B. P.**; Bak-Jensen, B.; Mahat, P.; Pillai, J. R., "Voltage controlled dynamic demand response," *in Proc. 4th IEEE Innovative Smart Grid Technologies (ISGT) Europe*, pp. 1-5, Oct. 2013.

C.3. **Bhattarai, B. P.**; Bak-Jensen, B.; Mahat, P.; and Pillai, J. R., "Two-stage electric vehicle charging coordination in low voltage distribution grids," *in Proc. IEEE PES APPEEC*, pp 1-5, Dec. 2014.

C.4. **Bhattarai, B. P.**; Bak-Jensen, B.; Pillai, J. R.; and Maier, M., "Demand flexibility from residential heat pump," *in Proc. IEEE PES General Meeting*, pp. 1-5, Jul. 2014.

C.5. Astaneh, M. F.; **Bhattarai, B.P.;** Bak-Jensen, B.; Hu, W.; Pillai, J. R.; and Chen, Z., "A novel technique to enhance demand responsiveness: An EV based test case," *6th IEEE PES Asia Pacific Power and Engineering Conference, Nov. 2015.*

C.6. **Bhattarai, B. P.**; Bak-Jensen, B.; Pillai, J. R.; Gentle, J. P.; and Myers, K. S., "Coordinated control of demand response and grid-tied rooftop photovoltaics for overvoltage mitigation," *3rd IEEE SusTech2015*, Jul.–Aug. 2015.

C.7. **Bhattarai, B. P.**; Mendaza, I. D. D. C.; Bak-Jensen, B.; and Pillai, J. R., "A local adaptive control of solar photovoltaics and electric water heaters for real-time grid support," *CIGRE Session2016*.

C.8. **Bhattarai, B.P.;** Bak-Jensen, B.; Chaudhary, S. K.; and Pillai, J. R.; "An adaptive overcurrent protection in smart distribution grid," in Proc. *IEEE PES PowerTech*, Jun.–Jul. 2015.

This present report combined with the above listed scientific papers has been submitted for assessment in partial fulfilment of the PhD degree. The scientific papers are not included in this version due to copyright issues. Detailed publication information is provided above and the interested reader is referred to the original published papers. As part of the assessment, co-author statements have been made available to the assessment committee and are also available at the Faculty of Engineering and Science, Aalborg University.

To:

My parents,

My wife, and

Whole family

For their exceptional love and support in my life.

PREFACE

I am very thankful to *ForskEL* for providing financial support for this research as a part of the project "*Control, Protection, and Demand Response in Low Voltage Distribution Grid*". Further, I am thankful to the project partners, namely Aalborg University, Danish distribution system operator, SEAS-NVE, and KK-electronics, for their financial support as well as the technical inputs during entire study.

I would like to express my deepest gratitude and appreciation to my supervisors, Associate Professor Birgitte Bak-Jensen (main supervisor) and Associate Professor Jayakrishnan Radhakrishna Pillai for their valuable feedbacks, encouragements, and exceptional guidance throughout the entire PhD duration. Their invaluable supports, scientific expertise, and understanding have been very important in accomplishing this study.

I would also like to express sincere thanks to Jens Ole Pihl-Andersen and Lars Elmegaard from the SEAS-NVE and Paul Bach Thøgersen from kk-electronics for their help with required data and discussions during the course of this work. I would also like to appreciate Pukar Mahat, Professor Martin Maier, Professor Claus Leth Bak, and Associate Professor Sanjay Chaudhary for providing valuable suggestions and guidance at different stages of the study. In addition, I would also like to appreciate Jake P. Gentle and Kurt S. Myers from Idaho National Laboratory for their encouragements, help and feedbacks.

I would like to thank my friends, especially Martin Levesque, Konstantinos Kouzelis, Iker Diaz de Cerio Mendaza, and Reza Ahmadi Kordkheili for their encouragements and supports.

Last but not least, I would like to deeply thank my parents, wife, and rest of the family members for their unconditional love, patience, understanding, and support throughout the entire PhD study.

ENGLISH SUMMARY

Increased environmental concern and favorable government policies in the recent years have resulted in rapid growth of Renewable Energy Sources (RESs), such as Solar Photovoltaics (PVs) and Wind Turbine Generators. Despite creating several benefits, the high integration of the RESs in an electrical network imposes potential problems. In particular, limited dispatchability of the RESs on top of intermittent generation is creating key scientific challenges to the research community. On the other hand, increased trends of electrifying heating, transportation and gas sectors have resulted in new electrical loads, such as Electric Vehicles (EVs), Heat Pumps (HPs), and Electric Water Heaters (EWH), in the distribution network. In addition to the increase in power demand, those loads create high, rapid and random fluctuations in the demand, thereby impacting the power balancing scenario negatively.

Conventional solutions to address the aforementioned issues include building excess generation or grid scale storage to compensate the power imbalances resulting from intermittent generations and fluctuating demands. Even though those approaches perform technically well, they are capital intensive to be implemented with the existing technology. One of the potential alternatives is to intelligently control the electrical loads to make them follow the intermittent generation. This not only enables the end consumers to get reliable and cheap electricity but also enables the utility to prevent huge investment in counterpart. Therefore, the theoretical foundation of this research work is based on a paradigm shift in 'generation following demand' to 'demand following generation' scenario.

The primary aim of this research work is to develop intelligent control architecture, control strategies, and an adaptive protection methodology to ensure efficient control and operation of the future distribution networks. The major scientific challenge is thus to develop control models and strategies to coordinate responses from widely distributed controllable loads and local generations. Detailed models of key Smart Grid (SG) elements particularly distribution network, controllable loads, namely EV, HP, and EWH, and local generation, namely PV, are developed. The outcome of the projects is demonstrated mostly by simulations and partly by laboratory setups. The research outcome will not only serve as a reference for ongoing research in this direction but also benefit distribution system operators in the planning and development of the distribution network. The major contributions of this work are described in the following four stages:

In the first stage, an intelligent Demand Response (DR) control architecture is developed for coordinating the key SG actors, namely consumers, network operators, aggregators, and electricity market entities. A key intent of the architecture is to facilitate market participation of residential consumers and prosumers. A Hierarchical Control Architecture (HCA) having primary, secondary, and tertiary control loops is developed to establish coordinated control of widely distributed loads and generations. Moreover, a heterogeneous communication

network is integrated to the HCA for enabling control and communication within each control loop of the HCA. In particular, each control loop of the HCA is designed with specific control latency and time coordinated with the other loops to establish coordination among each other. The outcome of a power and communication co-simulation demonstrated that the proposed architecture effectively integrate responses from widely distributed loads and generations.

Detailed models of the controllable loads, local generation, and distribution network are done in the second stage. Transportation loads, namely EV, and heating loads, namely HP and EWH, are modeled as controllable loads, whereas the solar PV is modeled as local generation. Control strategies are developed to realize various DR techniques, namely autonomous, voltage controlled, incentive based, and price based. The performance of the developed models and control strategies are demonstrated in a low voltage distribution network by utilizing the intelligent architecture developed in the first stage. Even though the developed models and control strategies are tested in a particular low voltage network, they are generic to apply to any network. The outcome from this part of the study enables to exploit demand flexibility from the consumers/prosumers for technically supporting the grid as well as for enabling to trade the flexibility in electricity markets.

In the third stage, a scaled down SG testbed is developed and implemented for practical demonstration of developed DR models and control strategies. A LV test case network is scaled down to a 1 kVA testbed and is built in a laboratory. An optical fiber and TCP/IP based communication is integrated on the testbed to enable data communication and control. Moreover, a centralized and decentralized control approach is implemented for optimized EV charging coordination in the testbed. As practical demonstration of the SG is significantly lagging, the developed scaled down testbed based approach provides not only a novel approach for practical demonstration of the SG control but also a new research perspective in the SG field. More importantly, the proposed method provides an economic and riskless approach compared to the existing pilot project based SG developments.

In the final stage, an adaptive overcurrent protection is developed for the future distribution system having high share of RESs and Active Network Management (ANM) activities. In the future grid, the protection is affected not only by bidirectional power flow due to RESs but also due to the ANM activities such as demand response, network reconfigurations etc. Therefore, unlike the conventional protection methodology where the protective settings are made static, an approach to adapt relay settings based on dynamic network topologies and power infeed is developed. In particular, the developed methodology integrates the protection and ANM such that the protection is ensured for every change in network operation mode and topologies. A two-stage protection strategy, whereby an offline proactive stage combined with online adaptive stage is designed to realize the intended protection approach. The proactive stage determines settings of the relays for every mode of operation using offline short circuit analysis and dispatches the settings to the respective relays. The adaptive stage in turn identifies the operating status of distributed energy resources and operating modes (grid-connected, islanded,

network reconfiguration etc.) in real time to adapt/activate proper settings. The performance of the developed method is demonstrated in a medium voltage distribution network using real time digital simulator. The simulation results demonstrated that the proposed adaptive protection approach reliably discriminate the faults and establishes protection coordination in dynamic network topologies.

Overall, the research outcomes provide an innovative approach to exploit demand flexibility from controllable loads and establish the integrated ANM and protection to ensure effective control and protection of the future distribution grids. This not only enables the end consumers to get reliable and cheap electricity but also enables the utility to prevent huge investment in counterpart. Moreover, distribution system operators can implement the findings of the projects in their operational stages to avoid grid bottlenecks and in the planning stages to avoid or delay the grid reinforcements.

DANSK RESUME

Øget interesse for miljøet og favorable regeringspolitikker i de senere år har resulteret i en hurtig stigning i vedvarende energikilder (VE) såsom solceller (PV) og vindmøller. Foruden at skabe flere fordele, skaber den store integration af VE også forskellige problemer for el-nettet, herunder i særdeleshed særlige videnskabelige udfordringer for forskerne omkring begrænset styring af VE sammen med deres fluktuerende drift. På den anden side har elektrificeringen af biler (EV), varmepumper (HP) og el-vandvarmere (EWH) skabt nye laster i distributionsnettet. Udover at forøge forbruget, skaber disse laster høje, hurtige og tilfældige fluktuationer i forbruget, og påvirker derved effektbalances negativt.

De konventionelle løsninger til at adressere ovennævnte problemer inkluderer ekstra produktionsfaciliteter eller energilagre til at kompensere for effektubalancen fra den fluktuerende produktion og forbrug. Selvom disse løsninger fungerer udmærket teknisk er de dyre at idriftsætte med den eksisterende teknologi. Et af de mulige alternativer er intelligent at styre de nye elektriske belastninger så de følger den fluktuerende el-produktion. Dette vil ikke kun få forbrugerne til at få pålidelig og billig elektricitet men vil også sikre at forsyningsselskaberne ikke skal have store investeringer i nye linjer. Derfor er den teoretiske fundering af dette projekt baseret på et scenarie med et paradigme skifte fra ”produktion følger forbruget” til ”forbruget følger produktionen”.

Det primære mål med projektarbejdet er at udvikle en intelligent styringsarkitektur, styringsstrategier og en adaptiv beskyttelsesmetode to at sikre effektiv styring og drift af det fremtidige distributionsnet. Den tekniske hovedudfordring er at udvikle styrings modeller og strategier til at koordinere responsen fra distribuerede laster og lokal produktion. Der opstilles detaljerede modeller af hovedelementerne i det smarte el-net, såsom el-nettet, de styrbare laster (EV og HP) og lokal produktion fra solceller (PV). Resultaterne fra projektet vil fortrinsvist blive demonstreret ved simuleringer og til dels via laboratorieopstillinger. Forskningsresultaterne vil ikke kun kunne anvendes som reference for den løbende forskning, men også komme distributionsselskaberne til gode under deres planlægning og udvikling af distributionsnettet. Hovedbidragene fra projektet beskrives i de følgende fire dele.

I første del er der udviklet en intelligent forbrugsrespons (DR) styringsarkitektur for at koordinere det intelligent nets aktører i form af forbrugerne, net operatørerne, net-selskaberne og andre el-markeds aktører. Hensigten med arkitekturen er at bidrage til at private forbrugere og producenter kan deltage i el-markedet. Der er opbygget en hierarkisk styringsarkitektur (HCA) med en primær, sekundær og tertiær sløjfe, til at koordinere styring af distribuerede laster og produktion. Derudover er der integreret et heterogent kommunikationsnetværk til HCAen for at muliggøre styring og kommunikation indenfor hver styringssløjfe i HCAen. Hver styringssløjfe i HCAen er designet med en specifik styringsventetid og

tidsresponstid koordineret med de andre sløjfer. Resultaterne fra en effekt og kommunikations co-simulering har vist, at den opstillede arkitektur effektivt integrere responsen fra distribuerede laster og produktioner.

I anden del af projektet er der opstillet detaljerede modeller for styrbare laster, lokale produktionsenheder og distributionsnettet, herunder er især elbiler og varmepumper modelleret som variable laster og solceller er modelleret som en lokal produktionsenhed. Der er udviklet styringsstrategier til at realisere forskellige DR teknikker nemlig: autonom, spændingsstyret, incitaments- og prisbaseret. Virkningen af de forskellige modeller og styringer er demonstreret for et lavspændingsnet under anvendelse af den hierarkiske styringsstruktur opstillet i første del. Selvom de udviklede modeller og styringsstrategier er testet på et bestemt lavspændingsnet er de generiske og kan anvendes også for andre net. Resultatet fra denne del af studiet sikrer at forbrugsfleksibilitet fra forbrugeren/producenten kan anvendes dels for teknisk at supportere el-nettet men samtidig også for handel på elmarkedet.

I tredje del af projektet er der udviklet en nedskaleret laboratoriemodel af det intelligente el-net for praktisk demonstration of de udviklede forbrugsresponsmodeller og styringsstrategier. Et scenarie for et lavspændingsnet er nedskaleret til en 1 kVA laboratorieopstilling. Et optisk fiber TCP/IP baseret kommunikationssystem er integreret med laboratorieopstillingen for at sikre data behandling og styring. Derudover er der opbygget en central og en decentral styringsmetode for at optimere og koordinere el-bilopladningen i systemet i forhold til net-betingelserne. Der mangler praktisk demonstration af muligheder i det intelligente net, som den nedskalerede laboratorieopstilling kan medvirke til at afdække samtidig med at opbygningen af en sådan model også i sig selv er et forskningsområde. Det er også vigtigt, at den forslåede metode med en nedskaleret model giver en økonomisk billig og risikofri analyse i sammenligning med eksisterende pilotprojekter.

I sidste del af projektet er der udviklet en adaptiv beskyttelse for fremtiden distributionsnet med en stor andel af vedvarende energikilder og aktiv net management (ANM). I fremtidens net vil beskyttelsen ikke kun være påvirket af strømme fra begge retninger pga. vedvarende energikilder, men også af ANM aktiviteter så som forbrugsrespons, netkoblinger m.m. Derfor i modsætning til den konventionelle beskyttelse, hvor relæerne er indstillet med statiske værdier, er der lavet et forslag til en adaptiv relæindstilling baseret på netstrukturen og effektproduktionen. Den udviklede metode integrerer beskyttelsen og ANM sådan at beskyttelsen virker ved alle ændringen i driften af nettet og ved alle topologier. Der er opbygget en to-niveau beskyttelsesstrategi, hvor et off-line proaktivt niveau kombineret med et on-line adaptivt niveau er designet til at realisere ideen. Det proaktive niveau udregner indstillingerne på relæet for alle tænkelige måder nettet kan drives med ud fra kortslutningsberegninger og sender de forskellige indstillinger til relæerne. Det adaptive niveau identificerer den aktuelle driftsstatus for de distribuerede energikilder (net-tilsluttet, i ødrift) samt netstrukturen i real tid og bruger herefter de rigtige indstillinger. Performance for den udviklede metode er

demonstreret for et mellemspændingsnet scenarie under anvendelse af en ”real time digital simulator”. Simuleringsresultaterne viser at den foreslåede adaptive beskyttelse pålideligt er i stand at klarlægge de rigtige fejl og udføre den korrekte beskyttelse under dynamisk netdrift.

Alt i alt giver projektet et innovativt forslag til at udnytte forbrugsfleksibilitet fra styrbare laster og til at etablere en integreret ANM og beskyttelse for sikre en effektiv styring og beskyttelse af fremtiden distributionsnet. Det giver ikke kun mulighed for forbrugerne til at få pålidelig og billig elektricitet men giver også forsyningsselskaberne mulighed for at modvirke at skulle bruge store investeringer i udbyggelsen af nettet. Distributionsselskaberne kan implementere resultaterne af projektet i deres drift til at modvirke flaskehalse og i planlægning til at undgå eller udskyde netforstærkninger.

TABLE OF CONTENTS

Thesis Details v
Preface ix
English Summary xi
Dansk Resume xv
Table of Contents xix
List of Figures xxiii
List of Tables xxv
Acronyms xxvii
THESIS REPORT 1
Chapter 1. Introduction 3
1.1. Background and Motivations 3
1.2. Problem Description 4
1.2.1. RES Integration 4
1.2.2. Electrification of Heating, Gas, and Transportation 6
1.2.3. Intelligent Power Grids 8
1.3. Project Objectives 12
1.4. Project Scope and Limitations 13
1.5. Thesis Organization 14
Chapter 2. Literature Review 17
2.1. Introduction 17
2.1.1. Organization of Demand Response Programs 18
2.1.2. Benefits of Demand Response 18
2.2. Intelligent DR Deployment Architecture 19
2.2.1. Multi-disciplinary Aspects of SG Architectures 21
2.3. Modeling of Flexible Loads and Local Generation 21
2.3.1. Electric Vehicles 21
2.3.2. Heat Pump 22
2.3.3. Solar Photovoltaic 23
2.4. Development of DR Control Strategies 24

2.4.1. Impact of Active Load and Generation in LV Grids 24
2.4.2. Active Loads and Generation Control Strategies 25
2.5. Impact of ANM on Protection 28
2.6. Chapter Summary 30
Chapter 3. Intelligent Smart Grid Control Architecture 31
3.1. Introduction 31
3.1.1. DR Deployment Framework 32
3.2. Implementation of HCA Architecture 33
3.2.1. HCA Implementation from Power Perspective 34
3.2.2. Communication Perspective of HCA 37
3.2.3. Power and Communication Co-simulation 39
3.3. Test System Modeling and Characterization 40
3.4. Observations and Discussions 42
3.4.1. Power Performance 42
3.4.2. Communication Performance 46
3.5. Chapter Summary 47
Chapter 4. Development of DR Control Strategies 49
4.1. Introduction 49
4.2. Constraints Violations Management 49
4.2.1. Proposed Methodology 50
4.2.2. Observations and Discussions 51
4.3. Voltage Controlled Dynamic DR 53
4.3.1. Proposed Methodology 53
4.3.2. Observations and Discussions 53
4.4. DR Control Strategies for EVs 56
4.4.1. Proposed Methodology 56
4.4.2. Observations and Discussions 56
4.5. DR Control Strategy for HP 58
4.5.1. Proposed Methodology 58
4.5.2. Observations and Discussions 59
4.6. Increasing Demand Responsiveness 61

4.6.1. Proposed Methodology 61
4.6.2. Observations and Discussions 62
4.7. Chapter Summary 63
Chapter 5. Control of Active Load and Local Generation 65
5.1. Introduction 65
5.2. Control Strategies for Solar PV and EV 65
5.2.1. System Modeling 65
5.2.2. Proposed Methodology 66
5.2.3. Observations and Discussions 67
5.3. Integrated Adaptive Control of EWH and PV 69
5.3.1. Modeling of EWH and PV 69
5.3.2. Proposed Adaptive Control Strategies 69
5.3.3. Observations and Discussions 70
5.4. Chapter Summary 72
Chapter 6. Development of Scaled Down SG Testbed 73
6.1. Introduction 73
6.2. Development of Smart Grid Testbed 74
6.2.1. Electric Power Distribution Network 74
6.2.2. Communication Network 76
6.2.3. Integration of Power and Communication Network 76
6.3. SGT Performance Demonstration 77
6.3.1. Centralized Control 77
6.3.2. Decentralized Control 78
6.3.3. Coordination of Decentralized and Centralized Control 79
6.4. Observations and Discussions 79
6.4.1. Power Performance 80
6.4.2. Computation Performance 82
6.4.3. Communication Performance 83
6.5. Chapter Summary 83
Chapter 7. Proactive and Adaptive Protection Design 85
7.1. Introduction 85

7.2. Key Issues to Protect Future Distribution Grids 86
7.2.1. Impacts of DERs in Distribution Protection 86
7.2.2. Impacts of Network Operation in Protection 87
7.3. Implementation of Proposed Algorithm 88
7.3.1. State Detection of Distributed Energy Resources 88
7.3.2. Detection of Islanded/Grid-connected Modes 89
7.3.3. Detection of Changes in Network Topologies 89
7.4. Observations and Discussions 89
7.4.1. Adaptive Relay Update for Protection Blinding 91
7.4.2. Adaptive Relay Update for False Tripping 92
7.4.3. Adaptive Updates for Grid-connected/Islanded Mode 93
7.5. Chapter Summary 94
Chapter 8. Conclusion 95
8.1. Summary and Conclusions 95
8.2. Major Contributions 97
8.3. Future Work 98
Bibliography 101

LIST OF FIGURES

Fig. 1.1 Danish roadmap to be independent of fossil fuel by 2050....3
Fig. 1.2 Current and future generation technologies in Denmark....4
Fig. 1.3 Estimation of wind and solar PV capacity growth in Denmark....5
Fig. 1.4 Intermittency on wind production a) Variation of wind power generation & consumption in 2050, b) Fast ramping down and up of wind turbines in Horns Rev....5
Fig. 1.5 Location of heating technologies & Natural gas network, in Denmark....6
Fig. 1.6 EV charging and battery swapping stations in Denmark....8
Fig. 1.7 Anticipated transformations of power system and its potential solutions....9
Fig. 1.8 Expected demand flexibility from various load types....9
Fig. 1.9 Nordic power exchange market....11
Fig. 1.10 Roles and responsibility of different actors in flexibility market....12
Fig. 2.1 Demand side management activities....17
Fig. 2.2 DR classification and potential benefits....19
Fig. 2.3 Intelligent control architecture. a) Centralized-decentralized and b) HCA....20
Fig. 2.4 a) Coefficient of performance vs. ambient temperature for a HP, b) PV array current vs. solar irradiance....23
Fig. 2.5 Various perspectives to develop DR control strategies....26
Fig. 3.1 DR Interaction framework for SG actors....32
Fig. 3.2 Hierarchical DR control architecture....34
Fig. 3.3 Proposed communication infrastructure for HCA implementation....38
Fig. 3.4 Proposed co-simulation framework....39
Fig. 3.5 Single line diagram of test network....40
Fig. 3.6 Yearly variation of demand and generation....41
Fig. 3.7 Daily load profile for maximum and minimum demand day....42
Fig. 3.8 EV arrival/departure and availability over a day....42
Fig. 3.9 Optimal configuration of electricity price and feeder load demand....43
Fig. 3.10 EV charging profiles with and without periodic charging control....43
Fig. 3.11 SDRC performance with load and regulation events....44
Fig. 3.12 SDRC performance in a) 100kW down & b) 75 kW up, regulations. (P_I/P_F: EV power before/after SDRC)....44
Fig. 3.13 EV charging profiles demonstrating PDRC performance....45
Fig. 3.14 Amplified plot to illustrate PDRC....45
Fig. 4.1 Sample results. a) Minimum voltage at the feeder, b) Maximum overcurrent recorded at the feeder, c) Transformer load, and d) Available versus activated flexibility....51

Fig. 4.2 Simulation results with (green) and without (blue) control a) Flexibility of consumer 14, b) Voltage at N14, c) Flexibility of consumer 26, and d) Voltage at N26. 52
Fig. 4.3 Demand regulation potential. a) Case I and b) Case II. 55
Fig. 4.4 Total demand regulation potential for various cases. 55
Fig. 4.5 EV scheduling in scenario-I a) EV charging profiles and b) Electricity prices. 57
Fig. 4.6 EV schedules in scenario II a) EV charging profiles and b) Electricity prices. 57
Fig. 4.7 Terminal voltage at farthest node (N13) for various cases. 58
Fig. 4.8 Adaptive update of charging profile based on monitored voltage. 58
Fig. 4.9 a) HP scheduling with load and price variation, b) Normal and deviated price. 60
Fig. 4.10 a) Impact of voltage on HP schedules and b) Variation of terminal voltage (N_{13}) ...60
Fig. 4.11 Adaptive control of a single HP connected at Node 13. 61
Fig. 4.12 Price modification mechanism. a) Optimal price and b) Corresponding load shift ..62
Fig. 4.13 Profiles of a) EV demand and b) Sum of EV and base load demand. 63
Fig. 5.1 Coordination between centralized and decentralized control. 67
Fig. 5.2 PV power injection and EV charging power. 68
Fig. 5.3 Decentralized control results. 69
Fig. 5.4 Simulation results of EWH control. a) SOE, b) Active/reactive power consumption, c) POC Voltage, and d) Thermal demand, for a consumer. (WC: without & C: With control) 71
Fig. 5.5 PV results with/without control a) Active and reactive power b) POC Voltage. 72
Fig. 6.1 Schematic diagram of 13-node scaled down network. 74
Fig. 6.2 Laboratory implementation of the testbed. 75
Fig. 6.3 Communication infrastructure implemented in the testbed. 76
Fig. 6.4 Optimized EV charging power profile (price based optimization). 80
Fig. 6.5 EV charging optimization considering network constraints. 81
Fig. 6.6 Voltage profile of node 13 with local voltage control. 81
Fig. 6.7 Computation time for optimization process. 82
Fig. 6.8 Communication performance. a) Synchronization performance using time-based and coordinated sensors, and b) Captured traffic of the DMS port to/from optical load terminal..83
Fig. 7.1 Protection blinding and false tripping due to DER penetration. 86
Fig. 7.2 a) Relay settings and b) Time-overcurrent characteristics. 90
Fig. 7.3 Maximum fault current seen by relays for different cases. 91
Fig. 7.4 a) Protection blinding of relay R_{34} and b) Solution by proposed adaptive method. 92
Fig. 7.5 a) False tripping of relay R_{26} and b) Solution by proposed adaptive method. 92
Fig. 7.6 a) Relay settings for islanded operation and b) Time-current curve of relays. 93

LIST OF TABLES

Table 1.1 Correlation between the thesis chapters and publications. 16
Table 2.1 Key features of different battery technology. 22
Table 3.1 A Novel control requirement based DR categorization. 33
Table 3.2 Communication requirements for HCA. 37
Table 3.3 Test network characteristics. 41
Table 3.4 Line parameters of test network. 41
Table 3.5 Communication configuration. 46
Table 3.6 Communication performance in terms of stage delay. 47
Table 4.1 Configuration of demand dispatch signals. 54
Table 6.1 Network parameters before and after scaling down. 74

ACRONYMS

ADR	Autonomous Demand Response
ANM	Active Network Management
CA	Central Aggregator
CVR	Conservative Voltage Reduction
DDDR	Demand Dispatch based Demand Response
DER	Distributed Energy Resource
DLCDR	Direct Load Control based Demand Response
DMS	Distribution Management System
DR	Demand Response
DRR	Demand Response Resource
DSM	Demand Side Management
DSO	Distribution System Operator
EPON	Ethernet Passive Optical Network
EV	Electric Vehicle
EWH	Electric Water Heater
HAN	Home Area Network
HCA	Hierarchical Control Architecture
HP	Heat Pump
ICT	Information and Communication Technology
IFC	Informative Control
ISC	Instructive Control
IZR	Intra-Zone Relay
LAC	Local Adaptive Control
LV	Low Voltage
NAN	Neighborhood Area Network
MV	Medium Voltage
PDR	Price Based Demand Response
PDRC	Primary DR Control
PF	Power Factor

POC	Point of Connection
PV	Photovoltaic
RES	Renewable Energy Source
RPM	Regulating Power Market
RTDS	Real Time Digital Simulator
SDRC	Secondary DR Control
SG	Smart Grid
SGT	Smart Grid Testbed
SOC	Stage of Charge
SOE	Stage of Energy
SS	Substation
TDRC	Tertiary DR Control
TMS	Time Multiplier Setting
VCDR	Voltage Controlled Demand Response
ZSR	Zone Separating Relay

THESIS REPORT

Chapter 1. Introduction

This chapter outlines a short summary of project concepts, objectives, and limitations. The motivation behind this research and its future prospects are also outlined. Moreover, the project relevance seen from both the Danish and international perspectives are also emphasized.

1.1. Background and Motivations

Increased environmental and energy security concerns in the recent years are compelling many countries to seek alternatives to fossil fuels based electricity generation. Accordingly, several countries have set their national targets for electricity production from RESs. Recently, EU has set the following climate and energy targets for 2030 as a roadmap for its member states [1].

- Reducing EU's greenhouse gas emissions by at least 40% below 1990 level,
- Increasing the share of RES to at least 27% of the EU's energy consumption,
- Increasing energy efficiency by at least 27%.

In addition to these EU targets, its member countries have their own RESs targets. The targets varies widely, for instance from 10% for Malta to 49% for Sweden [2]. The increase in RESs production by 83.13% from 2002 to 2012 in EU-28 clearly demonstrates EU's future direction [3]. Therefore, the new targets are expected to create a huge transformation from the existing fossil fuel based generation to future RESs based generation [4]. Being one of the pioneering countries of wind power technologies, Denmark stands at the front end on RESs development. In particular, the Danish Ministry of Climate, Energy, and Building has set very ambitious targets, illustrated in Fig. 1.1, to make the country independent of fossil fuel by 2050 *[5]*.

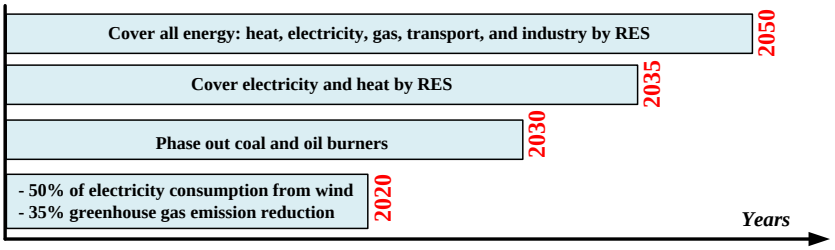

Fig. 1.1 Danish roadmap to be independent of fossil fuel by 2050 [5].

Two major transformations in the Danish electricity sectors are expected while moving forward to these 2050 targets. First, the conventional fossil-fuel based generations will be continuously substituted with RES generation [6]. Second, existing fossil fuel based heating, gas, and transportation sector will be electrified [7]. On the one hand, the increased RES integration creates intermittency in generation. On the other hand, the electrification of the heating, gas, and

transportation sectors results in several new electrical loads, such as EVs, HPs etc., which creates huge and random fluctuations on the demand. Consequently, the fluctuations on demand add up to the intermittent generation to worsen the power balancing scenario. The existing generation following demand scenario, whereby the generation is adjusted to cope with the load variations, will not work due to limited dispatch capability of the RESs. In this regards, one of the great motivations for this study is to exploit the demand flexibility from the new electrical loads to move towards demand following generation, whereby the demand is regulated to compensate the intermittent generations from the RESs.

1.2. Problem Description

The previous section briefly reveals the energy policies and roadmaps set by EU and Danish government. In this section, technical initiatives taken by Danish government and concerned authorities to meet the aforementioned targets and their anticipated challenges on the electrical grids are detailed. Specifically, the initiatives taken on *RES development and electrification of the heating, gas, and transportation* are investigated to identify their key technical impacts on future distribution system.

1.2.1. RES Integration

Over the last few decades, Danish power system has undergone significant transformation in relation to electricity generation technologies. In particular, conventional centralized power plants are continuously displaced by increased penetration of DER technologies, namely by combined heat and power plants and wind turbine generators [8]. As illustrated in Fig. 1.2 several conventional power plants have already substituted by thousands of combined heat and power plants and onshore/offshore wind turbines. This trend is expected to continue further in the upcoming years, thereby substituting more conventional plants as in Fig. 1.2 [8].

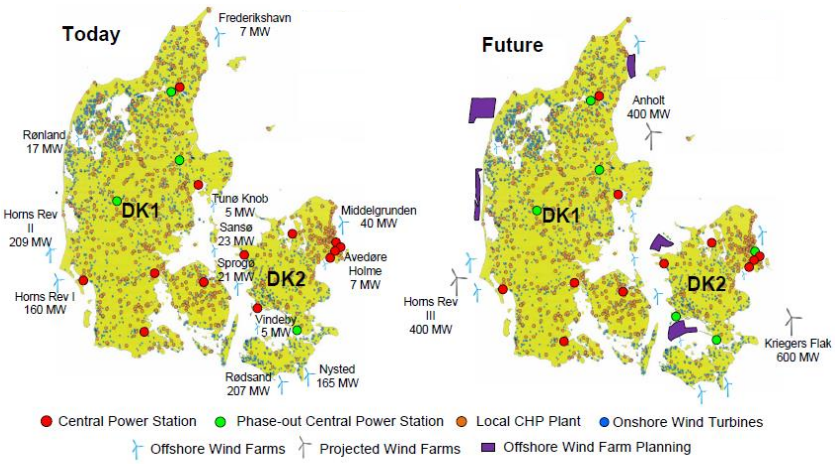

Fig. 1.2 Current and future generation technologies in Denmark [8], [9].

Undoubtedly, the wind power constitutes a major share in Danish electricity production, thereby playing a key role on the substitution of the conventional power

plants [10]. In fact, the wind turbine generators provided 39.1% of the total electricity consumption of the country in 2014 from the installed capacity of 4845 MW. It was a world record in relation to the highest percentage consumption from wind [11]. It can be seen from the wind power predictions made by the Danish transmission system operator, Energinet.dk, as shown in Fig. 1.3a) that an accelerated growth of wind power production is expected in the years to come. Consistent with the wind, the growth of the solar PV is also very promising. Indeed, the PV generation is projected to grow steadily as shown in Fig. 1.3b) [12].

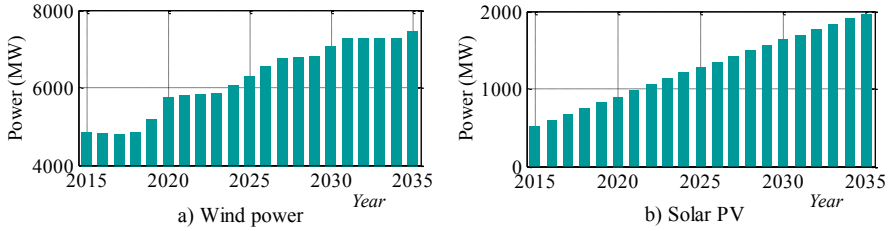

Fig. 1.3 Estimation of wind and solar PV capacity growth in Denmark [12].

Despite having several technical and environmental benefits of those RESs, their increased share creates a number of control and operational complexities in the existing power system. In particular, greater dependency of the power generation from the wind and PV on weather condition creates a potential problem on the system balancing. Fig. 1.4a) illustrates an electricity generation and consumption scenario by 2050 in Denmark. It is seen that power generation from wind farms exceeds the consumption. More importantly, the predicted fluctuations in the wind power range from few MWs to thousands of MWs which inherently results in potential issues to maintain system balance.

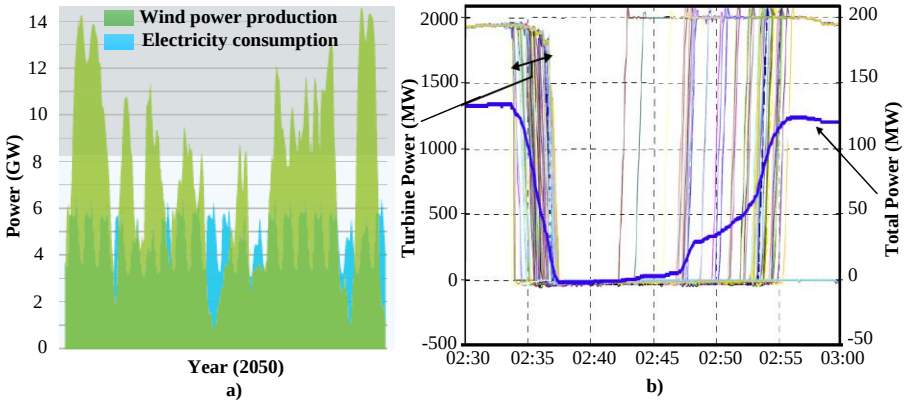

Fig. 1.4 Intermittency on wind production a) Variation of wind power generation & consumption in 2050 [7], b) Fast ramping down and up of wind turbines in Horns Rev [13].

The condition is even worse when those variations occur very rapidly as shown in Fig. 1.4b) where 80 Vestas V80 wind turbines, each having 2MW in Horns Rev

offshore wind farm in Denmark, has shut down due to wind storm. As a result, a ramping down of about 140 MW is seen in less than 4 minutes [13]. In the case of high wind penetration, ramping amount could be significant high and can severely threaten the power balance scenario. Consequently, reliable spinning reserves are desired to alleviate such rapid ramping up/down in the generation.

In addition, the power system is progressively losing rotational inertia due to continuous displacement of the conventional large power plants [5]. Consequently, system stability and security get threatened as conventional power plants are responsible for the stability [14]. Moreover, the loss of conventional power plants from the system results in significant decrement on the short circuit current [15]. As a result, the existing protection system which is designed based on the short circuit current level needs renovation. Furthermore, the addition of distributed energy resources (DERs) in the distribution system disturbs direction and distribution of the fault current. Consequently, the conventional protection design faces several issues to discriminate faults.

1.2.2. Electrification of Heating, Gas, and Transportation

Total energy consumption in the heating, gas, and transport sectors constitute a major portion of the national energy consumption in Denmark [12]. Therefore, to move towards fossil fuel independent state, electrification of the sectors consuming huge amount of the fossil fuels is inevitable. Key initiatives taken by the Danish government on those sectors and their implication in the future electrical system is outlined in this section.

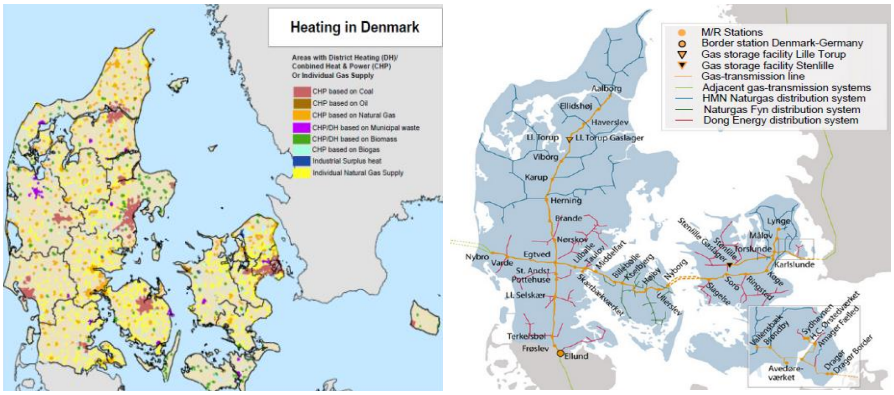

a) Heating system b) Natural Gas system

Fig. 1.5 Location of heating technologies [16] & Natural gas network [18], in Denmark.

1.2.2.1 Electrification of heating

Currently, heating demand, comprising space heating and hot water, in Denmark is fulfilled by a combination of district heating and individual heating. Typically, the district heating covers the majority of the urban population; amounting 60% of the Danish households [16]. In fact, 670 centralized and decentralized combined heat and power plants are distributed throughout the country as in Fig. 1.5a) to fulfill urban heating demand.

As the district heating may not be cost-effective in the rural areas where the consumers are widely spread, most of the rural populations in Denmark are still using oil-fired boilers for the heating purpose [17]. However, the Danish government has banned to use oil-burner and natural gas furnaces in new homes from January 2013 and in existing buildings from beginning of 2016 [5]. Similarly, as can be seen from Fig. 1.5a), the majorities of the combined heat and power plants are based on coal, oil, and natural gas and should be shifted towards renewables. Such anticipated transformation in the heating will greatly impact the existing electrical system as it results in new electrical loads such as HPs and EWHs particularly in distribution systems. As a result, many of the electrical distribution systems need upgrades or reinforcement to accommodate anticipated load growth.

1.2.2.2 Electrification of Gas

The gas system comprising natural gas and biogas constitutes a significant energy share in Danish energy consumption [12]. In particular, the gas system is serving a majority of the country through several transmission and distribution links as shown in Fig. 1.5b). However, Energinet.dk estimates that the gas supplies from the North Sea, the main source of the natural gas in Denmark, will decline during 2019 – 2042 and most likely be exhausted by 2045–2050 [19]. Therefore, immediate technological alternatives are desired not only to move towards 100% fossil-fuel free but also to seek alternatives to natural gas. On one hand, initiatives are taken to decrease the consumption of natural gas by electrifying natural gas based combined heat and power plants, cooking, and heating. As a result, new types of electrical loads such as the HPs (individual or central), electric ovens, electric boilers, are increasing. On the other hand, initiatives are taken to reduce the natural gas dependency by substituting it with renewable fuels such as hydrogen, biogas etc. In particular, biogas is a growing technology and is expanding very rapidly in Denmark. According to the estimates, the biogas production will increase with more than 300% (6.6 PJ in 2013 to 20 PJ in 2022) within the coming decade [20]. Recently, generating hydrogen using renewable energy and injecting it to the current natural gas system is emerging as an alternative solution [21]. With the advancement of this hydrogen fuel based technology, new electrical loads such as electrolyzer is expected to increase in the system. As such, the electrification of the gas system also results in new loads which were not foreseen when electrical networks were built.

1.2.2.3 Electrification of Transportation

Being one of the largest energy consuming sectors in the Danish energy mix, electrification of the existing fossil-fuel based transportation possesses significant challenges. According to the 2010 statistics, the fleets in the road transport constitute around 2.16 million private vehicles, 14496 busses, and coaches, and 148766 motorcycles [22]. The Danish government has taken various initiatives such as tax exemptions and development of infrastructures to boost the number of electric cars [5]. In particular, stations for battery charging and battery swapping are built to overcome the driving distance limits possessed by a vehicle battery. Distribution of EV charging and battery swapping stations throughout Denmark is illustrated in Fig.

1.6 [23]. The effects of those initiatives have started to be seen with the increased penetration of electric cars in the road. According to the prediction made by the Energinet.dk, the number of EVs is expected to grow from 1.390 in 2013 to 400.000 in 2035 [12]. This anticipated EV growth impacts the existing electric grids by introducing new loads having sizable ratings.

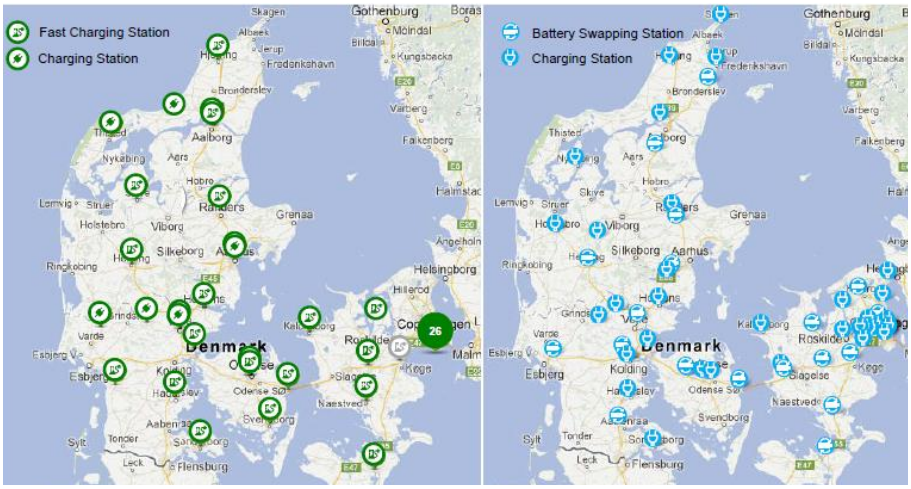

Fig. 1.6 EV charging and battery swapping stations in Denmark [23].

Therefore, one of the common issues with the electrification of the **heating, gas, and transport** sector is that they result in new electrical loads in the existing system, perhaps the loads having significant rating compared to the normal household loads. Those loads not only congest the network but also increase random and rapid fluctuations on the demand. As the existing networks were not designed to accommodate those loads, several distribution networks might need reinforcement.

1.2.3. Intelligent Power Grids

The anticipated transformation of the electrical system due to the increased integration of RESs and the electrification of the heating, gas, and transport sectors, as shown in Fig. 1.7, demands an intelligent grid so called SG. Considering existing and anticipated changes in the power system, Energinet.dk has set the following strategies to address the future power system issues *[24]*.

- Building large energy storages exploiting new technologies,
- Expansion and upgrade of existing network and cross-border interconnections,
- Development of advanced techniques for accurate wind power forecast, and
- Exploit flexibility from the electrical loads using various DR techniques.

Studies regarding grid support capabilities from battery **storage** have shown that large scale power storage can be a technically viable option to compensate the intermittency on generation [25]. However, the exploitations of large storages for system level balancing are economically less attractive with the existing

technologies and market structure. Building new infrastructure to ***upgrade or expand the existing grids and international connections*** can help maintain the system balance with import/export of the electricity with the neighboring countries. However, it should also be noted that the interconnection increases the country's energy dependency.

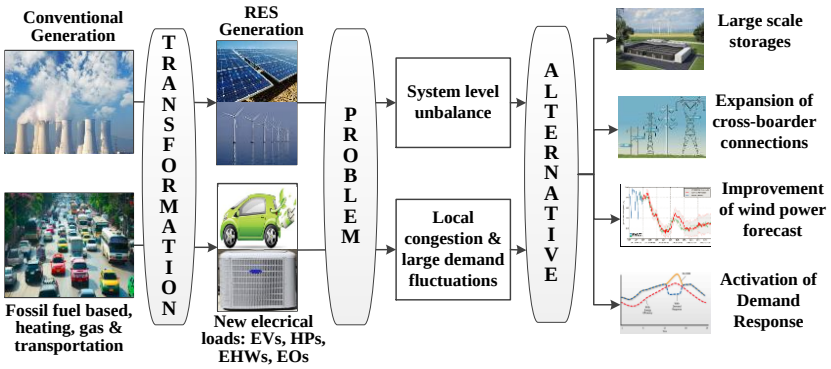

Fig. 1.7 Anticipated transformations of power system and its potential solutions [24].

More importantly, this concept might face technical challenges when the energy mix in the neighboring countries is similar to that of Denmark. Similarly, the development of ***advanced wind power forecast*** techniques helps to make better operational plans and to better utilize and trade the wind power in the electricity markets. However, it serves as a planning tool, rather than regulating the power. Therefore, one of the potentially attractive approaches is to activate DR for exploiting the demand flexibility from various electrical loads.

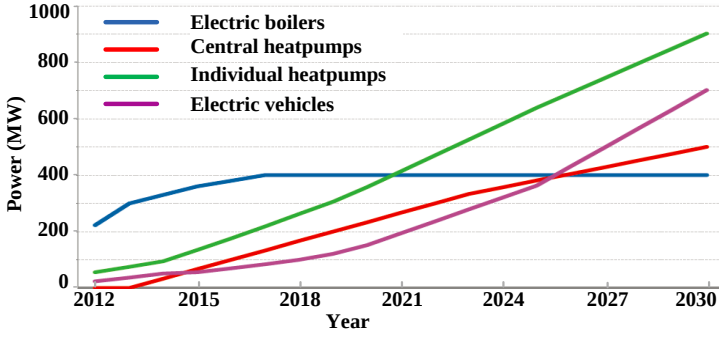

Fig. 1.8 Expected demand flexibility from various load types [8].

1.2.3.1 Technical Challenges to Deploy DR

According to the Nordic power market, DR is a voluntary and temporary adjustment of the electricity consumption in response to an electricity price or reliability requirements [26]. The DR can not only support the electrical network in several ways but also decrease the country's energy dependencies to the other

country. Currently, common consumer loads such as freezers, refrigerators, washing machines, tumble dryer etc. are considered as key resource for providing demand flexibility. However, new electrical loads such as HPs, EWHs, EVs etc. resulting from the electrification of heating, gas and transport sectors are foreseen as potential resource to provide great amount demand flexibility in the future [12]. According to the estimates, the demand flexibility from major flexible loads is expected to increase as per the projection presented in Fig. 1.8. It can be observed that the demand flexibility from HPs (both centralized and individual) and EVs is expected to increase exponentially in the upcoming years.

However, the introduction of such anticipated loads inherits both challenges and opportunities. Due to the sizable ratings of those loads, most of the existing distribution networks get congested as they were not designed with those scenarios accounted. As a result, many DSOs are forced to invent on the grid reinforcement. Nevertheless, due to sizable rating and storage capability, those loads provide great demand flexibility. The flexibility can not only be used to manage the grid congestion but also be applied for system level balancing. A key idea is to exploit the demand flexibility to compensate the intermittent generation from the RESs and to delay or defer grid reinforcement. Nonetheless, there are several technical challenges, listed below, that need to be addressed prior to the DR deployment.

- Assessment of the demand flexibility potential of different load types,
- Quantification of the impacts of active loads in existing distribution grids,
- Development of intelligent architectures for control and coordination of widely distributed loads,
- Control strategies development to maximize technical benefits of the DR, and
- Development of control strategies to deploy DR for network applications.

1.2.3.2 Financial Challenges to Deploy DR

In addition to the aforementioned technical challenges, financial aspects also impose potential barriers to the DR deployment. As consumers normally want financial benefits in return to their participation in DR programs, development of proper market frameworks to aggregate and trade the flexibility is very essential. As illustrated in Fig. 1.9, there are primarily three market platforms available for trading in NordPool electricity market, where Denmark trades and exchanges most of its energy. Spot and balancing market are owned and managed by NordPool, while RPM is owned by the TSOs of different countries. The RPM is owned and managed by Energinet.dk particularly for Danish case.

The spot market is a day ahead hourly market which trades almost 80% of the energy consumption in the Nordic countries [27]. Every interested seller and buyer of electrical energy submits its demand/supply bid to the Elspot from 8:00 until 12:00. Based on the demand and supply bids, the hourly electricity prices for the following day are computed between 12:00 through 13:00 and all the traders are invoiced between 13:00 to 15:00 [28].

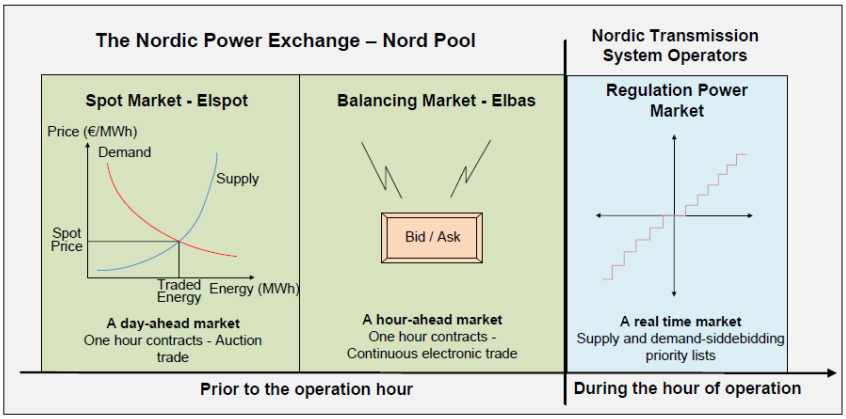

Fig. 1.9 Nordic power exchange market [27].

As the trading in Elspot takes place from 24 to 36 hours ahead of the actual delivery of the bids, deviations in the supply and/or demand of the electricity from the Elspot trading may be observed while moving closer to the power delivery. As a result, the balancing market so called Elbas is designed to compensate power imbalances during near actual operation. Basically, this is an hour ahead market, whereby different parties make their offers for buying and selling the balancing power until one hour before delivery [29]. The Elbas prices are set based on a first-come, first-served principle where the lowest selling price and the highest buying price come first, regardless of when an order is placed [29].

Even though Elbas ensures an hour ahead balance in the system, power imbalance may occur even after Elbas closes. Therefore, RPM is designed to maintain power balance in the system during actual operation (real-time). In particular, the RPM accept bids for up-regulation and down-regulation separately until 45 minutes before the operating hour [30]. The bids are then sorted with increasing prices for up-regulation and with decreasing price for down-regulation. The transmission system operator activates the cheapest regulating bid as per up-/down-regulation requirement. The accepted parties get paid for both the energy (based on the activation) and the capacity (for being available for regulation) [30].

In order to maximize the DR potential and financial incentives to the participating consumers, there must exists a proper framework to trade the demand flexibility on every market. As the payment from RPM and Elbas is normally higher compared to the Elspot, deployment of DR types and DR control strategies to ensure their participation on those markets could be an effective approach to provide additional incentives to the consumer to participate in DR programs.

1.2.3.3 Danish Roadmap for Flexibility Market

Even though the aforementioned market framework provides a transparent platform for electricity trading, it is not favorable especially for residential consumers to trade the flexibility. Indeed, market regulation such as minimum limit on the amount to be traded is becoming a key barrier to trade flexibility directly

from the customers. As such, Energinet.dk and Danish energy association jointly developed a roadmap to trade flexibility from the residential consumers [31]. The roadmap has defined distribution of roles of major actors, namely private players, commercial players, and system operators, as depicted in Fig. 1.10.

Fig. 1.10 Roles and responsibility of different actors in flexibility market [31].

The private players are basically the customers who are having flexible loads and are capable of offering flexibility. The commercial actors handle the flexibility offer from the private players and provide the flexibility to the system operators such as grid companies and transmission system operator. In the proposed roadmap, the grid companies will no longer be in direct contact with the consumers. A third party, such as an aggregator or retailer, takes an intermediate role to act on their behalf to provide aggregated flexibility to the grid companies. Nevertheless, proper algorithms need to be designed not only to deploy demand flexibility from individual customers but also to aggregate the flexibilities for system support in accordance with the proposed roadmap of the flexibility market.

1.3. Project Objectives

As mentioned in the previous section, exploitation of the demand flexibility provides a great opportunity not only to manage congestion in the local network but also to establish system level power balancing. However, there are several challenges related to quantification of the demand flexibility potential, development of proper DR control architecture and strategies, which needs to be addressed to exploit the flexibility. The overall objective of this research is to solve the aforementioned issues by intelligent control and operation of the flexible loads in a distribution system. More specifically, the objectives of this research are as follows:

- Develop suitable control architectures for exploiting demand flexibility from residential consumers in LV distribution networks,
- Develop proper models of potential flexible loads and suitable control strategies for activating DR considering a dynamic electricity market,
- Coordinated control of active loads and local generation to provide economic and efficient operation of the LV grid,

- ❖ Develop a smart grid testbed considering multi-disciplinary aspects of the smart grid for practical demonstration of the developed DR models and control strategies, and
- ❖ Develop an adaptive and proactive protection scheme to ensure protection coordination in a MV distribution grid during varied network topologies.

1.4. Project Scope and Limitations

The scope and limitations of this research are as follows:

- The consumer demand is modeled as a three-phase balanced load and the studies are performed assuming three-phase balanced system. One of the main reasons for this assumption is the lack of phase-wise data of the test network. Nonetheless, this assumption also helps to make the network analysis simpler. Unlike in distribution systems where the consumers are supplied with single-phase connection and are widely sparse, the extent of unbalancing is very low in the Danish network as the consumers are supplied with a three-phase connection and settled closely. Therefore, the considered assumption does not alter the findings of the research.
- The consumer demand is modeled using the hourly electricity consumption, where the hourly demand in a specific hour is assumed to be same as the total energy consumption on that hour. Therefore, the consumers load profile is same as the hourly energy consumption profile. Any demand peaks within a specific hour are neglected. However, while analyzing from the grid perspective those individual peaks are compensated due to consumer's diversity.
- This study is based on a deterministic load model, where the consumer load/profile is modeled with the deterministic demand/profile. The stochastic behavior of the consumers is not considered in this study. However, the developed methods and control strategies are made adaptive such that any load models can be used simply by changing the existing deterministic load input by any desired load models.
- The application of active demand control is demonstrated in relation to its capability for supporting the network for voltage control and congestion management. However, the DR application for supporting the frequency is not demonstrated. A major reason behind this consideration is that the frequency is a system level parameter and does not change significantly with small changes on the demand. Nonetheless, the proposed architecture and control strategies can be applied for frequency support with no or minimal modification.
- The intelligent SG architecture is developed to establish coordination and control of the small scale consumers for utilizing their demand flexibility. Communication infrastructure is integrated and power and communication co-simulation is performed to realize the control and exchange data in the proposed

architecture. However, the communication performance is demonstrated in terms of the latency and bandwidth only. Other parameters like throughput, jitter, and error rates are not explicitly considered.

1.5. Thesis Organization

The thesis is written as a collection of papers and is structured in two parts. The first part contains description on research contribution of this study as a brief report and the second part contains the scientific publications in relation to this research. In particular, the first part of the thesis is structured as eight chapters as follows:

- **Chapter 1** introduces the ongoing transformation on electric grid due to increased penetration of the RESs and electrification of gas, heating, and transport sectors. The opportunities and challenges of this transformation to the future electric grid have been presented. Further, the research scope, objectives, and limitations are defined and its relevance seen from the Danish and international perspective is described.
- **Chapter 2** is the state of the art which summarizes major scientific contribution made in SG research area. In particular, this chapter focuses on the ongoing developments on smart grid architecture, multi-disciplinary aspects of the SG, modeling of active loads and local generations, and adaptive protection in the future distribution system. Finally, the chapter outlines the scientific contribution of this study on top of the current state of the art.
- **Chapter 3** introduces the intelligent control architecture for the future distribution grids. In particular, a HCA is developed to establish control and coordination of various DR techniques and exploitation of the demand flexibility for grid applications. A multi-disciplinary aspect of the SG is demonstrated in a power and communication co-simulation environment.
- **Chapter 4** summarizes control strategies developed during the course of this study to exploit demand flexibility from residential consumer. First, control strategy is developed to manage constraints violations in SG using two-stage control. Next, a voltage controlled dynamic DR is developed to realize demand flexibility at substation level without impacting consumer. Control strategy to exploit demand flexibility from active loads, namely EVs and HPs, are then developed. Finally, a strategy to increase consumer's demand responsiveness is implemented. In this chapter, both the technical and economic aspects of the DR deployment have been addressed.
- **Chapter 5** presents integrated control of active loads and local generation so as to increase both load and generation hosting capacity of the LV grid. First, coordinative control of EVs and PVs is developed to alleviate both under-voltage and overvoltage issues in the network. As EVs are mobile loads which are unavailable at home during the day when PV has maximum production, an adaptive control of EWH and PV is developed to alleviate overvoltage issues.

- **Chapter 6** summarizes a scaled-down SG testbed developed for practical demonstration of the DR control strategies and intelligent control architecture developed in this study. A detailed description on testbed implementation, integration of power and communication infrastructure, and implementation of local and central control scheme are included. The testbed performance is demonstrated from both power and communication perspectives.
- **Chapter 7** summarizes the adaptive protection designed to ensure protection coordination in the varied network condition. In particular, an integrated local and central communication assisted protection strategy is developed for dynamically setting the protective devices based on ON/OFF status of the DGs and changes in network topologies. Impact of ANM on the protection of the medium voltage network is also described briefly.
- **Chapter 8** is the concluding chapter which summarizes the project and underlines the major outcomes and scientific contribution of this research. In addition, the chapter outlines the future prospect of this research and presents the potential extension.

The second part of this thesis contains manuscripts prepared along the course of this study. In particular, the research contribution is documented with the following peer-reviewed conference proceedings and journal publications. The relationship between the manuscripts and thesis chapters is illustrated in the Table 1.1.

Journal Contributions

J.1. **Bhattarai, B. P.**; Levesque, M.; Bak-Jensen, B.; Pillai, J. R.; Maier, M.; and David Dipper, "Design and co-simulation of a hierarchical control architecture for demand response coordination," *IEEE Transaction on Power Delivery (To be submitted)***.**

J.2. Kouzelis, K.; **Bhattarai, B. P.**; Mendaza, I. D. D. C.; Bak-Jensen, B.; and Pillai, J. R., "Smart grid constraint violation management for balancing and regulating purposes," *IEEE Transaction on Power System (*Under Review*).*

J.3. **Bhattarai, B. P.**; Levesque, M.; Maier, M.; Bak-Jensen, B.; and Pillai, J. R., "Optimizing electric vehicle coordination over a heterogeneous mesh network in a scaled-down smart grid testbed," *IEEE Transaction on Smart Grid*, vol. 6, no. 2, pp. 784-794, Jan. 2015.

Conferences Contributions

C.1. Bhattarai, B. P.; Bak-Jensen, B.; Mahat, P.; Pillai, J.R.; and Maier, M., "Hierarchical control architecture for demand response in smart grid scenario," in *Proc. IEEE PES Asia Pacific Power and Energy Engineering Conference (APPEEC)*, pp. 1-6, Dec. 2013.

C.2. Bhattarai, B. P.; Bak-Jensen, B.; Mahat, P.; Pillai, J. R., "Voltage controlled dynamic demand response," in *Proc. 4th IEEE Innovative Smart Grid Technologies (ISGT) Europe*, pp. 1-5, Oct. 2013.

C.3. Bhattarai, B. P.; Bak-Jensen, B.; Mahat, P.; and Pillai, J. R., "Two-stage electric vehicle charging coordination in low voltage distribution grids," *in Proc. IEEE PES APPEEC*, pp 1-5, Dec. 2014.

C.4. Bhattarai, B. P.; Bak-Jensen, B.; Pillai, J. R.; and Maier, M., "Demand flexibility from residential heat pump," in *Proc. IEEE PES General Meeting*, pp. 1-5, Jul. 2014.

C.5. Astaneh, M. F.; **Bhattarai, B. P.**; Bak-Jensen, B.; Hu, W.; Pillai, J. R.; and Chen, Z, "A novel technique to enhance demand responsiveness: An EV based test case," *IEEE PES APPEEC 2015*. (Under review)

C.6. Bhattarai, B. P.; Bak-Jensen, B.; Pillai, J. R.; Gentle, J. P.; and Myers, K. S., "Coordinated control of demand response and grid-tied rooftop PVs for overvoltage mitigation," in *Proc. IEEE SusTech2015*, pp. 1-7, Jul.–Aug. 2015.

C.7. Bhattarai, B. P.; Mendaza, I. D. D. C.; Bak-Jensen, B.; and Pillai, J. R., "A local adaptive control of solar photovoltaics and electric water heaters for real-time grid support," To be submitted to CIGRE Session2016 (synopsis accepted).

C.8. Bhattarai, B.P.; Bak-Jensen, B.; Chaudhary, S. K.; and Pillai, J. R.; "An adaptive overcurrent protection in smart distribution grid," in Proc. *IEEE PES PowerTech*, pp. 1-6, Jun.–Jul. 2015.

Table 1.1 Correlation between the thesis chapters and publications.

Chapters	1	2	3	4	5	6	7	8
Related Publication	-	-	C1, J1	J2, C2, C3, C4, C5	C6, C7	J3	C8	-

Chapter 2. Literature Review

This chapter summarizes current knowledge about intelligent control and operation of future distribution networks. Specifically, the state of the art in relation to: intelligent control architecture of SG, modeling of controllable loads, control strategies to deploy flexible demand, and protection of distribution systems, are presented to illustrate research gaps from which the key contributions of this study are developed. Additionally, recent progresses in multi-disciplinary aspects of the SG to exploit DR are presented.

2.1. Introduction

Conventionally, DSM has been practiced by electric utilities to efficiently utilize their electricity consumption [32], [33]. Several programs, such as energy efficiency, energy conservation, strategic load growth, peak shaving/shifting etc., were designed as a part of the DSM to influence the electricity consumption in the long run [33], [34]. Nevertheless, the conventional DSM approaches as illustrated in Fig. 2.1a) were not designed for short-term load regulation, for instance, to compensate intermittent generation [35]. DR is a concept which is designed for intentional modifications in consumption patterns of the consumers for altering the timing, level of instantaneous demand, or total electricity consumption [36]-[38]. As illustrated in Fig. 2.1b), a key idea of the DR is to make temporary load adjustment, such as turning off, adjusting, or deferring power consumptions of electrical loads for various applications, such as to smooth-out intermittent generations, decongest network, support frequency and voltage regulations, and so forth. The DR is essentially a subset of the DSM [39].

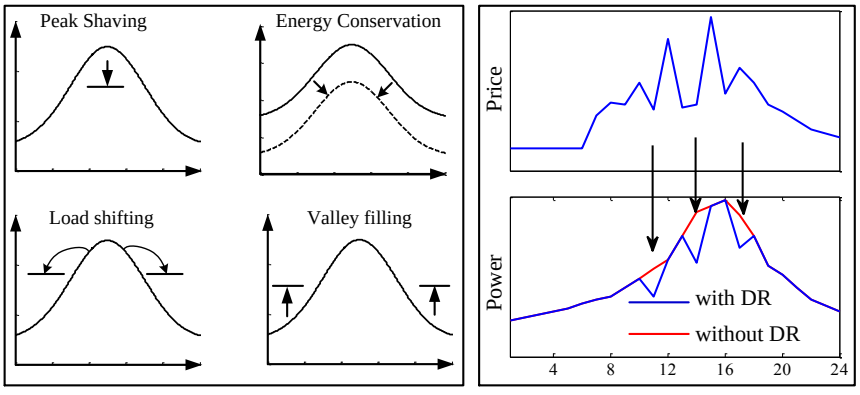

a) Conventional DSM activities b) Demand response

Fig. 2.1 Demand side management activities [33], [34].

There are two potential issues to deploy DR in the existing system. First, a majority of today's electrical loads at the customer level are passive. Second, the

demand of consumer rarely stay constant, rather it varies rapidly and randomly over time [40]. Therefore, controlling the consumer's loads to make them follow the intermittent generation is challenged themselves by their intermittent consumption. Nevertheless, proper mobilization of currently unused flexible electricity consumption is foreseen as a potentially cheaper resource for balancing the intermittent generations as well as supporting the local grids [38].

2.1.1. Organization of Demand Response Programs

Several DR programs have been designed based on consumer preference, load types, and intended applications, to exploit demand flexibility. At first, existing DR programs are broadly classified into incentive based DR and price based DR, as illustrated in Fig. 2.2a) [38]. The DR techniques which act in response to change in electricity price are basically the PDR. Demand price elasticity of the consumers is exploited in PDRs for shifting electrical loads from peak or any critical periods to off-peak periods. Depending on utility strategy and available infrastructure, different types of PDR as illustrated in Fig. 2.2a) can be implemented. Nevertheless, a key intent of the PDRs is to influence the consumer consumption pattern via dynamic electricity pricing without forcing the consumers to do so [41]. Consequently, PDR response is non-dispatchable and is accompanied with high level of uncertainties in consumer responsiveness.

The DR programs in which consumers get incentives in return to their demand flexibility belongs to incentive based DRs. Based on prior contract with the consumers, the DR enabling entity, hereafter called aggregator, executes one or more incentive based DRs, [42]-[44]. A key advantage of the incentive based DRs is that they have dispatchable response, for instance, the amount of regulation from say DLCDR is more predictable than that of the PDRs [45]. In addition to the incentive based DRs and PRDs, recently a new DR category, called ADR, is becoming increasingly popular. The ADR is basically a technique which acts in response to a variation in system parameters, such as frequency or voltage [46], [47]. Device continuously monitors the given parameters and automatically adjusts its setting once the monitored parameter goes beyond preset limits [37].

2.1.2. Benefits of Demand Response

As depicted in Fig. 2.2b), DR programs provide several technical and economic benefits to customers, DSOs, and system operators, they get benefited quite differently though [48], [49]. The system operators can deploy the DR to balance supply and demand, thereby lowering electricity cost in wholesale markets. This, indeed, avoids the need of expensive reserves and helps to reduce price volatility in the market [50], [51]. Similarly, the grid operators or DSOs can use the DR as a resource to avoid grid congestions expected to be created due to increased integration of new electrical loads such as EVs, HPs [52]. The DR can additionally be applied for local network support in several ways, such as peak reduction, congestion management, real-time voltage support etc. [53]. Therefore, the grid operator can get not only operational benefits by effectively using the DR for network support, but also financial savings by delaying or avoiding grid expansion or reinforcement. Similarly, the electrical customers are expected to be benefited mainly in two ways. First, they can have savings on their electricity bills by

reducing the consumption during peak or critical periods. Second, they can trade their flexibility to the market, thereby getting financial gain in return [38].

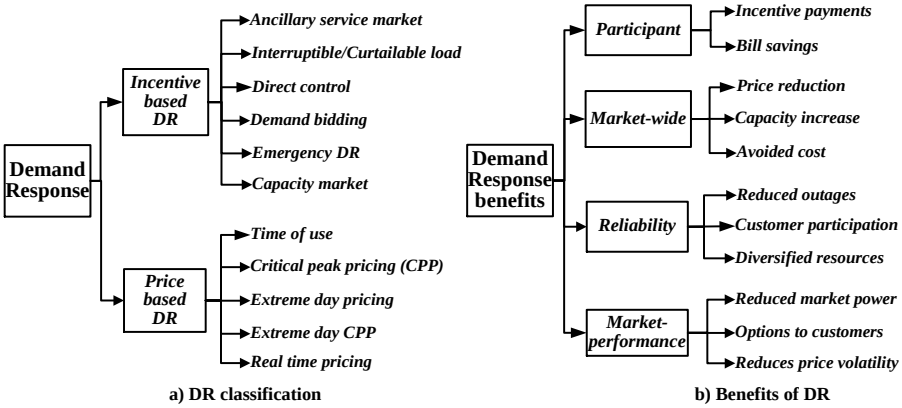

Fig. 2.2 DR classification and potential benefits [38].

In addition to the aforementioned benefits, several system wide benefits, such as improved reliability and market performances can also be realized. As illustrated in Fig. 2.2b), improved reliability can be achieved through reduced outages, whereas, improved market performance can be realized through reduced price volatility. Despite having several benefits, the DR deployment especially for residential consumers is still at a primitive stage [54]. Several technical issues, such as intelligent control architecture, control models, and control strategies, need to be designed to effectively deploy the DR for residential consumers [55].

2.2. Intelligent DR Deployment Architecture

The supply of and demand for electricity must be kept in balance in real-time to keep a secure operation of the electric power system. Therefore, the primary objective of power system control is to maintain system parameters, namely voltage and frequency within pre-defined operational limits during normal as well as abnormal operating conditions [56]. Traditionally, the distribution system is treated as a passive network. So, most of the controls are implemented in the generation and transmission system. However, increased integration of RESs and controllable loads in the distribution network are turning the traditional passive distribution into an active [57], [58], thereby providing various control possibilities.

A centralized and decentralized control architecture is a well-established concept in the power system particularly for transmission and generation. The centralized control has been used for better controllability, predictability, and wider network visibility, whereas, the decentralized control has been implemented for autonomous and prompt responses [59]. Fig. 2.3a) illustrates a brief summary of key characteristics of the centralized and decentralized controls presented in [59]. As the combination of a centralized and a decentralized control scheme has been successful in generation and transmission for years, it has also shed some light on

the design considerations for the future distribution system, especially for the DR deployments [59].

Control architectures for deploying DR vary greatly depending on the utility strategy, available infrastructure, and type of DR to be deployed [60]. For instance, if the utility strategy is just to exploit the DR for peak shifting/clipping, a simple time of rate based strategy might be sufficient, whereas, an extensive approach is needed provided the DR is applied for real-time network support. A centralized control is implemented when dispatchable demand regulation is desired, such as DLCDRs. On the contrary, consumers decide themselves about the control action in response to the DR signal in decentralized control architectures, such as PDRs and ADRs [61]. The authors in [59] demonstrated that coordinated centralized and decentralized control can capture both prompt response and better controllability.

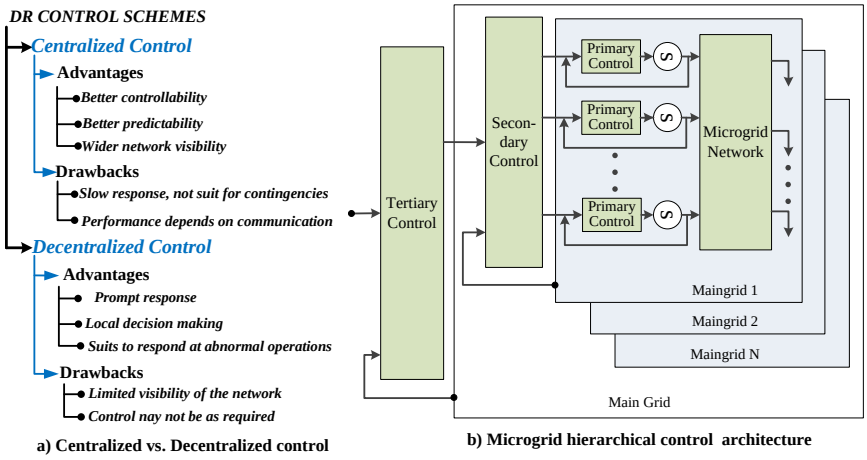

Fig. 2.3 Intelligent control architecture. a) Centralized-decentralized [59] and b) HCA [63].

Recently, several architectures have been developed to integrate advantages of both the centralized and decentralized control. The authors in [62] implemented a simplified HCA to exploit the demand flexibility from HPs and EVs, where the higher level controller ensures equalization of SOC of the EVs and SOE of the HPs and the lower level controller acts in real-time to support the network locally. A very similar HCA strategy can be realized by using primary and secondary control loops of the micro-grid control hierarchy as illustrated in Fig. 2.3b) [63]. Nevertheless, proper design of time and level of control interactions among the hierarchical loops significantly impact the performance of the HCA architecture. The assumption of real-time data availability at the centralized controller, as proposed in [62], may not be realistic. In [64], the authors presented theoretical prospects on coordination strategy among various multi-objective actors, namely fleet operator, DSOs, consumers, and market entities, for realizing EV charging. It has been shown that the presence of several multi-objective actors greatly complicates required DR architectures. Despite some architecture, such as OpenADR [65], has been practiced in the recent years, formally accepted standards to deploy various DR under a single framework are still unavailable.

2.2.1. Multi-disciplinary Aspects of SG Architectures

As stated in IEEE P2030 standard [66], the SG is a multi-disciplinary field comprising the power system, information technology, and communication perspectives. Therefore, deployment of DR depends not only on the power performance, but also on the performance of the ICT. Given this multidisciplinary aspect, several co- and multi-simulation frameworks were proposed for detailed multidisciplinary studies [67]. A co-simulation of power and ICT for EV coordination was investigated in [68] to maximize RESs utilization. Moreover, the authors in [69] developed a multi-agent simulation environment to meet the cross-disciplinary requirements of the SG, particularly DR. In [70], authors investigated impacts of ICT on power system using power and communication co-simulation.

Very few studies, [67]-[70], have been done in investigating the multidisciplinary architecture to deploy various DR schemes. These researches presented co-/multi- simulations to deploy a specific DR, which may not be the case in the future distribution system. The future system will rather have a number of DR programs running simultaneously. In particular, presence of a new DR program may significantly impact the performance of the existing DR and vice versa. Therefore, a HCA is designed and the power and communication co-simulation is performed in this thesis to control and coordinate a number of DR programs under a single architecture. This provides a novel approach to integrate responses from various loads considering both power and communication aspects.

One of the greatly lagging parts in SG, particularly in DR, is the practical demonstration and investigation of the multi-disciplinary aspects. Indeed, very few attempts, [71]-[73], have been done towards practical implementation of multidisciplinary aspects of the SG in physical setups. University laboratory setups, [74]-[76] often involve several real-time or offline simulators rather than having a complete physical setup. Therefore, one of the best approaches to demonstrate their practical implementation and to avoid huge investments in large pilot projects is to downscale the system in the laboratory environment. Indeed, this forms a riskless way to investigate new control and coordination mechanisms for integrating DR.

2.3. Modeling of Flexible Loads and Local Generation

Demand flexibility potential greatly depends on load type, their characteristics, and consumer behaviors. For instance, the demand flexibility of lighting load is significantly low compared to high rated flexible loads provided with storage capacity, such as EVs, HPs etc. Therefore, proper load models are desired to satisfy consumer comforts/requirements and to extract flexibility potential. State of the art on modeling of active loads and local generation is presented as follows.

2.3.1. Electric Vehicles

The sizable ratings provided with energy storage capability makes EV to stand as a potential DR resource [79]. From the power system perspective, an EV is essentially a battery which acts as an electrical load while charging and a source while discharging back to the grid. Therefore, battery model (e.g., electrical, chemical, electro-chemical etc.) often forms a core of the EV modeling [80]. Electrochemical models normally involve non-linear algebraic and partial differential equations for verification of the battery performances [81]-[83]. In fact,

the model performance varies greatly per battery technology. In particular, key parameters, such as efficiency, energy and power density, cycle life etc., for different battery technologies are illustrated in Table 2.1[84]. Due to high power and energy density, longer life time, and high efficiency, Lithium-ion is the most commonly used for EVs [84], and is also the considered technology in this study.

Table 2.1 Key features of different battery technology [84].

Technology	Li-ion	Lead-Acid	Ni-CD	Ni-MH	Nas
Efficiency (%)	70-85	70-80	60-90	50-80	70
Energy Density (Wh/kg)	100-200	20-35	40-60	60-80	120
Power Density (Wh/kg)	360	25	140-180	220	120
Life (no of cycles)	500-2000	200-2000	500-2000	<3000	2000
Self-discharge	High	Low	Low	High	Medium

Nevertheless, electrical models are undoubtedly the most common in studying the impacts and grid support capabilities of the EVs [84]. Indeed, an electrical model of the EV is an equivalent circuit comprising voltage source, resistors, capacitors, etc. [84], [86]. Among several existing electrical models, a Thevenin model consisting of an ideal voltage source in series with an internal resistance and parallel RC circuits is the common one [86]. However, despite having simplicity in the model, its accuracy, for instance for SOC estimation might need to be compromised [86]. As the EV can be seen both as a load and a generator, separate models are normally designed. A common method is to model the EV as a constant power load. Different statistical or stochastic models, as in [87], [88], are used to create EV demand, availability, and charging profiles. Similarly, a static generator model is used for the EV while feeding energy back to the grids [89]-[90]. Currently, there are no established standards in Denmark on EV capability curve; rather the capability curves of the general static generators are applicable [90]. In this study, the EV has been modeled as a constant power load having unity PF.

2.3.2. Heat Pump

The HP is a thermostatic load working in either heating or cooling mode to supply thermal demand of the customers. It transfers heat energy from lower temperature to the higher temperature in heating mode and vice versa. Since the primary use of HPs in Denmark is heating, the entire study has seen the HPs from heating perspective. Depending on the modes of heat transfer, the HPs are broadly classified into: Ground to Water, Air to Water, and Air to Air [9]. The first medium is a source from where heat is extracted and the second refers to the sink. The modeling of HP is primarily seen from two perspectives: thermal and electrical. Thermo-dynamic models include thermodynamic cycles and thermal models of the room, and thermal demand of the consumers [92], [93].

However, thermos-electric models play a greater role since the focus of this study is on accessing the demand flexibility from the HPs for supporting electrical network. In particular, coefficient of performance which is defined as a ratio of thermal energy demand to electrical energy demand performs an interface between the thermal and electrical models [94]. In order to simplify the HP models, many studies assumed constant coefficient of performance [95]-[97]. Nevertheless, in

reality, the coefficient of performance depends greatly on ambient conditions, namely on the temperature difference between source and sink [98]. Authors in [99]-[100] have developed a mathematical model of the coefficient of performance as a function of source and sink conditions. The coefficient of performance as a function of ambient temperature for an air source HP is shown in Fig. 2.4a).

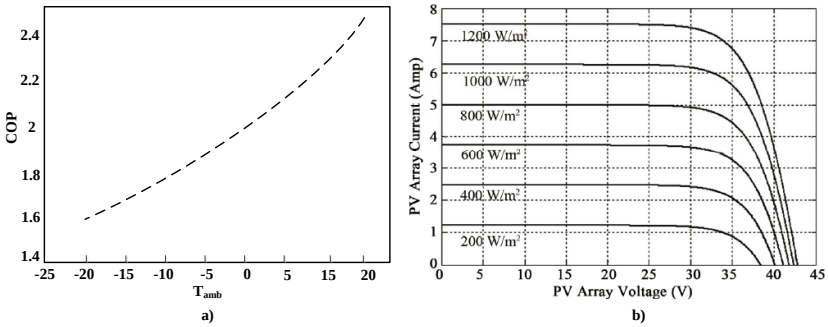

Fig. 2.4 a) Coefficient of performance vs. ambient temperature for a HP [101], b) PV array current vs. solar irradiance [102].

Since a thermal storage tank is often integrated to provide thermal demand of the consumers, a storage tank model is also included in the thermo-electrical model [103]-[104]. Indeed, the storage tank provides two functionalities. First, the storage tank provides operational flexibility, and hence the electrical demand flexibility to the HPs. In addition, it helps to decouple the thermal and electrical system, thereby providing simplified HP models for electrical studies. Nevertheless, the tank size is becoming a key factor in determining cost and technical performance of the HPs. For instance, if the tank size is very small, the HP may not fulfill the consumers demand during worst climate conditions even with full operation, whereas, if the tank size is very large, stratification problem might occur in the tank [9].

2.3.3. Solar Photovoltaic

In Denmark, integration of rooftop solar PV is increasing significantly over the last few years. The PV modeling is basically seen from technological development and application perspectives. There are significant developments on PV technology over the last few years [105], thereby resulting in continuous decrement on cost of the PV cells/modules. Nevertheless, PV modeling seen from electrical application perspectives is the major focus for this study. While seeing the PV from electrical perspective, it is modeled as a static generating source whose power output is a function of environmental factors, such as solar irradiance and ambient temperatures [106], [107]. In particular, the power output varies widely with those parameters. Typical variation of the PV power array current per solar irradiance is illustrated in Fig. 2.4b). In [106], authors presented a probabilistic model to compute power output of the PV considering geostrophic wind variations and in [107], the authors developed artificial intelligence based models for PV power forecast. A key objective of such models is to better estimate the PV power output to ease better operational planning [106].

Solar PV is normally modeled as a current source while studying from grid perspectives. Nevertheless, significant progress on the control capability of the grid-tied PV inverter provides several operational flexibilities to the PVs, thereby different modeling possibilities. In particular, depending on grid application and modes of controls, several detailed electrical models of the PVs, as presented in recent literatures [108] - [110], can be implemented. The authors in [109] have developed a dynamic PV model for local voltage support in the network and the authors in [110] presented very similar modeling approach for congestion management. As this study is intended to deploy DR for residential consumers, the PV is modeled as a static generator integrated with controllable loads.

2.4. Development of DR Control Strategies

Integration of flexible loads and local generation in the distribution system come up with several potential issues. A method of accessing and quantifying those impacts is the foremost step in developing the DR control strategies. The following sections first present potential impacts of flexible loads and generations and subsequently control strategies to overcome those issues are presented.

2.4.1. Impact of Active Load and Generation in LV Grids

Electrification of the heating, gas, and transport sector, introduce new electrical loads, such as EVs, HPs, and EWHs. Due to their sizable ratings, the distribution system particularly the LV networks get greatly affected followed by their higher penetration [111]. Consequently, many of the grids are expected to face one or many problems, such as voltage deviations beyond limits, unacceptable voltage unbalances, voltage flicker, thermal overloading and so on. The authors in [112] has pointed out that some of the LV networks in the Netherlands have already faced such problems due to increased penetration of HPs. Many LV grids which are near to the thermal or voltage limits get congested even with low or moderate penetration of the HPs [113].

Similar to the HPs, simultaneous charging of EVs can easily overload the LV feeder and distribution transformers [114]. Several researches, [115]-[117], has shown that uncontrolled charging of EVs result in several power quality issues, such as excessive voltage drops during peak periods, voltage flicker due to simultaneous switching of EVs etc. The extent of impacts becomes even more when both EVs and HPs are integrated in the LV network since many of the LV networks were not designed to address such scenario. A combined analysis of HPs and EVs in LV showed that uncontrolled operation of such loads leads to immediate reinforcement of majority of the LV networks [9].

On contrary to the impacts of loads, high integration of rooftop PVs, which is an expected scenario in Denmark, will create additional issues, such as overvoltage and harmonic distortions in the network [118]. It has been shown in [119] that the voltage rise is observed as the foremost issue in residential feeders having relatively longer feeder length. Consequently, several rural feeders face overvoltage issue even under relatively low PV penetration. Authors in [120] have further demonstrated that the PVs not only cause overvoltage in the network, but also create intermittent voltage rises on the network due to intermittency in generations.

Reverse power flow and introduction of harmonics in the system are additional issues contributed due to integration of the PVs [120].

The impact assessments of those loads and generations in the network are of great importance especially from DSO's perspective as they should ensure the hosting capacity of the network within limit to maintain reliability and quality of supply. Normally, DSO performs worst case analysis, often deterministically, [121], to identify maximum hoisting capacity of the network. Nevertheless, the worst case analysis may be pessimistic, thereby allowing lower penetration of the loads or generation. This will in turn lead to higher economic investments on the grid reinforcement. As the distribution of the EVs, HPs, and PVs in a feeder significantly vary the level of impacts, stochastic studies considering random load distribution often gives better results [122]. Nevertheless, the study may end up without capturing the worst case.

The impacts of loads and generation on the network are often complementary to each other. Nevertheless, their operation rarely coincides. The PVs normally produce maximum power during the day when the consumption is very low. Similarly, active loads, such as EV, HP, EWH etc., normally consumes high power in the morning and evening when the PV has low/no generation. Nevertheless, exploiting the thermal storage of the HPs and the electrical storage of the EVs, proper control strategies can be designed to complement those conflicting impacts.

2.4.2. Active Loads and Generation Control Strategies

Intelligent control strategies are desired not only to address the aforementioned impacts but also to deploy the demand flexibility for various grid applications. However, there are very limited control possibilities in existing distribution, particularly, in LV distribution systems. Commonly available options are off-load tap changing of the secondary transformer, voltage regulator and/or capacitor banks [123]. Nevertheless, those control techniques are pretty passive since their operation cannot adapt to dynamic operating conditions. Moreover, such control techniques have several technical limitations in relation to regulation capacity, stepwise control, mean lifetime, tracing difficulties and so on [9]. Active control techniques are therefore desired to establish coordinated control and automation of various DERs and loads [124]. As shown in Fig. 2.5 control strategies can be developed and designed from different perspectives. In particular, various control strategies for potential DR resources for grid applications and objectives, are presented next.

2.4.2.1 Control Strategies for EVs

In the recent years, significant attentions from researchers, academia, and government has been invested to develop control methods and strategies to manage high EV penetration, particularly in the LV distribution grids. Price based charging strategies, as proposed in [125], [126], form simple and basic control techniques, whereby consumers reduce their consumptions during high price periods, and consequently shift their loads towards low price periods. A very similar approach, where an optimum EV charging algorithm is seen from the consumer perspectives, is proposed in [127]-[128]. Nevertheless, implementation of purely price based control does not respect network constraints and creates peaks at low price periods.

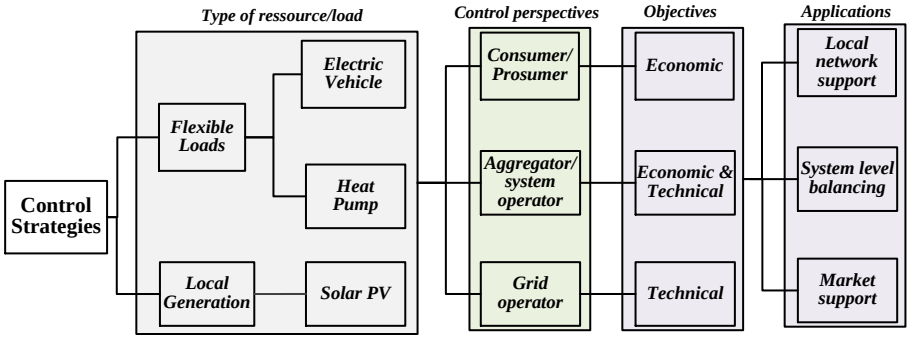

Fig. 2.5 Various perspectives to develop DR control strategies.

On contrary to the aforementioned techniques, several control strategies, [129]-[132], are developed for EV charging management considering network constraints; particularly the voltage and thermal constraints. A flexible EV charging optimization using a reference load curve is proposed in [131] to consider network constraint, particularly the thermal constraints. Similarly, a local voltage and current sensitivity based EV charging algorithm is proposed in [130] to address both the thermal and voltage constraints in the network. In addition, EV charging strategies are developed for several network applications, such as for peak clipping, maximization of load factor, and minimization of feeder loss [130]-[132]. However, seeing the EV charging only from technical perspectives is often insufficient since the EV owners do not concern about the network condition, they rather have financial motivation in return of operational flexibility.

In order to complement the shortcomings of economic and technical perspectives in EV charging, control strategies integrating both aspects are desirable. The authors in [129] presented a two stage optimum EV charging strategy taking thermal loading as a constraint. However, the network constraint, simply taken as the feeder capacity, is often insufficient since voltage is a foremost concern in majority of the LV networks. To address this issue, the authors in [132] presented EV charging algorithms considering voltage, overloading, and electricity costs. In particular, a coordinative EV charging algorithm where an offline scheduling is performed for charging cost minimization and a shadow pricing is performed for congestion management. The proposed approach perfectly suits to formulate optimum EV charging schedules which simultaneously respect both the voltage and thermal constraints. Nevertheless, optimum scheduling based on the forecasted loads and EV arrival/departure might need to be adjusted during actual operations as the loads may vary rapidly and randomly over time.

2.4.2.2 Control strategies for HPs

The sizable rating provided with energy storage capability of the HP possesses substantial demand flexibility. In addition, large thermal time constant further provides operational flexibility, without impacting the consumers' comfort [9]. Nevertheless, proper control strategies are desired for exploiting the demand flexibility not only to provide grid support in several ways but also to ensure the financial motivations of the consumers. Authors in [133] presented optimum HP

scheduling by minimizing total energy cost of the HPs. Similarly, the authors in [134] presented a distributed HP scheduling to optimally shift the operation of HP according to local generation from wind and solar PV. It has been assumed that the HP is provided with sufficient storage capability so that its operation can be shifted to any period of the day, which may not always be the case since the storage capacity depends greatly on the tank size. Moreover, those price based control strategies ignore one of the important aspects, the network constraints.

In order to address the network technical limitations, the authors in [135]-[136] proposed different control techniques incorporating network constraints and consumer comforts. The authors in [135] proposed a methodology to ensure maximum utilization of the local network by simultaneously respecting the consumer comfort. Similarly, the authors in [136] proposed an aggregated approach for the thermostatic loads and EVs for the frequency support. Even though the aforementioned methods perform technically better than price based strategies, integration of the economic aspects is vital especially to incentivize the consumers.

To support the network in real-time, a direct load control approach has been proposed in [137] where the HPs get disconnected for 1-2 hours for several times per day, provided the storage tank has full energy before the next disconnection. A very similar approach is presented in [138] where a load dispatch algorithm based on an ON-OFF control strategy is implemented to control HPs for supporting the network in real-time. Even though the direct load control based methods respect the electricity prices as well as provides the dispatchable demand regulation, consumer flexibility and comforts needs to be compromised. Alternatively, the authors in [139] proposed a simple voltage control strategy for peak shaving in distribution feeder. This method provides an adaptive control to the HPs, and hence has great potential for grid support without noticeable impact to the consumers. Nevertheless, as the HP compressor is supplied normally by induction motors, the decrease in voltage may degrade the HP performance.

2.4.2.3 Coordinated control of PVs and EVs

As mentioned in the previous section, increased PV penetration creates several impacts in the existing electrical grid. In particular, voltage rise is one of the foremost concerns that need immediate attention even under moderate PV penetration [119]. Several control strategies have been developed recently to alleviate the grid overvoltage resulting from the PV penetration. Authors in [140] - [141] presented various reactive power control techniques to alleviate grid overvoltage, where the key idea is to increase reactive power consumption of the grid-tied PV inverter during overvoltage. However, increased reactive power consumption to alleviate OV creates additional power loss in the grid. To overcome this issue, the authors in [142] proposed a droop based active power curtailment method. Despite its superior performance for voltage support, it incurs revenue loss to PV owners, thereby reducing the probability of acceptance by the PV owners.

Alternatively, integration of battery storage is presented in [143] and a coordinated control of distributed energy storage and transformer tap changer is proposed in [144] for the voltage control in distribution grids. In spite of their better grid support capability, extra investment in storage makes them economically less

attractive. To avoid additional investment on storage, battery storage of the EVs is often integrated with the PV control. Utilization of battery storage of EVs is proposed in [145] to reduce reverse power flow from the PVs. Similarly, a real-time EV charging control is proposed in [146] to reduce impacts of solar irradiance intermittency. Nevertheless, both the forecasting based predictive control, [145], and real-time based adaptive control, [146], are desired to effectively address the overvoltage issue. Therefore, a combined predictive and real-time control of the EV charging to mitigate grid OV due to PVs is developed in [147]. However, the proposed EV control is often insufficient to fully mitigate the overvoltage in residential feeders due to the fact that EVs are normally unavailable at home when PV has maximum production.

2.4.2.4 Voltage control DR

CVR is a technique conventionally deployed by many electric utilities as a mean of energy conservation [148]. The authors in [149] - [154] proposed CVR for various applications, for instance, peak shaving, energy conservation etc. Nevertheless, a key idea of the CVR is to reduce the consumer demand and hence the consumption by reducing the operating voltage. Exploiting the fact that the demand of a device is a function of voltage, both up/down regulation can be realized by voltage control. This method gained less attention over the last few decades due to the risk of voltage deviations beyond the limits [155]. Moreover, lack of accurate estimation of voltage dependency of loads is acting as additional barriers on its easy acceptance. Nevertheless, this method is gaining relatively increased attention with the advancement on automatic metering infrastructure and with a greater need of demand flexibility in the future grids.

The actual demand regulation potential of the voltage control is subjected to the voltage dependencies of the loads and available range of voltage control [156]. The authors in [157] performed voltage control experiments by changing the voltage of the secondary smart transformer on a representative urban LV feeder to compute the voltage dependency. They have demonstrated significant demand regulation potential with the proposed techniques. The variations on regulation potential are dependent of with season, geographical location, and loading conditions of the network. Typical variations of voltage dependencies of feeder loads for different seasons are listed in [158]. Therefore, an adaptive control method is anticipated to determine real-time voltage dependencies of the load.

This method serves as a potentially effective tool in regulating the demand as most of the existing DR techniques are accompanied with greater uncertainties and lack of dispatchability [155]. Moreover, a clear advantage of this technique is that the consumers get minimally affected due to its deployment and it cause very low energy recovery effect [157]. Therefore, this technique serves as an effective tool for the various applications such as emergency DR, peak reduction, participating in regulating market etc. However, in order to make it easily acceptable, voltage at every consumer POC should be within the acceptable limits.

2.5. Impact of ANM on Protection

Future distribution systems are expected to be characterized with high adaptation of DERs and ANM activities, such as DR, dynamic network

reconfiguration. Despite having several technical benefits of the DERs, their high penetration inherits several control and operational complexities in the existing system. Protection of the electric distribution network is considered as one of the potential issues caused due to high penetration of the DERs. Conventional protection approaches where the protective devices use static settings may not properly discriminate the fault in the future grids characterized with high DER penetration [159]. In addition, presence of various ANM approaches also threatens the existing protection practice since they may change the network topology. Therefore, unlike the conventional approach where the protection is decoupled from the network control, an integrated protection and ANM is desired. Particularly, the protection should be a part of the ANM such that protection coordination is ensured dynamically consistent with the ANM activities.

Recent studies have developed various algorithms to address the protection problem in the distribution system due to DER integration. The authors in [159] proposed a simplified method to disconnect all the DERs followed by fault detection. A key idea behind this approach is to keep protection settings intact as that of without having DERs. Nevertheless, disconnecting all the DERs after fault is undesirable since it causes significant revenue loss and decreased reliability. Alternatively, authors in [160], [161] proposed techniques to determine the maximum penetration of DERs without impacting the protection system. In line with this, various faults current limiting methods, [162] - [163], are recently proposed to limit the fault current contributions from the DERs such that the existing protection can be used without modification. For the inverter interfaced DERs, the authors in [163] demonstrated that the fault current contribution can be reduced to zero. Particularly, the main idea on those techniques, [160]-[163], is to limit the fault current to such an extent that it does not demand change in setting.

Therefore, an AP scheme, where the relay settings are updated dynamically consistent with varying network topologies, is gaining increased momentum in the recent years. Authors in [164] presented a local adaptive overcurrent protection where each relay locally detect connection status of the DERs and update their setting. Similarly, local adaptive protection where the relay settings are updated based on locally measured voltage is proposed in [165]. Even though those local adaptive protection approaches effectively updates the relay settings based on the connection status of the DERs, any changes in network topologies due to ANM or connection of additional DERs cannot be addressed by those techniques.

In order to resolve those issues with the local adaptive protection, the authors in [166] proposed communication assisted adaptive protection integrated with ANM. Similarly, communication assisted protection for micro-grids is proposed in [167], [168]. Nevertheless, those approaches used a centralized communication assisted protection, in which a central protection unit gather data from every DER and relay to update relay settings consistent with the change in network topology. Such centralized protection scheme not only requires increased communication burden but also creates a single point of failure. To simplify the problems of the centralized schemes, authors in [169], [170] proposed zonal based decentralized protection, whereby each zone separating breaker communicate to the others [169] and to the central relay [170] to identify the faulted section.

2.6. Chapter Summary

Despite having significant research efforts, deployment of DR at the residential consumer level is still at the developmental stage. As discussed in the previous sections, intelligent DR control architecture, proper DR control strategies, and adaptive and proactive protection are the key issues that need to be addressed to realize intelligent control and operation of the future distribution system. State of the art on DR architecture has shown that there is no standard common framework for deploying various types of DR. Moreover, multi-disciplinary aspect for DR exploitation is still unsolved. Therefore, an intelligent hierarchical DR control architecture is developed in this study to provide a common framework to establish control of different DR types. A communication infrastructure is integrated to the HCA to address the multi-disciplinary aspect of the DR deployments.

It has been seen from the state of the art that DR strategies simultaneously addressing both technical as well as economic perspective are still under development. Therefore, a novel two-stage algorithm, where the first stage prepares an economic optimization considering electricity price, network constraints, and consumer requirement and the second stage makes a real-time network support by adjusting power consumption from active loads, namely EVs and HPs based on a locally monitored voltage is proposed in this study. Moreover, periodic interaction between two stages is established to adapt any operational uncertainties.

As existing DR control strategies are mainly based on directly/indirectly controlling the consumer loads, there are always very high uncertainties in the consumer responsiveness and participation. To address this aspect, a new voltage control dynamic DR is presented in this study, whereby SS voltage is adaptively regulated consistent with need of demand regulation.

The state of the art has shown that practical demonstration of the DR is one of the greatly lagging parts in the SG development. As such, a scaled down SG testbed is developed in this study for practical investigation of the developed DR solutions. Additionally, multi-disciplinary aspects of the DR deployment are demonstrated from power and communication perspective by implementing a combination of centralized and decentralized control strategy.

The state of the art on protection of future distribution system reveals that both the local adaptive protection and centralized protection approach inherits limitations in terms of their fault discrimination capability. Moreover, protection is normally decoupled with ANM activities, which is not realistic in future. Therefore, a two-stage protection strategy is proposed in this study to address protection issues resulting from increased DERs and ANM integration. Particularly, a combination of local adaptive and communication assisted centralized protection scheme is implemented.

Chapter 3. Intelligent Smart Grid Control Architecture

*This chapter presents intelligent control architectures to apprehend anticipated control and operations of the future distribution grids for deploying DR. In particular, the key functionalities of an HCA, documented in manuscripts **C1** and **J1** are summarized and the effectiveness of the HCA to deploy existing DR techniques is demonstrated. Moreover, multi-disciplinary aspects to the DR deployment are investigated through power and communication co-simulation in a LV test network considering EVs as potential DRRs.*

3.1. Introduction

One of the major objectives of the SG is to deploy DR for enabling consumers to interact with the power system by means of intelligent control of their electrical appliances. However, lack of standardized DR architecture is becoming a key barrier to deploy DR, particularly for residential consumers. Further, the passive nature of most of the current LV distribution networks and electricity consumers is being a potential issue for practical deployment of the DR. Therefore, intelligent DR control architecture is designed in this study to effectively deploy various types of DR programs with the aim of producing the following functionalities:

Commercial functionality: *A key idea of the commercial functionality is to ensure profitability to the participating consumers. Therefore, the architecture provides a coordination framework among key SG actors, namely consumer, aggregator, and DSO, to facilitate trading of consumers' demand flexibility in the dynamic electricity markets.*

Technical functionality: *A key purpose of the technical functionality is to utilize the flexible demand from widely distributed consumers/prosumers for supporting the electrical network. Proper coordination among the actors is established to exploit the demand flexibility in supporting the network at the local level (e.g. local voltage support, congestion management etc.) as well as at the system level (e.g. system level balancing). Moreover, consumer's comfort, operational preferences, and needs are ensured through coordinated control of the potential DRRs.*

This chapter presents intelligent DR control architecture designed for realizing the aforementioned technical and commercial goals. In particular, the HCA proposed in the publications $\mathbf{C_1}$ and $\mathbf{J_1}$ is implemented to maximally exploit demand flexibility, particularly, from the residential consumers. First, a control-requirement based classification of the existing DR techniques is presented to quantify control needs of each DR category. The HCA containing three DR control loops, namely primary, secondary, and tertiary, is then designed to establish coordinated control among all DR categories. As control latency of HCA loops

increase from the inner primary towards the outer tertiary loop, every outer loop provides time-delayed backup to the immediate inner loop. Moreover, every inner loop supports the outer loop by activating their control with shorter latencies. This indeed leads to increased control and operational flexibility to every loop, thereby supporting the network maximally. More importantly, a heterogeneous communication network is integrated into the HCA to realize anticipated control. The HCA performance is demonstrated from power and communication perspectives in a LV test network considering EV as a potential DRR.

3.1.1. DR Deployment Framework

In general, a DR deployment framework as illustrated in Fig. 3.1 is required to establish coordination among major SG actors, namely DRR, DSO, aggregator, RPM, and electricity market. In particular, the RPM and electricity market are system level actors, whose influences to deploy DR are taken in the form of regulating signal or price signal. On the other hand, DRR, DSO, and aggregator are local actors, which play key roles to deploy DR in a particular distribution system. Indeed, the DRR is a consumer or directly controllable load, which receives DR control signals, such as electricity price, power/temperature set-points etc., from the higher level and reacts to them as per the instruction contained in the signal. The DRR either adjust or shift the consumption in response to the DR signal.

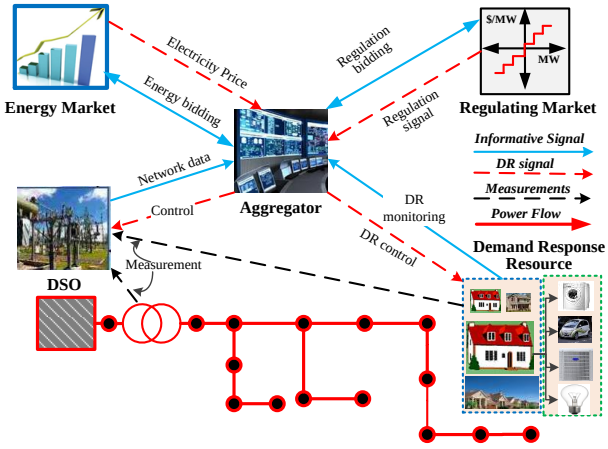

Fig. 3.1 DR Interaction framework for SG actors.

Similarly, the aggregator is a commercial actor who is responsible for ensuring coordination among the actors to execute DR. As illustrated in Fig. 3.1, the aggregator plays an intermediate role to enable market participation of DRRs, which otherwise cannot directly trade their flexibility to the market. The aggregator additionally ensures coordination with the DSO to avoid grid bottlenecks that might result from DR deployments. Similarly, the DSO, who is an owner of a physical network, is responsible for ensuring operational constraints within the limits.

In particular, a novel control requirement based DR categorization is proposed in this study to establish a common framework to deploy DR. In particular, existing DR techniques are categorized into ADR, DLCDR, DDDR, and PDR, on the basis

of control schemes, response time, and communication requirement. In ADR**,** DRR continuously monitors system parameter, such as frequency or voltage, and automatically adjusts their setting once the monitored parameter deviates beyond the preset limits. Prompt response in the range of fraction of seconds can be realized by the ADR as monitoring and control take place locally at the DRR level. Similarly, DLCDR is realized by directly controlling status of individual devices. As the aggregator executes the DR control centrally, the DLCDR has slower response ranging from few seconds to minutes.

Similarly, in DDDR, the aggregator centrally dispatches a DR signal invoking a specific instruction, such as power/temperature set-points, to candidate DRRs, who in turn takes the final control action. Depending on load characteristics, the response time of the DDDR varies from few minutes to several hours. Similarly, DR techniques which act in response to electricity price belong to PDR. In particular, the electricity price is regulated centrally by the aggregator and dispatched to every DRR such that consumers are free to respond to the electricity price. The PDRs typically exhibit slower response (in order of several hours) since consumer should know the price in advance to be able to shift or reschedule their loads. Key characteristics of each DR category are summarized in Table 3.1 and details are presented in Section II of **C1**.

Table 3.1 A Novel control requirement based DR categorization.

DR Type	Control Signal	Signal type	Decision place	Control action	Response time	Communic-ation need
ADR	Frequency/Voltage	Directive	Local	Local	< 1 sec	No
DLCDR	ON/OFF, Setpoints	Directive	Central	Central	sec. - min	Yes
DDDR	Demand dispatch	Instructive	Central	Local	min. - hour	Yes
PDR	Price	Informative	Central	Local	hour - day	Yes

The aforementioned DR categorization is done such that limitations of each DR category are compensated by the other. For instance, high uncertainties in consumer responsiveness of the PDRs can be compensated by exploiting the specific demand regulation capability of the DDDR, whereby the consumers are instructed to regulate their demand by a specific amount. Similarly, the DLCDR is designed as a potential resource to provide demand regulations during emergency conditions when the PDRs and DLCDRs are unable to do so due to their longer control latencies. Moreover, the ADR is designed for real-time network support which otherwise cannot be realized from other DR categories.

3.2. Implementation of HCA Architecture

A HCA is designed in this study to establish coordination among the aforementioned DR categories, especially to compensate limitations of the individual DR categories as well as to maximize demand regulation potential. In particular, implementation of the HCA is realized in three stages. First, the HCA is designed to establish coordinated control among aforementioned DR categories from power perspectives. Second, appropriate ICT infrastructure is integrated into the HCA. Finally, a power and communication co-simulation is performed considering multi-disciplinary aspects of the HCA.

3.2.1. HCA Implementation from Power Perspective

As illustrated in Fig. 3.2, the HCA is designed with three DR control loops, namely primary, secondary, and tertiary, such that each loop is responsible for deploying a specific DR category. In particular, each loop exhibits a specific response time which increases from the inner primary loop towards the outer tertiary loop. Therefore, every outer loop provides time-delayed backup to the immediate inner loop and hence the increased control and operational flexibility. Similarly, every inner loop backup the performance of the immediate outer loop by compensating their uncertainties in shorter time resolutions. Indeed, the HCA loops run in succession to back-up each other and maximally exploit the DR potential. However, the HCA loops are not identical to the frequency regulation loops; the same naming is intentionally used to emphasize that each HCA loop can serve the respective frequency regulation. For instance, the primary DR loop can serve the primary frequency regulation and so on. Nevertheless, the HCA loops can additionally be applied to support the network in several ways, such as peak shaving, congestion management, local voltage support etc.

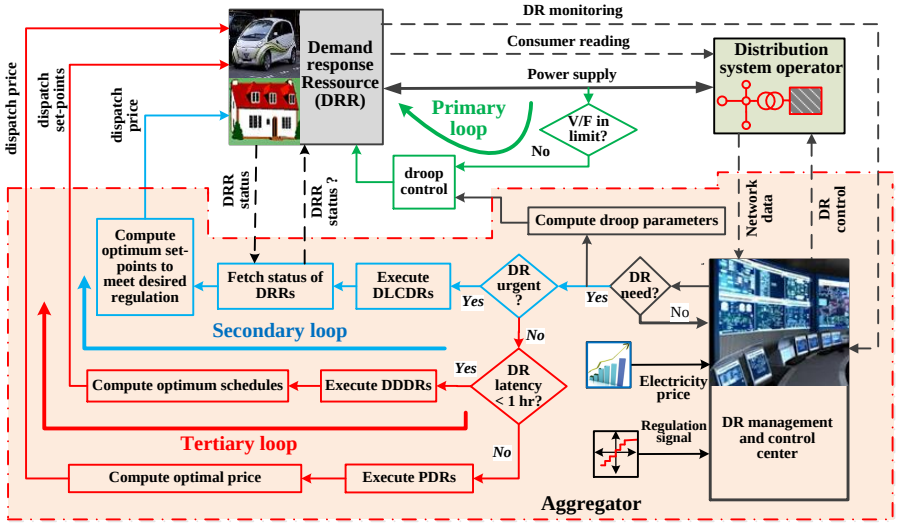

Fig. 3.2 Hierarchical DR control architecture.

3.2.1.1 Tertiary DR control

The TDRC loop is the slowest, outermost loop in the HCA which is primarily designed to execute the PDRs and DDDRs. Depending on desired response time the TDRC executes IFC to deploy the PDRs or ISC to deploy the DDDRs. In particular, the ISC is executed when faster responses ranging from few minutes to an hour are desired, thereby leaving the IFC to work for DR where slow response is acceptable.

Informative control: The IFC is designed to optimally adjust hourly electricity prices so as to incentivize the consumers for reducing or rescheduling their consumption. Since the consumers should know the electricity price well in advance to be able to shift their loads, the IFC normally exhibits slow response.

Therefore, the IFC in this study is proposed to be executed once per day, typically at the beginning of the day. Since the consumers are not specifically instructed for any particular action, they have complete flexibility to respond to the electricity price. Therefore, IFC is designed based on aggregated feeder load with an objective to maximize profit by shifting loads from high to low price periods as follows:

$$\max . \sum_{t=1}^{T} \{C_t . L_t - (C_t + \Delta C_t).(\mathrm{L}_t + \Delta L_t)\} \tag{3.1}$$

$$\begin{aligned} &\text{Subjected to,} \sum_{t=1}^{T} \Delta L_t = 0 \\ &|\Delta C_t| \le \alpha * C_t \\ &|\Delta L_t| \le \beta * L_t \\ &C_t / \Delta C_t = \lambda * L_t / \Delta L_t . \end{aligned} \tag{3.2}$$

where C_t and L_t are original electricity price and feeder load respectively; ΔC_t and ΔL_t are the optimum changes in electricity price and corresponding change in feeder load; and α and β are the allowable percentage changes in electricity price and load, respectively. Moreover, subscript *t* represents value of corresponding variable at t^{th} hour, *T* represents total number of hours, and λ represents demand-price elasticity. The 1st and 2nd part of the objective function represent total electricity cost to be paid before and after applying IFC. Therefore, the higher the positive difference, the higher the saving is. The 1st constraint keeps the total energy consumption in a day constant, the 2nd and 3rd constraints limit the price and load changes, and the 4th constraint sets price responsiveness of the aggregated load. The optimization provides optimum electricity prices $(C_t+\Delta C_t)$ to be dispatched to every consumer.

Instructive control: The ISC is designed to instruct the consumers to regulate their demand by a specific amount. In particular, based on type of load and prior contract with the consumers, the ISC is executed by dispatching proper signals such as power or temperature set-points. In this study, the ISC is configured to be periodic with a period of 15 minutes to compensate any uncertainties, such as deviations in demand, generation, or electricity prices, within the period. EVs are taken as potential DRRs, whereby the EV charging schedules are periodically updated considering observed variations in preceding time-slots. As such, the aggregator prepares optimum EV schedules by minimizing total charging cost as in (3.3) and dispatches the schedules to the corresponding EVs as an ISC signal.

$$\min . \sum_{k=1}^{K} \sum_{i=1}^{N_{EV}} C_k . \mathrm{P}_{i,k} . \delta_{k,} \tag{3.3}$$

$$\begin{aligned} &\text{Subjected to: } P_{\min,\mathrm{i}} \le P_{\mathrm{i,k}} \le P_{\max,i} \\ &SOC_{\min} \le SOC_{\mathrm{i}} \le SOC_{\max} \\ &SOC_{\mathrm{T}_{out},\mathrm{i}} = SOC_{\max} \\ &\sum_{i=1}^{N_{EV}} \mathrm{P}_{i,k} + \mathrm{P}_{\mathrm{base},k} \le \mathrm{P}_{cap,k} . \end{aligned} \tag{3.4}$$

where *P*, *SOC*, and *C* are power, state of charge, and hourly electricity prices, respectively. The subscript *i*, *k*, and *min/max* represent the EV number, slot number, and minimum/maximum values of the associated parameters. Similarly, N_{EV} and *K* denote the total number of EVs and time-slots respectively. $SOC_{Tout,i}$ is the desired

SOC by plug-out time and $P_{cap,k}$ and $P_{base,k}$ are the feeder capacity and feeder base load respectively. The objective function is formulated to minimize the sum of electricity cost for EV charging. Further, the 1st constraint ensure that the EV charging power stay within the charger limits, whereas the 2nd and 3rd constraints are used to fulfill charging requirement of the EV owner such that the EV get fully charged by its plug-out time. The 4th constraint ensures that the EV charging does not violate the feeder capacity. A linear optimization is then implemented to determine the optimum schedules $P_{i,k}$. The optimization is repeated periodically at every 15 minutes by considering observed variations in demand, electricity prices, and plug-in and plug-out of the EVs in the preceding slot(s).

3.2.1.2 Secondary DR control

A SDRC is implemented to execute the DLCDRs, whereby the DRRs are directly controlled by the aggregator. Typically, the SDRC is executed when emergency demand regulation is desired and the TDRC is incapable to meet the strict up/down regulations requirements. Exploiting the prompt response capability, ranging from few seconds to minutes, the SDRC can be realized as an intra-hour or intra-day balancing resources. As illustrated in SDRC loop in Fig. 3.2, the aggregator optimally distribute the demand to be regulated among the candidate DRRs based on their current operating mode. The desired demand regulation, P_{DR}, is optimally allocated among the candidate EVs as follows:

$$\min . \sum_{i=1}^{N_{EV}} C_i . (P_i^{'} - P_i) \tag{3.5}$$

$$such\,that\, C_i = \begin{cases} SOC_i & if\ P_{DR} > 0 \\ (1 - SOC_i) & if\ P_{DR} < 0 \end{cases}$$

$$\sum_{i=1}^{N_{EV}} (P_i^{'} - P_i) = P_{DR} \tag{3.6}$$

$$P_{\min,i} \le P_i^{'} \le P_{\max,i} .$$

where P_i and P'_i denote charging power of i^{th} EV before and after SDRC execution, and C_i is an optimization coefficient which is $(1\text{-}SOC_i)$ for up-regulation and SOC_i for down-regulation. The objective is formulated such that EVs having lower *SOC* contribute first during down-regulation and vice versa. The constraints are designed to ensure the desired demand regulation as well as to respect the charger limits. It should be noted that the P_{DR} is limited to the maximum regulation capacity of the EVs if the P_{DR} exceeds the regulation capacity of the EVs.

3.2.1.3 Primary DR control

A PDRC is implemented for executing the ADRs, where the DRRs automatically adjust their power when locally monitored system parameter deviates beyond the preset limits. The PDRC is suitable for real-time local voltage support leading to its prompt response (in the order of seconds). The PDRC is designed with a power-voltage (P-V) droop and is implemented at every DRR such that the DRR continuously monitors voltage at the POC to adaptively adjust the power as:

$$P = \begin{cases} P_i & V > V_{th,i} \\ P_i\left(1 + \dfrac{V - V_{th,i}}{V_{th,i} - V_{\min,i}}\right) & V_{th,i} < V < V_{\min,i} \\ o & V \le V_{\min,i} \end{cases} \quad (3.7)$$

where P_i is the charging power, $V_{th,i}$ is the threshold voltage beyond which the droop starts operating, $V_{min,i}$ is the minimum allowable voltage beyond which the EV stop operation, and the subscript 'i' depicts the EV index. It should be noted that EVs connected to different nodes in the network have different voltage thresholds. Particularly, the EV connected to a node closer to a SS has higher V_{th} and V_{min} compared to the EV connected to the node far from the SS. This is established to enable a fair participation of every EV in supporting the network rather than stressing the farthest node EV by using constant V_{th} and V_{min}. Procedure to compute V_{th} and V_{min} sets for every EV is described in Section II.C of **J1**.

3.2.1.4 Coordination among the HCA loops

The aforementioned DR control loops are designed such that action of each loop provides time delayed backup to the others, thereby creating increased operational flexibility to every loop. Any deviations that might be caused due to TDRC can be compensated in real-time by the PDRC, thereby providing increased operational flexibility to the TDRC. Similarly, any deviations in the operational schedules of the DRRs due to PDRC get compensated while updating the schedules by the TDRC in the succeeding slot, thereby providing time-delayed backup to the PDRC. In addition to the TDRC and PDRC, an event driven SDRC is integrated to take care of any emergency conditions requiring up/down regulations. As such, the HCA establish coordination among the loops to exploit the demand flexibility for supporting network from day ahead planning up to the real-time operation.

3.2.2. Communication Perspective of HCA

A combination of wired and wireless technologies should be integrated to the HCA to establish bidirectional communications among the actors. In particular, a robust fiber-wireless access network and a wired optical network are implemented to exploit high capacity, longevity, and reliability of optical networks with the ubiquity and availability of their wireless counterparts. Communication technologies are selected based on the requirement at various control levels of the proposed HCA. As presented in Table 3.2, the message interval and required latency are specified for each control loop to exploit them for various grid applications, such as real-time voltage, congestion management, peak saving etc. In addition, communication distance is chosen on the basis of maximum expected distance between the involved actors to execute the particular control action.

Table 3.2 Communication requirements for HCA.

Level	From	To	Distance (km)	Interval	Latency (sec)
TDRC	CA	DRR	0-25	15 min	60
SDRC	CA	DRR	0-25	Variable	15
PDRC	HEM	DRR	0-0.05	Variable	1

The communications infrastructure for the proposed control scheme depicted in Fig. 3.3 is selected on the basis of aforementioned communication requirement as well as the cost of currently available communication technologies. In particular, a ZigBee for HANs, WiMAX for cost-effective NAN coverage, and dedicated optical fibers for reliable interconnection of CA and data concentrator, are integrated into the HCA to make it operational. Basically, communication framework as illustrated in Fig. 3.3, has been used to realize the proposed HCA control and coordination. However, the whole framework may not be needed for execution of every control level. For instance, HAN is adequate to execute PDRC, whereas, all HAN, WiMAX, and dedicated fiber are desired to execute the TDRC and SDRC. The communication technologies which are presented in detail in Section IV of the '**J1**' are briefly outlined as follows.

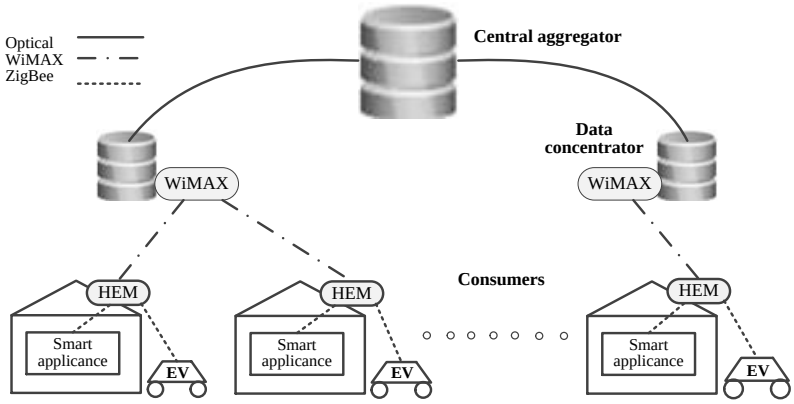

Fig. 3.3 Proposed communication infrastructure for HCA implementation.

1) **HAN - ZigBee:** ZigBee compliant with IEEE 802.15.4 is used for HANs with a capacity of 250 Kbps per zone (e.g., per home). According to Eq. (2) in [16], the access delay of IEEE 802.15.4 can be approximated by

$$D_{HAN}^{ac} = T_{BO} + T_{frame}(x) + T_{TA} + T_{ACK} + T_{IFS} \tag{3.8}$$

where T_{BO} takes into account the backoff period, $T_{frame}(x)$ is the transmission delay for a payload of x bytes, T_{TA} is the turnaround time, T_{ACK} is the transmission time for an acknowledgement frame, and T_{IFS} is the interframe space time. For payload sizes of L greater than x_{max}, the adjusted access delay is approximated as follows:

$$D_{HAN}^{ac} = a.\bar{L} + \bar{L}/x_{\max}.b. \tag{3.9}$$

where 'a' denotes the delay to transmit a single byte, 'b' is the overhead delay while transmitting a frame, and L is the number of bytes in the message. The maximum achievable throughput in a given household is approximated by $\bar{L}.8/D_{HAN}^{ac}$ and the overall delay corresponds to $D_{HAN} = D_{HAN}^{ac} + \phi$.

2) **DRRs and data concentrator** – WiMAX: For the access network area, which interconnects the DRRs and data concentrator, WiMAX is used. The overall transmission process in WiMAX consists of successive upstream and downstream sub-frames, whereby both form a WiMAX frame. In the upstream direction, a given

subscriber station first competes for sub-channels by sending a bandwidth request frame to the base station at the beginning of a WiMAX frame. Note that WiMAX frames have a fixed duration of T_{wi} frame. Then, the base station sends back a bandwidth response containing the scheduling allocations to the subscriber station. Therefore, the approximate upstream delay D^{wi}_{up} consists of a number of WiMAX frames with duration T_{wi}, which largely depends on the traffic intensity.

3) **Interconnection of CA and Data Concentrator** – Dedicated Fiber: For reliable communication between the CA and data concentrator, dedicated fiber links with 1 Gbps (denoted by *c*) duplex capacity is considered. Since point-to-point optical links are deployed, the upstream delay is estimated as follows:

$$D^{op}_{up,l} = \phi(\rho l) + \frac{\bar{\text{L}}.8}{c} + \frac{\text{d}_{l,ca}}{200000}. \tag{3.10}$$

where *Ø(pl)* corresponds to the queuing delay with a traffic intensity of *pl* from a data concentrator *l* to the CA, the second term is the transmission delay, and the last term is the propagation delay (including the distance (km) from data concentrator *l* to the CA, $d_{l,ca}$). The downstream delay (from CA to a data concentrator) $D^{op}{}_{down,l}$ can be defined similarly, but based on the traffic intensity $p_{ca,l}$ at the CA interface. Therefore, a message from a given node in the HAN to CA will experience a total delay equal to (3.11) and a delay equal to (3.12) from the CA to a node in the HAN.

$$D_{HAN-CA} = D_{HAN} + D^{wi}_{up} + D^{op}_{up,l} \tag{3.11}$$

$$D_{CA-HAN} = D^{op}_{down,l} + D^{wi}_{down} + D_{HAN} \tag{3.12}$$

3.2.3. Power and Communication Co-simulation

To investigate the performance of the proposed HCA, a power and communication co-simulation model is developed using off-the-shelf simulators, particularly using RTDS for the power simulation and OMNeT++ for communication simulation. In addition, MATLAB is used for computations and to make interface between the OMNeT++ and RTDS, thereby establishing overall co-simulation framework as depicted in Fig. 3.4.

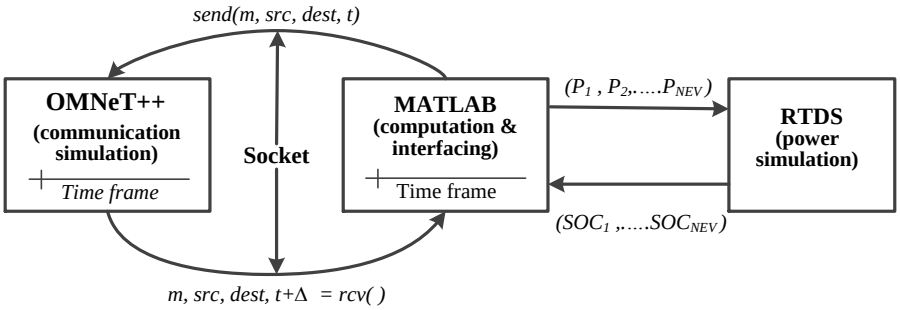

Fig. 3.4 Proposed co-simulation framework.

In particular, droop based PDRC is implemented at every EV location in the RTDS, whereas the TDRC and SDRC are implemented in MATLAB for computing optimum set-points for every EV. The computed set-points are then channeled

through the OMNeT++ to the respective EVs in the RTDS for control realization. Moreover, MATLAB continuously records actual charging power and SOC of each EV and voltages at every node from the RTDS using '***Listenonport'*** feature of the RTDS. The optimization is updated periodically in MATLAB based on the recorded data from the RTDS and dispatched to the respective EVs using the aforementioned procedure.

The overall co-simulation is application-driven. At the beginning of a co-simulation, a TCP socket between MATLAB and OMNeT++ is established so that both simulators interact each other. Both simulators maintain a time frame as the co-simulation progresses. As the application written in MATLAB runs the HCA model, when a message must be send from a given source '*src'* to destination '*dest'*, a message is sent to the OMNeT++ co-simulation scheduler containing the message '*m'* and current time '*t*'. Then, OMNeT++ progresses until a delay 'Δ' and sends back message *m* to MATLAB when it has reached the destination. As delays are experienced in the communication network, the delay Δ is specified such that MATLAB is aware of the exact reception time *(t + Δ)*. Whenever the message from the OMNeT++ is received by the MATLAB, the message is dispatched to the respective EV(s) at the RTDS. By doing so, the communication end-to-end delay is quantified and both simulators affect each other.

3.3. Test System Modeling and Characterization

As illustrated in Fig. 3.5, a LV distribution grid fed by a 10/0.4kV, 400 kVA distribution SS is taken as a test case network. It should be noted that same network is used unless specified. The test network supplies 45 detached residential houses.

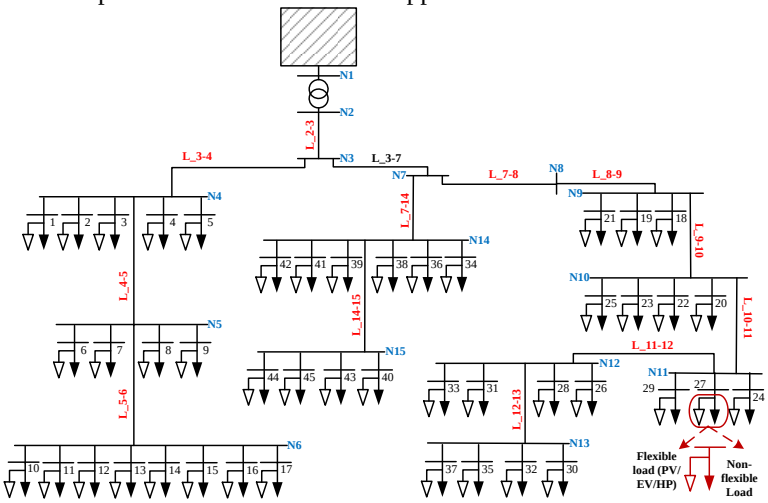

Fig. 3.5 Single line diagram of test network.

Key technical parameters of the transformer and cable are illustrated in Table 3.3 and detailed line parameters of each cable branch is depicted in Table 3.4. Since the cable lengths are relatively short, 'short-line model' has been used for modeling the cables. Due to relatively shorter length and higher cable size, the test network is

significantly strong with regards to accommodate additional load and/or generation. Therefore, minimum and maximum voltage limits in this study are taken as 0.94 and 1.04 pu respectively even though permissible voltage in Denmark is ±10%.

Table 3.3 Test network characteristics.

Equipment	Rating	Ressistance/Reactance	Type
Transformer	400 kVA	4.64/18.64 mΩ	10/0.4 kV
Main Cable	335 A	4.64/18.64 mΩ	4*150 mm2 (AL PEX)
Consumer Cable	25 A	-	4*10 mm2 CU/ 4*16 mm2 AL

Table 3.4 Line parameters of test network.

S. N.	1	2	3	4	5	6	7	8	9	10	11	12	13	14
From	N1	N2	N3	N4	N5	N3	N7	N8	N9	N10	N11	N12	N7	N14
To	N2	N3	N4	N5	N6	N7	N8	N9	N10	N11	N12	N13	N14	N15
R (Ω)	0.00464	0,0232	0,0101	0,0132	0,0180	0,0166	0,0052	0,0083	0,0072	0,0075	0,0072	0,0072	0,0095	0,0077
X (Ω)	0.01864	0,0087	0,0038	0,0050	0,0068	0,0062	0,0020	0,0031	0,0027	0,0028	0,0027	0,0027	0,0036	0,0029

Moreover, consumer loads are modeled as three phase constant power loads with a lagging PF of 0.95, unless specified. First, peak demand of every consumer is computed using Velander correlation as follows.

$$D^{P}_{\max,i} = \rho * W + q\sqrt{W} \tag{3.13}$$

where $D^{P}_{max,i}$ is the peak demand of i^{th} consumer (kW), W is the annual electricity consumption (MWh), and ρ and q are Velander coefficients which are taken as 0.29 and 2.09 respectively for this study. Those values correspond to values used by the DSO (SEAS-NVE) for planning. Fig. 3.6 illustrates a yearly variation, March 2012 through February 2013, of demand and generation in the test feeder. Demand profile of a maximum demand day over the year, Fig. 3.7a), is taken for analyzing worst case scenario from demand perspective. Similarly, generation profile of a maximum generation day Fig. 3.7b) is used for analyzing worst case scenario from generation perspectives.

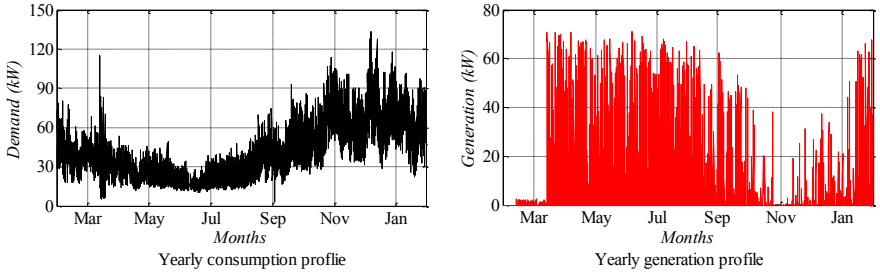

Fig. 3.6 Yearly variation of demand and generation.

It can be observed that generation is very low during maximum demand day and vice versa. Therefore, maximum demand with no generation is considered as the worst case from demand perspective and maximum generation is considered as the worst case from generation perspective.

Modeling of EVs: From the power system perspective, EVs are basically seen as electrical loads. In particular, two types of EVs, namely 11 kW, 25 kWh and 4 kW,

16 kWh, are considered for the analysis. The EVs are modeled as constant power load whose power changes dynamically over time as follows:

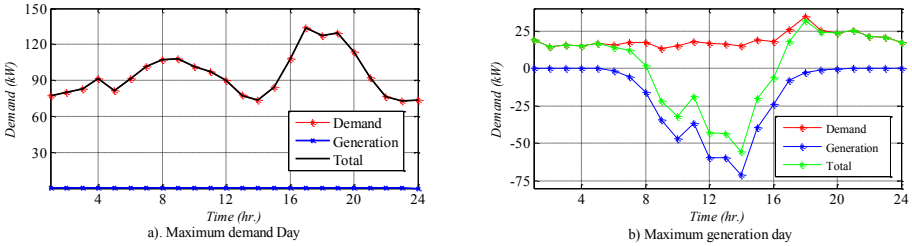

Fig. 3.7 Daily load profile for maximum and minimum demand day.

$$P_i \in \begin{cases} [0,\ P_i^{Rated}] & SOC_i < SOC_{i,max} \\ 0 & SOC_i \geq SOC_{i,max} \end{cases} \tag{3.14}$$

where P_i and P_i^{Rated} are charging power and rated power of the i^{th} EV. Demand flexibility (P_i) provided by an i^{th} EV is computed as provided the SOC of the EV stay within the predefined limits (i.e., $SOC_{i,min}<SOC_i<SOC_{i,max}$).

$$\begin{aligned} P_{i,up} &= P_i - P_{i,\min} \\ P_{i,down} &= P_{i,\max} - P_i \end{aligned}. \tag{3.15}$$

where $P_{i,up}$ and $P_{i,down}$ are the up and down regulation potentials, which depends greatly on current operating state of the EVs. Therefore, the demand flexibility of the EVs depends on their availability, namely arrival and departure time, and varies as a function of time. In this study, the EV availability data are configured based on national transportation survey of light cars in Denmark [15]. In particular, arrival and departure time of light cars and their availability in a typical working day in Denmark is illustrated in Fig. 3.8. In this study, plug-in and plug-out times for the EVs are configured as illustrated in Fig 4 of **'J1'** by considering national statistical data presented in Fig. 3.8.

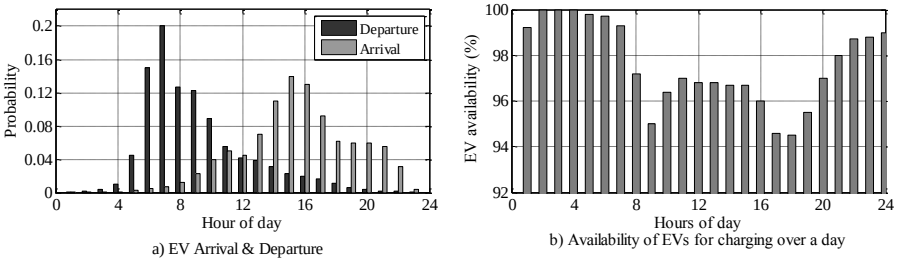

Fig. 3.8 EV arrival/departure and availability over a day.

3.4. Observations and Discussions

3.4.1. Power Performance

The performance of the HCA is investigated by means of 24 hours of power and communication co-simulation. As described in Section 3.2.1.1, the IFC of the TDRC is executed once per day, typically at the beginning of the simulation, to optimally adjust the electricity price. In particular, the IFC maximize the profit by

shifting loads from peak to off-peak periods by means of optimal price changes. Fig. 3.9a) illustrates a day-ahead electricity price before and after price adjustment using IFC. It can be observed that the original price is decreased to its maximum allowed value of -10 % during off-peak periods and vice versa. Such optimum price modification indeed incentivizes the consumers to shift their loads from peak price periods towards the lower price periods. The corresponding load adjustments with λ equals -0.1 is presented in Fig. 3.9b). Even though the load shifting due to IFC seems relatively small for the given λ, it increases significantly for higher penetration of flexible loads. Therefore, the IFC will be a potential solution to effectively regulate demand without forcing the consumers to do so.

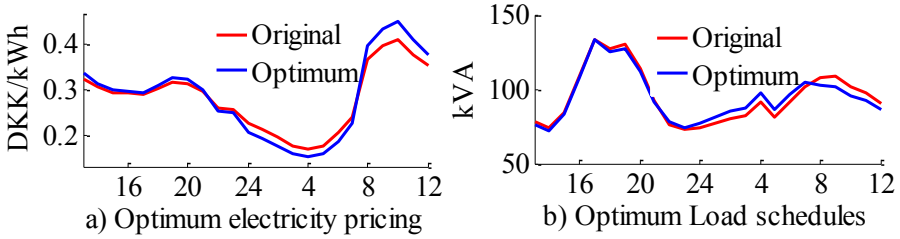

Fig. 3.9 Optimal configuration of electricity price and feeder load demand.

Since the IFC response ranges from hours to a day and includes higher uncertainties in relation to the consumer response, ISC is implemented to realize demand regulations with a smaller time resolution (from few minutes to few hours). This indeed can be used for an intra-day or intra-hour balancing purposes and is realized through an optimum operational scheduling of the flexible loads. For the presented study, the ISC is proposed to be executed periodically at every 15 minutes to update charging schedules of the EVs based on observed variations on load, electricity price, and plug in/out of the EVs in preceding slot(s). In order to demonstrate the effectiveness of the periodic optimization, electricity price from 2:00 through 3:00 is increased.

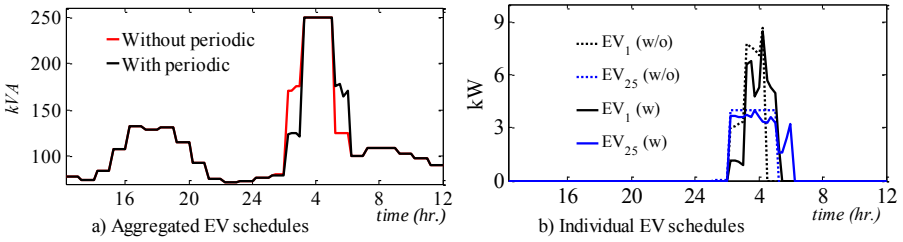

Fig. 3.10 EV charging profiles with and without periodic charging control.

Aggregated and individual (EV1 and EV25) EV charging profile with and without periodic optimization are illustrated in Fig. 3.10a) and Fig. 3.10b) respectively. It can be observed that the EV schedules without periodic optimization are insensitive to price fluctuations, but the EVs effectively adjust their charging schedules according to the observed price variations during periodic optimization. In fact, some of the EVs which were initially scheduled for charging during 2:00-

3:00 are shifted to 5:00-5:45 in response to the increased electricity prices. The ISC serves as an effective tool to adapt observed variations on day ahead schedules.

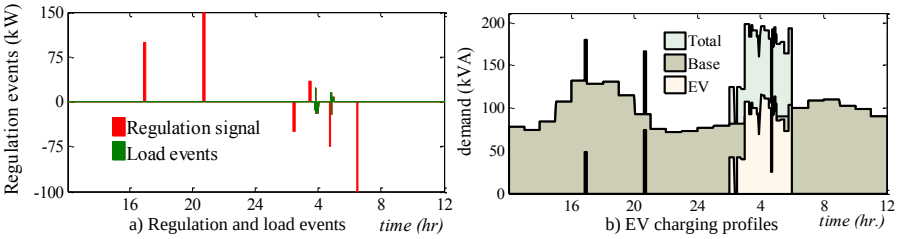

Fig. 3.11 SDRC performance with load and regulation events.

Even though the periodic optimization of the TDRC compensate observed variations in load, electricity price, plug-in/-out of EVs at every 15 minutes, it cannot achieve faster demand regulation (e.g., less than 15 minutes in this study). Since the demand has to be regulated promptly during emergency situations, the SDRC is designed to realize faster demand regulation so as to serve as an effective tool for intra-hour as well as intra-day power balancing. In particular, the SDRC realize the demand regulation by executing the DLCDRs such that the demand regulation can be realized within few seconds. To illustrate the performance of the proposed SDRC, up/down regulation events are configured as shown in Fig. 3.11a). Each event comprises demand to be regulated, regulation start time, and regulation duration. When regulation is desired, the EVs which were initially operating based on schedules from the TDRC were rescheduled to meet the desired regulation.

Modification in charging profiles of EVs due to the regulation events is illustrated in Fig. 3.11b). It can be observed that the EVs get rescheduled followed by demand regulation events such that desired regulation is achieved. The demand regulation potential of the SDRC depends greatly on current charging states of the EVs. The details on how the EV gets adjusted due to regulation events are illustrated in Fig. 3.12. Fig. 3.12a) illustrates a case when a down-regulation of 100 kW was desired at 17:00. It is observed that all the EVs were scheduled for idle (not charging) initially.

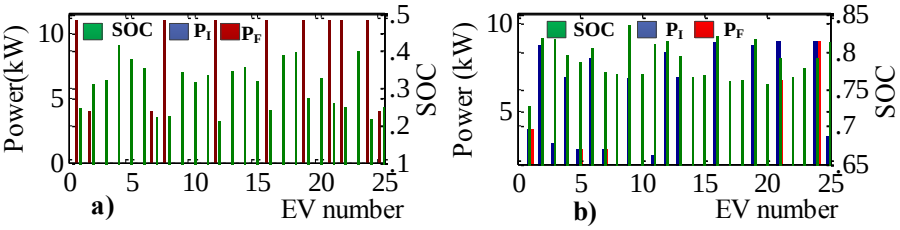

Fig. 3.12 SDRC performance in a) 100kW down & b) 75 kW up, regulations. (P_I/P_F: EV power before/after SDRC).

Following the down-regulation event of 100kW, the EVs get rescheduled in ascending order of the SOC to meet the down-regulation. Particularly, the EVs with lower SOC contribute first to meet the down-regulation. It should be noted that the number of EVs contributing to the down-regulation depends on regulation amount

as well as initial operating states of the EVs. Similarly, Fig. 3.12b) illustrates the case when an up-regulation of 75 kW was executed at 5:00. It is observed that most of the EVs which were initially scheduled for charging get adjusted to meet the desired up-regulation. In particular, the EVs contribute to the up-regulation according to descending order of the SOC, for instance, the EV having higher SOC contribute first to meet the up-regulation.

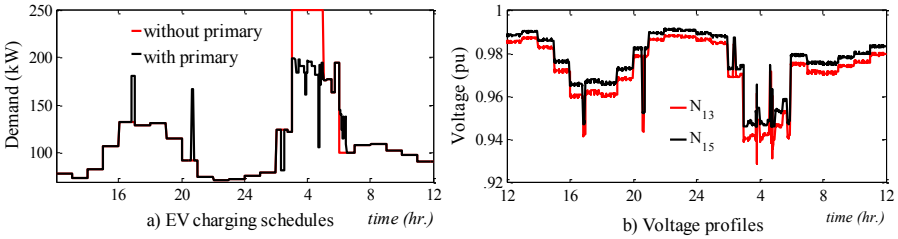

Fig. 3.13 EV charging profiles demonstrating PDRC performance.

Despite having superior performance of the periodic control capability of the TDRC and an event driven capability of the SDRC, they cannot provide real-time network support. Therefore, a droop based PDRC, as described in Section 3.2.1.3, is implemented at every EV location for real-time voltage support. In particular, the EV droop continuously monitors local voltage and automatically adjusts the EV charging once the monitored voltage deviates beyond predefined limits. Fig. 3.13 illustrates EV charging profile considering the PDRC and voltages at far end nodes (N13 and N15) respectively. It can be observed that the EV charging adapts their charging power when voltage has dropped below the acceptable limits of 0.94 pu due to load change events illustrated in Fig. 3.11a).

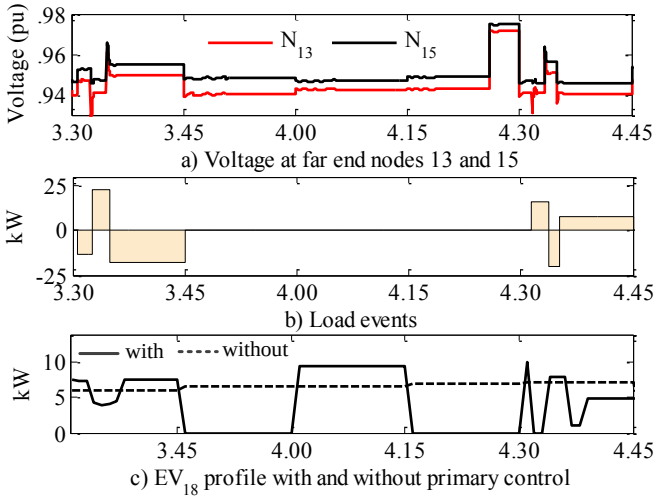

Fig. 3.14 Amplified plot to illustrate PDRC.

An amplified view of load events (Fig. 3.11a)), node voltages (Fig. 3.13b)), and charging profiles of single EV (EV_{18} connected to far end node N_{13}) are illustrated

in Fig. 3.14 to provide closer view on how the PDRC adapts to real-time load variations. It is observed that the EV droop is insensitive to a load variations (Fig. 3.14b)) unless the load change lead to violations in voltage. However, if the load variations event lead to the voltage violations, as seen from (Fig. 3.14a)), the EVs whose voltage at the POC get violated adjust their charging power to adapt to the load variations. In particular, the adaptiveness of the EV charging based on the voltage is presented in Fig. 3.14c). It can be seen that, following the voltage deviations at 3:34 and at 4:32, the EV is adjusting its charging power with an effort to bring the voltage back to limits. Thus, the primary control effectively support the network in real-time by acting on the voltage locally.

3.4.2. Communication Performance

The communication infrastructure proposed in Section 3.2.2 is implemented in OMNeT++ and the performance is demonstrated in terms of latency. In particular, delays at each stage namely primary, secondary, and tertiary are recorded for the entire simulation and the performance is evaluated in terms of average and maximum delays. The configurations of different communication technologies, namely ZigBee IEEE 802.15.4 HANs, WiMAX NAN, and dedicated fibers, are presented in terms of average distance and upstream/downstream capacity as shown in Table 3.5. Similarly, Table 3.6 shows the average and maximum delays observed at all stage levels. The stage delay is measured as the time elapsed between the first generated message and last message received in a given stage (PDRC, SDRC, or TDRC). The presented results represent the maximum and average delays of the entire 24 hours simulation. As shown, all stages meet the requirements listed in Table 3.5, even by taking the maximum stage delays.

Table 3.5 Communication configuration.

Network	Average distance	Upstream/Downstream capacity
ZigBee	50m	250 Kbps
WiMAX	10km	23.5/11.4 Mbps
Dedicated fibers	30km	1/1 Gbps

As shown in Table 3.6, the PDRC response is very prompt (approximately 10 milliseconds by considering maximum delays), thereby facilitates the DRRs to be effective for real-time voltage support. Similarly, the maximum delay of approximately 250 milliseconds in the SDRC shows that the SDRC can be effectively implemented to realize faster demand regulation particularly for emergency up/down-regulations. Similarly, the observed delay in TDRC is low enough to be implemented for tertiary frequency regulations as well as for other grid applications such as peak shaving, load shifting etc. due to time requirement for dispatching the optimal EV charging schedules and electricity prices from the CA to every consumer. It is observed that the delay in SDRC is higher than that of the PDRC and TDRC. In particular, the higher delays in the SDRC are observed as SDRC execution desire round trip communication between the CA and consumer.

Table 3.6 Communication performance in terms of stage delay.

Metric	Average delay (sec.)	Maximum delay /sec.)
PDRC	0.008923	0.010088
SDRC	0.2271	0.2313
TDRC	0.0389	0.0413

For instance, to execute the SDRC, the CA has to fetch the status of individual EVs, make the decision followed by receipt of the status from them, and dispatch the final schedules to the candidate EVs again. Nevertheless, the delay is reasonably lower to be implemented for secondary frequency regulations and for other emergency regulation requirements. Therefore, it can be seen that the proposed communication infrastructure and control strategies perform effectively to deploy various DR categories as well as to establish coordination among their response as intended for the HCA implementation.

3.5. Chapter Summary

A key idea of the DR is to make temporary load adjustment by reducing or rescheduling electricity consumption pattern of the consumers. Indeed, simultaneous deployment of multiple DRs is desired to deploy the flexibility for maximal network support. Therefore, a HCA is developed as a platform to establish coordinated control among simultaneously existing DRs in this study. Different control strategies, ranging from a day ahead to real-time, are executed by the HCA to maximize the grid support from the DRRs. The HCA ensures a time-graded coordination among available DRs such that actions of each DR category provides time-delayed backup to each other. In particular, the coordination among the DR categories is established by using three DR control loops, namely primary, secondary, and tertiary. As response time increases from inner primary loop towards the outer tertiary, each inner loop backup the outer loop by executing controls in shorter time resolutions. Moreover, every outer loop provides a time delayed back-up to the inner loop such that any deviation in the operation from the scheduled value is compensated using periodic control capability of the outer loops in the succeeding slots.

To investigate the proposed HCA in a multidisciplinary manner, power and communication co-simulation has been performed. In particular, the performance of the proposed HCA is demonstrated through power simulation performed in RTDS and the communication simulation performed in OMNeT++. Interface between the OMNeT++ and RTDS is ensured through MATLAB. The co-simulation results demonstrated that the HCA effectively coordinates simultaneously existing DRs, thereby facilitating maximum utilization of the DR potential. Moreover, the proposed communication infrastructure based on ZigBee, WiMAX, and dedicated fiber facilitates the HCA to operate as desired.

The HCA demonstrates an effective framework to exploit various DR programs for supporting network. In particular, the TDRC, which is deployed to execute PDRs and DDDRs, is used for day ahead operational planning. By using the periodicity of the TDRC, any intra-day power imbalances can be addressed. Further, any emergency demand regulation need is taken care of by the SDRC by

executing DLCDRs. As the SDRC response varies from few seconds to few minutes, the SDRC can be used as spinning reserve for intra-hour/-day balancing. Moreover, the PDRC acts to support the network in real-time by adjusting the consumption once the monitored network parameters deviates beyond limits. Therefore, the PDRC serve as an effective resource to support the network locally by acting to voltage. As such, the coordinated operation of three loops maximizes not only the network support capability of the DRRs but also the financial benefits to the consumers.

Detailed control strategies to manage constraint violations in the LV network are presented in the following chapter presents. Furthermore, further investigation on strategies to exploit demand flexibility from active loads, namely EVs and HPs, are presented in the following chapter such that the developed strategies fit to HCA framework presented in this chapter.

Chapter 4. Development of DR Control Strategies

*This chapter presents device specific DR control strategies designed for exploiting demand flexibility from various residential loads. In particular, the chapter contains a summary of DR control strategies documented in the publications **J2, C2**, **C3**, **C4**, and **C5,** and presents detailed on their effectiveness.*

4.1. Introduction

As mentioned in the preceding chapter, control strategies to exploit demand flexibility are contingent to load characteristics and operational behaviors of the consumers. For instance, the control strategies for HP may differ significantly compared to the one for EV due to difference in the nature of their operation. In addition, the DR control strategies also depend on applications. For instance, application of demand flexibility for real-time network support such as real-time voltage support desires control latency of fraction of seconds, whereas, for applications such as peak shaving, load shifting, congestion managements etc., control strategies with latencies of few minutes to few hours may be enough. To this end, control strategies are designed per load type and applications.

First, a DR control strategy is developed for management of constraint violations in SG. In particular, a combination of centralized and decentralized control scheme is implemented to exploit demand flexibility of the consumer to maintain voltage and current constraints within limits. Next, a voltage based dynamic DR, whereby the demand regulation is realized by regulating supply voltage at the SS level is presented. Load type specific DR control strategies are then presented considering EV and HP as potential flexible loads. In particular, the DR control strategies are designed to *i) address anticipated issues due to high penetration of flexible loads (EVs and HPs) and ii) exploit the demand flexibility from them for various network supports, such as real-time voltage support and congestion management etc*. Finally, a simple and effective approach to increase demand responsiveness of the consumers in a residential distribution system is presented. A brief summary of the control strategies presented in **J2, C2**, **C3**, **C4**, and **C5**, are described chronologically as follows:

4.2. Constraints Violations Management

This section presents a summary of control strategies developed for constraint violation management in LV distribution grids, which is documented in detail in **J2**. In particular, a combined centralized and decentralized control is implemented to exploit flexible demand of consumers to keep the grid constraints within limits. The details of the proposed methods and observed outcomes are presented as follows:

4.2.1. Proposed Methodology

The proposed active load control strategy to manage constraint violations in LV distribution grids is realized in two steps, namely a proactive centralized and a reactive decentralized control. The former is used to manage constraints violations (voltage and current) in a proactive way considering estimated operational scenarios while the latter is used to react to the observed voltage violations in real time. The key idea of implementing the combined centralized-decentralized control scheme is to deploy better controllability and network visibility of the centralized control together with prompt response capability of the decentralized control.

The centralized control operates every hour and is responsible for managing an hour ahead load distribution so as to relieve any upcoming grid limit violations. Thus, the controller utilizes expected load consumption at every node. Particularly, given the consumers' forecasted load, a load flow calculation is conducted to identify any current and/or voltage problems. If any violation exists, optimization is performed to compute minimum amount of flexibility to be deployed to alleviate the grid violation. The outcome of this optimization, which is flexibility offer requests to consumers, is then dispatched to the consumers. The detailed mathematical formulation of the centralized control is included in Section II of **J2**.

It is worth mentioning that consumers located at weak spots in the network have higher impacts in resolving the grid constraints. Therefore, minimization of total flexibility to be activated for resolving given grid constraints always utilizes flexibility from the consumers connected at the weak spot, which is not fair especially from consumer's perspective. Therefore, to ensure a fair utilization of flexibility from every consumer, their optimization coefficients are computed utilizing the history of flexibility utilization. This gives higher coefficient for the consumer whose flexibility is used more and vice versa and hence ensures fairness in terms of flexibility activation from different consumers.

Since the centralized control is executed periodically to exploit the average hourly flexibility, it does not facilitate intra-hour controllability. As such, any intra-hour power volatility stemming from forecast errors or load variations might lead to network violations during actual operation. Therefore, a decentralized control is implemented to provide real-time voltage support by adapting the observed variations. The decentralized control, which is designed as a linear P-V droop, is implemented at every consumer so as to execute control actions once the monitored voltage deviates beyond the predefined limits. The details of the decentralized control are presented in Section III of **J2**.

One of the potential challenges in designing the droop for the decentralized control is to enable every consumer to participate to support voltage. As the voltage is local problem, constant droop setting forces the consumers at the weak spot, normally the farthest end node, to use its flexibility at every voltage violations. To ensure fair participation of every consumer, droop parameters are set differently for the consumers connected at different nodes. In particular, higher threshold voltage (the voltage beyond which the droop start operation) and minimum voltage (beyond which the droop uses full flexibility) are set for the nodes closer to SS. The procedure of the aforementioned voltage assignment is detailed in Section III in **J2**.

Exploiting the capability of the proposed control scheme, the centralized control can additionally be used to trade flexibility in balancing market while the decentralized control can be used to trade flexibility in the regulating market.

4.2.2. Observations and Discussions

To demonstrate the performance of the proposed method, a LV distribution grid as shown in Fig. 2 in **J2** is used. To create violations in the grid, the consumption of each consumer is increased. Moreover, the flexibility limits of each consumer are set to 20% of the load. This might be a somewhat big number for contemporary grids, but might be more rational in the near future, when flexible device penetration will increase. The details of the test network and data used for simulation are presented in Section IV.A in **J2**.

Simulation results of the centralized control from the 22nd to the 31st of January are displayed in Fig. 4.1. In this figure, blue corresponds to the grid behavior without control whereas green refers to results obtained after applying the centralized control. Judging from Fig. 4.1a), it is apparent that the grid is heavily loaded, that is to say voltages up to 0.93 pu are recorded. By implementing the centralized control scheme, this threshold was respected most of the times. Nevertheless, there were some incidences where the available flexibility did not suffice to sustain the voltage at 0.95 pu, i.e., the voltage limit experienced relaxation. This is depicted by the gray spikes which can be observed in the green area. Similarly, Fig. 4.1b) illustrates the recorded overloading before control. In all occasions the relevant current problem is resolved using the centralized control. Then, Fig. 4.1c) depicts the total load at the transformer connection before and after implementing the control. In this figure, it is evident that the proposed framework resulted in peak shaving. Finally, the total available (blue) versus the total activated (green) flexibility is presented in Fig. 4.1d). As can be seen, only a percentage of the available flexibility is employed to solve most grid issues, except for some instances when voltage relaxation is needed.

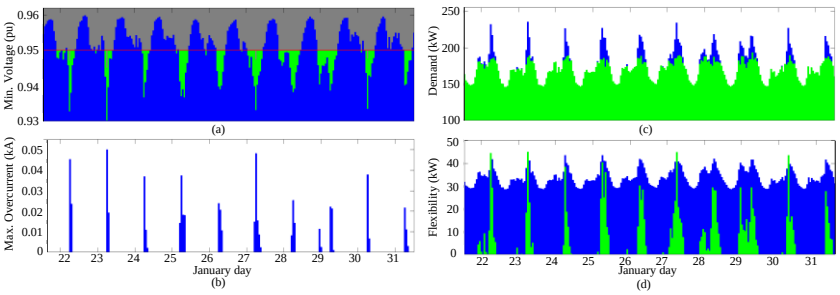

Fig. 4.1 Sample results. a) Minimum voltage at the feeder, b) Maximum overcurrent recorded at the feeder, c) Transformer load, and d) Available versus activated flexibility

As described in the preceding section, different weights are assigned to different consumers, using the procedure described in Section II in **J2**, to alleviate those violations in a fair way. To exhibit this feature, a problematic time, namely 8 p.m. January 28th, was chosen and the problem was repetitively resolved by the centralized control for different weights i.e. 0.1, 0.4, and 0.9. Since the weight

emulates a "forgetting" factor in exponential smoothing procedures, the simulation is performed with moderate weight, (0.4) to keep reasonable history of flexibility used by the consumer. The impacts of different weights in the fairness realization are depicted in Fig. 4 of **J2** and their significance is described in Section IV of **J2**.

To demonstrate the performance of the decentralized control, a 48 hour time-sweep simulation (28^{th} to 30^{th} January) is performed for three different cases. The first case is used to demonstrate the performance of the decentralized control in the perfect system where forecasting error and load variations are absent. In this case, the voltages throughout the network remain within the limit even without using the decentralized control as there are no load variations in the loads after the centralized control is executed. As shown in Fig. 6 of **J2**, the decentralized control utilizes flexibility at certain time slots and increases the voltage, even though there are no violations. The extra flexibility utilized by the decentralized control provides a safe operational margin to compensate any unexpected real-time variations of the load.

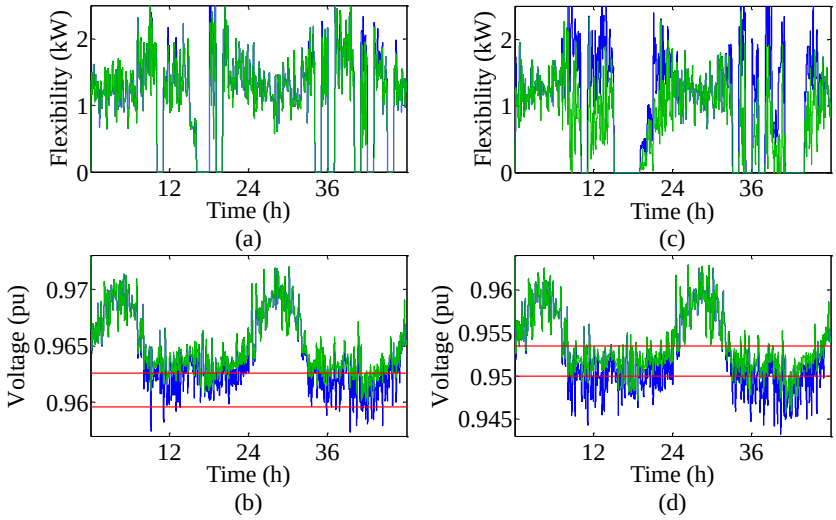

Fig. 4.2 Simulation results with (green) and without (blue) control a) Flexibility of consumer 14, b) Voltage at N14, c) Flexibility of consumer 26, and d) Voltage at N26.

The second case is used to demonstrate the performance of the decentralized control when random variations in load are present. In particular, random noise of ±20% is created to emulate the load variations. It is observed from Fig. 4.2 that the random noise leads to voltage violations if no control is implemented. However, when decentralized control is implemented, every consumer provides their flexibility based on availability to improve the voltage quality. It is observed that the voltage is improved significantly compared to the case without control. In particular, consumer 26 uses a significant amount of flexibility in an effort to support the voltage. Nevertheless, as illustrated in Fig. 4.2a) and Fig. 4.2b), upstream consumers also contributes towards voltage support. The contribution of upstream consumers to voltage support is clearly seen by the increase in voltage of consumer 26 when having no available flexibility. It should be noted that if the

voltage deviations are very large, the decentralized control improves the voltage with its available flexibility, but may not be able to fully solve the problem. This fact is depicted by small deviations of voltage at node 26 even using the control.

Finally, the last case is used to demonstrate impacts of voltage thresholds to the performance of the droop. Particularly, low, medium, and high values of voltage threshold are investigated. As observed in Fig. 8 of **J2**, high threshold voltage forces the consumer to use higher flexibility despite the voltage is above the limit. However, activating a lot of flexibility when not needed is undesirable. On the contrary, low threshold settings activate a very low amount of flexibility, thus restricts the use of extra flexibility when not needed. To avoid excess or limited activation of available flexibility, the aforementioned cases were studied with moderate threshold voltage. Thus, the combined centralized and decentralized control scheme is an effective way to manage grid violations. In addition, the proposed method can be used for trading flexibility in hourly balancing market through the centralized and in regulating market through the decentralized control.

4.3. Voltage Controlled Dynamic DR

The key idea of VCDR is based on the fact that power consumption of an electrical load is a function of operating voltage. As a result, demand of the load can be regulated to some extent by regulating the operating voltage. Since the degree of voltage dependency is contingent on load type (e.g., constant current, constant power, constant impedance, hereafter called ZIP), this study realizes demand regulation by exploiting the voltage dependencies of the loads. The effectiveness of the proposed method is investigated for various proportions of load types. The proposed methodology and outcomes, summarized on the basis of publication **C2,** are described in the following:

4.3.1. Proposed Methodology

The implementation of VCDR is accomplished in three stages. First, an adaptive model is developed to determine voltage dependency of the feeder level aggregated load. This is the foremost important step as demand regulation potential depends greatly on the voltage dependency of the loads. In particular, an adaptive voltage dependency computation method is implemented to compute near real-time voltage dependency of the load. Following the voltage dependency computation, the required voltage setting at MV/LV substation is computed to realize desired demand regulation by using the voltage dependency of the load computed in the first stage. Finally, a new voltage estimation technique, whereby the voltage estimate of nodes is updated with periodic measurement data, is implemented to ensure that node voltages are within acceptable limits following the realization of the proposed control methodology. The details of the mathematical formulation of each stage are described in Section II of **C2** and the details about the implementation of the proposed VCDR are illustrated in Fig. 2 of **C2**.

4.3.2. Observations and Discussions

The implementation of VCDR is accomplished in three stages. First, an adaptive model is developed to determine composite voltage dependency of the feeder level

aggregated load. This is the foremost important step as demand regulation potential depends greatly on the voltage dependency of the loads. In particular, an adaptive voltage dependency computation method is implemented to compute near real-time voltage dependency of the load. Following the voltage dependency computation, the required voltage setting at MV/LV SS is computed to realize desired demand regulation by using the voltage dependency of the load computed in the first stage. Finally, a new voltage estimation technique, whereby the voltage estimate of nodes is updated with periodic measurement data, is implemented to ensure that node voltages are within acceptable limits following the realization of the proposed control methodology. The details of the mathematical formulation of each stage are described in Section II of the **C2** and the details about the implementation of the proposed VCDR are illustrated in Fig. 2 of the **C2**.

The performance of the proposed method is investigated through simulation studies performed for different compositions of ZIP loads as shown in Table II of the **C2**. Particularly, four different cases as illustrated in Table 4.1 are presented to demonstrate the effectiveness of the proposed method.

Table 4.1 Configuration of demand dispatch signals.

Dispatch Time (min)	Dispatched Demand (kVA)			
	Case I	Case II	Case III	Case IV
60	133	150	160	190
120	144	144	175	200
180	125	125	185	180

In order to demonstrate the performance of the proposed method, each case is configured with different demand dispatch signals as illustrated in Table 4.1. Fig. 4.3 illustrates the demand regulation in case I and case II. It is observed that when a demand dispatch signal of 133 kVA is dispatched from an aggregator at 60 min., the proposed method regulate the SS voltage by exploiting real-time voltage dependency of the loads as per the technique described in Section II of **C2** so as to decrease the aggregated demand from 135 to 133 kVA. Similarly, following the DD signal of 144 kVA at 120 min., the model determines the corresponding voltage to increase the demand to 144 kVA. Nevertheless, with the dispatched demand of 125 kVA at 180 min., the estimated voltage at the farthest end node violates V_{min}. Therefore, the model fixes the voltage at the limit violating node to V_{min} (0.9 pu) and back estimate the SS voltage according to the method presented in Section II of the **C2**. In this case, even though the dispatched demand is 125 kVA, a demand regulation of 131 kVA is realized. For the given load compositions and voltage limits, approximately 5.88% and 3.68% of up and down regulation can be realized.

The demand regulation potential increases significantly when the percentage of constant impedance load increases. Fig. 4.3c) and Fig. 4.3d) illustrate results of case II, where the percentage of constant impedance loads is increased as shown in Table 4.1. It is demonstrated that total demand regulation potential has increased from 9.5% in Case I to 14.82% in Case II. Similar to Case I, the dispatched demand cannot be met fully when a DD signal of 150 kVA is dispatched at 60 min., therefore the minimum voltage limits are violated at consumer POC. Similarly, *Case III* and *Case IV* represent cases with same load proportions as case II but with

increased demand. Indeed, those cases have been analyzed to access impact of load growth due to increased penetration of new loads, such as EV and HP, on the demand regulation potential. For the same load composition, increased demand results in decreased demand regulation potential. Fig 7 and Fig. 8 in **C2** illustrates regulation potential of the proposed algorithm in case III and case IV respectively. In fact, the total regulation potential has decreased to 11.31% for 25% increase in loads and to 10.59% for the case of 40% increase in loads.

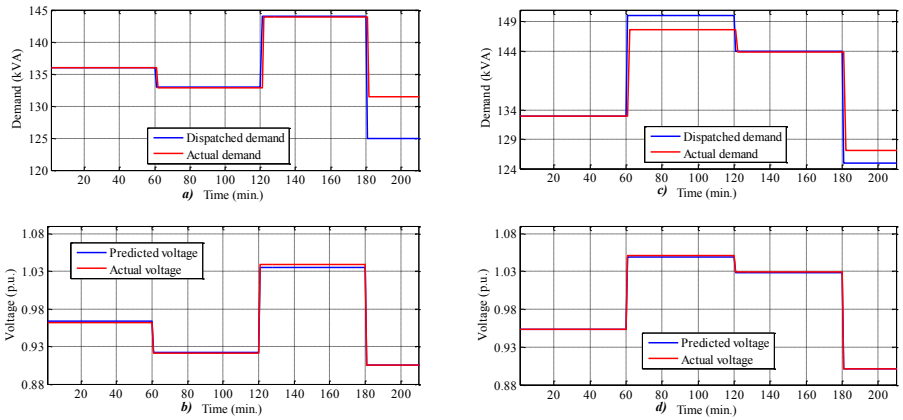

Fig. 4.3 Demand regulation potential. a) Case I and b) Case II.

Demand regulation potential for various study cases subjected to ±10% voltage variations are summarized in Fig. 4.4. It can be observed that the demand regulation potential increase significantly for the higher share of constant impedance loads. In addition, the regulation potential is a function of initial loading condition and allowable voltage variations. The higher the network loading, the lower the regulation potential is, whereas, the higher the allowable voltage variations, the higher the demand regulation potential. Unlike existing DR techniques which has greater uncertainty in consumer responsiveness, the proposed method exploits significant demand regulation without noticeable effect to the consumers.

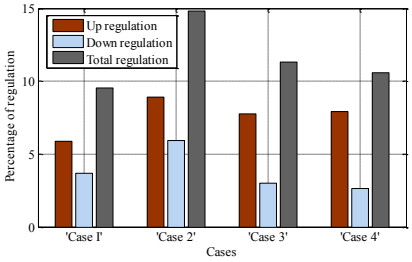

Fig. 4.4 Total demand regulation potential for various cases.

Moreover, the proposed method results in very low energy recovery effect after its deployment, which is often not the case with the existing DR techniques. Furthermore, the proposed algorithm can easily be implemented to any feeder provided real time measurement and on-load voltage control facility are available at

its SS. Moreover, the VCDR potential can be used for system level balancing as well as for local network support, such as peak reduction, congestion management etc. More importantly, the VCDR can effectively be used in combination with other DR techniques, thereby acting as back up resource to existing DR techniques.

4.4. DR Control Strategies for EVs

Due to sizable rating provided with storage capability, EVs can provide a significant amount of flexibility in future intelligent grids provided proper EV charging control strategies are developed. A summary of the proposed methodology and observed outcomes presented in **C3** are described in the following.

4.4.1. Proposed Methodology

A two-stage EV charging algorithm, namely local adaptive control encompassed by a central coordinative control, is proposed in this study to exploit the flexibility offered by the EV. In particular, the central coordinative charging prepares optimum EV charging schedules and the local adaptive control adaptively adjusts the EV charging in real-time according to monitored voltage. As such, the optimal EV charging scheduling is a centralized control stage, whereby an aggregator develops the charging schedule for every EV considering both technical as well as economic aspects. As EV owners want to minimize the EV charging cost and aggregator also tries to maximize its profit, the primary goal of the centralized stage is to minimize total EV charging cost. Technical requirements are considered by imposing constraints in the optimization. The EV schedules satisfying both voltage and thermal limits are finally dispatched to every EV.

In the second stage, a local adaptive EV control is implemented at every EV location to make real-time adjustment of EV charging power according to the consumer requirements and local network condition, namely voltage. Particularly, a simplified ON-OFF control is implemented to act over voltage in real-time. To avoid voltage oscillation resulting from frequent switching ON/OFF of the EVs, the EVs which are once turned off by the local controller are kept OFF until the next slot. This provides a simple but effective approach to avoid straining the EV battery as well as voltage oscillation due to frequent switching. Any deviations in the EV charging resulting from the local control are taken care of during updating EV schedules at the next slot. The centralized scheduling and local adaptive control work in coordination as illustrated in Fig. 3 of the **C3** to exploit the demand flexibility from the EV. The detailed formulation of the centralized and local adaptive control as well as their coordination is described in Section III of the **C3**.

4.4.2. Observations and Discussions

The effectiveness of the proposed algorithm is demonstrated through time sweep simulations for two different EV penetration scenarios. **Scenario I** is configured to investigate moderate EV penetration which is taken as 33% EV on top of feeder base loading. Fig. 4.5 illustrates electricity price and corresponding charging schedules of EVs for normal and deviated day ahead electricity price cases. The electricity prices at certain hours, particularly 18:00, 22:00, and 3:00, as shown in Fig. 4.5b) are adjusted to investigate adaptiveness of the proposed method. It is observed from Fig. 4.5a) that the EV scheduling is primarily influenced by

electricity price since most of the EVs have charged at lower price hours. Charging of some of the EVs even during high price periods (15:00 through 21:00is due to EV owner's travelling requirement, such as emergency charging whereby the EV should be charged anyway irrespective of the network and electricity price. Moreover, following the price deviations, the proposed periodic scheduling algorithm adapts to the adjusted electricity price for scheduling for downstream slots. In particular, the EV charging schedules are shifted to up/down stream slots depending on positive or negative price deviation. Note that voltage limits were not violated in this scenario due to relatively lower penetration of EVs.

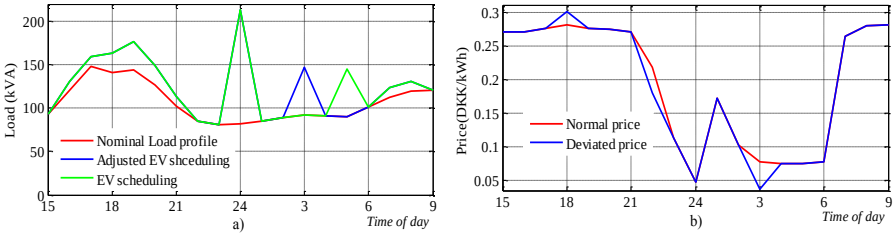

Fig. 4.5 EV scheduling in scenario-I a) EV charging profiles and b) Electricity prices.

Scenario II is configured to emulate high EV penetration in a heavily loaded feeder, which is realized by increasing the feeder base load by 50% and EV penetration to 66%. Electricity price and corresponding EV charging profiles in scenarios II are illustrated in Fig. 4.6a). In order to demonstrate adaptiveness of the proposed algorithm, the electricity price has been changes as shown in Fig. 4.6b) and feeder load has increased (shown by dotted red line in Fig. 4.6a).

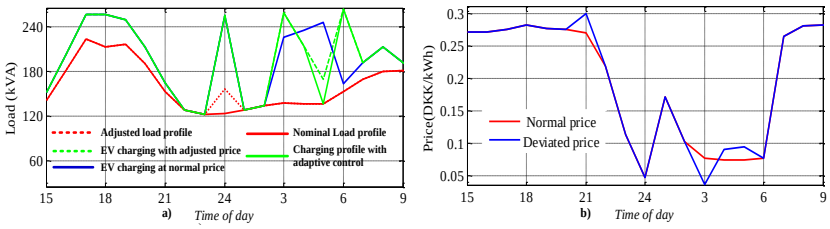

Fig. 4.6 EV schedules in scenario II a) EV charging profiles and b) Electricity prices.

It can be observed that the EV schedules adapts to the variation in electricity price as well as load. In particular, increase in load at 24:00 causes to decrease number of EV charging at that period. Further, decrease in electricity prices in upstream slots has shifted the EV charging to earlier slots. Charging of some of the EVs during high price periods is due to travel requirements of the EV owners.

Regardless of the adaptiveness to electricity price and/or load, the EV charging is subjected to real-time adjustment with network voltage. In particular, voltage based local adaptive control make real-time adjustment of EV charging when monitored voltage deviates beyond pre-defined limit. It can be seen from Fig. 4.7 that network voltage gets violated due to sudden increment in load (seen at hour 24 in Fig. 4.6a)). In response, some of the EVs whose voltage at POC was violated

adjust their charging power to bring the voltage back to the limit. In fact, two EVs whose voltage at the POC got violated were disconnected to support the voltage.

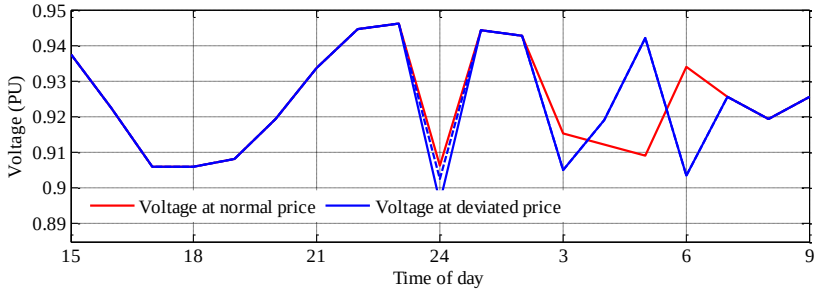

Fig. 4.7 Terminal voltage at farthest node (N13) for various cases.

The charging power profiles and SOC of a particular EV connected to farthest end node N13 are illustrated in Fig. 4.8. It can be observed that the voltage violation at hour 24 causes the EV to reduce its charging power to zero. The deviation in charging power resulted from the adaptive control is corrected by the centralized scheduling at the next time slot and thus schedule EV for charging at later time slots, mainly at 3:00. As such, any deviation resulting from the local adaptive control gets compensated by updating the EV schedules. In particular, the centralized scheduling periodically updates EV schedules at the beginning of each slot accounting for the observed variations in price and load.

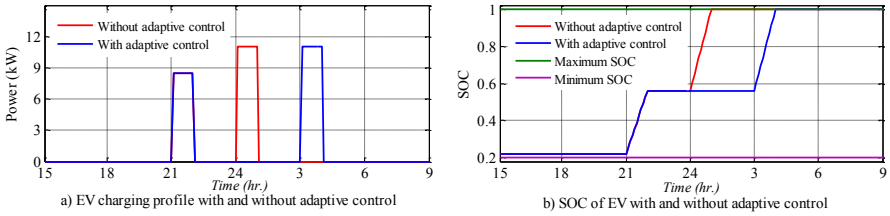

Fig. 4.8 Adaptive update of charging profile based on monitored voltage.

The proposed two-stage EV control is a simple and effective approach not only to support the network to accommodate increased EV penetration but also to support the network in various ways, such as real-time voltage regulation, congestion management etc. Moreover, the proposed method provides economic benefits to the participating consumers by reducing their EV charging cost.

4.5. DR Control Strategy for HP

Being a sizable load provided with thermal storage capability, HP is considered as a potential DR resource. A summary of the proposed methodology, HP modeling, and observed outcomes presented in **C4** are described in this section.

4.5.1. Proposed Methodology

Similar to the EV control strategies described in the preceding section, the exploitation of demand flexibility from HPs is also realized in two stages, namely centralized coordinative control and local adaptive control. This is done to keep the

control framework common for exploiting flexibility from different load types. However, it should be noted that control strategy at each stage varies significantly based on load types. In particular, the central coordinative control is adopted by an aggregator and determines optimum operational schedules for the HPs on the basis of electricity prices, consumer heating demands, and feeder demands. The primary objective of the central coordinative control is to achieve an economic objective with simultaneous consideration of network technical constraints. The central coordinative control then dispatches the final operational schedules for the HPs. In order to respect inherent ON-OFF control nature of the HP, a binary integer programming based optimization is implemented. The detailed formulation of the centralized control is presented in Section IV of the **C4**.

A LAC is integrated into each HP unit to ensure consumer comfort as well as to provide real-time network support. As long as the monitored voltage and SOE are within limits, the LAC follows the operating schedules from the central controller. However, when violations of voltage or SOE limits occur, the LAC executes predefined control, namely (4.1) for the SOE violations and (4.2) for the voltage deviations. Unlike in the case of EV, the LAC is realized for not only POC voltage but also SOE limits violations such that consumer's thermal demand is always fulfilled regardless of the network condition.

$$HP = \begin{cases} ON & SOE_i \le SOE_{\min} \\ OFF & SOE_i \ge SOE_{\max} \end{cases} \tag{4.1}$$

$$\begin{aligned} V_i \le 0.92\ p.u \quad & HP = OFF \\ V_i > 0.92\ p.u \quad & No\ Action \end{aligned} \tag{4.2}$$

Since both the controls are running in successions, any deviation in operational schedules resulting in due to LAC is compensated by the central controller periodic scheduling feature. The coordination procedure for the central coordinative control and LCA is described in Fig. 2 and Fig. 3 in **C4**. In addition, details of the modeling of HP and network are presented in Section II of **C4**.

4.5.2. Observations and Discussions

The effectiveness of the proposed HP control strategies are investigated considering 80% HP penetration (i.e., 80% of the consumer have HPs). The location of HPs in the network is assigned randomly to reflect a more realistic scenario. Further, HP rating is taken as 3.1 kW and equal proportions of two tank capacities (300 and 500 liters) are considered. As described in Section 4.5.1, optimum HP schedules are first prepared on the basis of electricity prices, feeder loading, and consumer comforts. Further, to investigate adaptiveness of the proposed method, electricity price has been changed at some hours as shown in Fig. 4.9b). Aggregated HP operating schedule for normal as well as deviated electricity price is illustrated in Fig. 4.9a). It is observed that HP schedules are adjusted to adapt to the changes in electricity prices. It is observed that increase in electricity price at 2:00 decreases the HP power at that time slot and shifts towards low price downstream slots at 5:00 and vice versa. Hence, depending on positive or negative price deviation, the charging schedule is advanced or delayed. Small amount of

scheduled HP power even at high price periods are due to the deviations imposed by consumer comfort, namely SOE and local voltage.

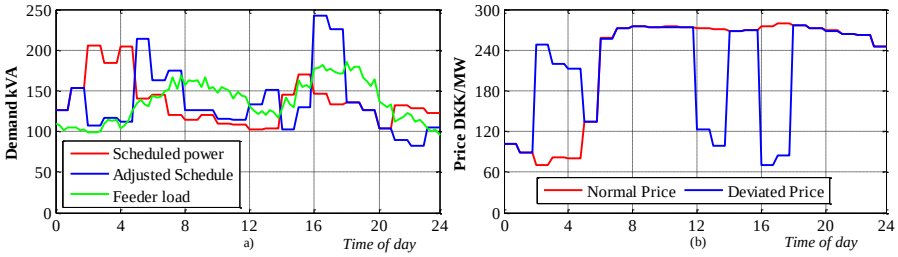

Fig. 4.9 a) HP scheduling with load and price variation, b) Normal and deviated price.

In addition, HP operation is subjected to real time adjustment based on voltage at POC and SOE in the tank. When voltage at POC of a HP drops below specified limit (taken as 0.92 pu), the LAC disconnects the HP as an effort to bring voltage back to the acceptable limit. Fig. 4.10a) illustrates HP operation profiles with and without LAC operation and Fig. 4.10b) illustrates the corresponding voltage at the farthest node (N_{13}) in the feeder. In particular, violation of voltage at 5:00, as shown in Fig. 4.10b), results in disconnection of 5 HPs to bring the voltage back to the acceptable limit. The disconnection of the HPs reduces power at 5:00 and shifts that power to later lower price slots. Similarly, violation of voltage at 16:00 results in disconnection of several HPs whose voltage got violated.

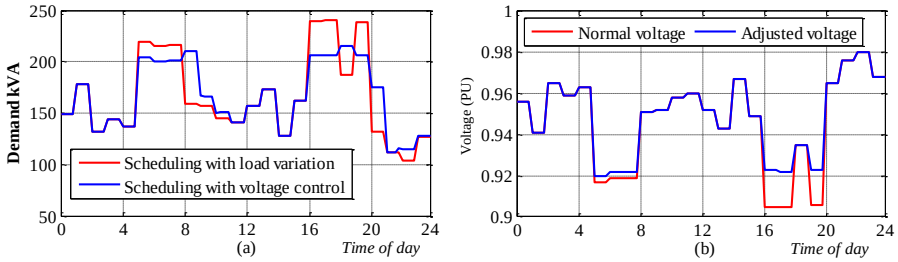

Fig. 4.10 a) Impact of voltage on HP schedules and b) Variation of terminal voltage (N_{13})

The variation of operational profiles of a single HP is illustrated in Fig. 4.11. It is clearly observed from Fig. 4.11a) and Fig. 4.11b) that the HP operational schedules have changed during 5:00-8:00 and 16:00-20:00 due to violations of terminal voltage. Particularly, the HP is turned OFF several times during the voltage violation periods to respond to the voltage violations. The actual turning off period is constrained due to the minimum and maximum SOE limits (illustrated in Fig. 4.11c) and thermal demand of the house (Fig. 4.11d)). The observed deviations on operational profiles due to LAC are compensated while updating the schedules by the central controller at next time-slot.

The proposed two-level control algorithm effectively exploits demand flexibility from HPs for supporting the grid in several ways. In particular, the central scheduling supports the network for congestion management, peak-shaving etc. by optimally scheduling the HPs, whereas the LAC provides a real-time voltage

support to the network. Therefore, the combination of the two controls helps to realize both economic as well as technical objectives. Moreover, simulation results demonstrated that any variations in electricity price, loads etc., are adapted by running two controls in successions.

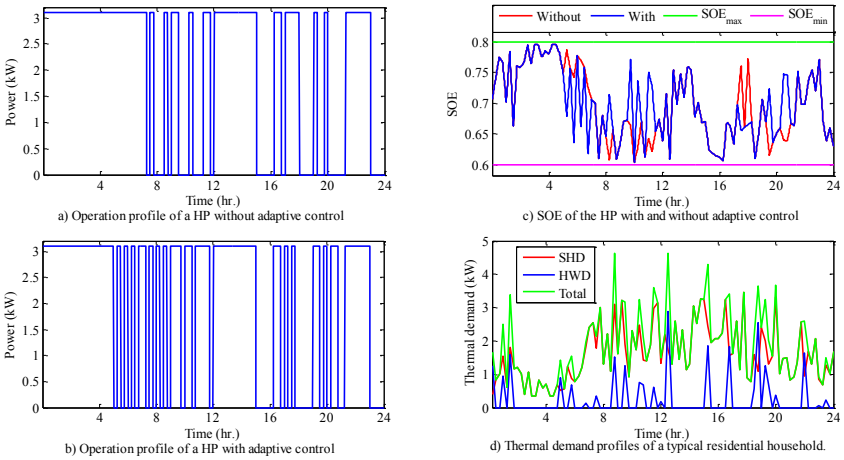

Fig. 4.11 Adaptive control of a single HP connected at Node 13.

4.6. Increasing Demand Responsiveness

Lack of active consumer participation to DR program is becoming one of the potential barriers for DR deployment, particularly at residential consumer level. A novel algorithm which works on the basis of optimal pricing adjustment is developed in this study to increase consumers' demand responsiveness. The effectiveness of the suggested method is investigated for a high EV penetration case in the test network.

4.6.1. Proposed Methodology

The proposed method is realized in two stages, namely optimal price adjustment to increase demand responsiveness and optimal EV charging. In the first stage, a day ahead electricity price is optimally adjusted using demand price elasticity of the consumers. It is assumed that the aggregator, who is responsible for DR control and management, has the right to optimally adjust the price before dispatching to the consumers. The key idea of the proposed technique is to incentivize consumers to create intended load shifts by offering lower electricity prices during off-peak or non-critical periods. This is realized by creating price differences between peak and off-peak hours. In fact, hours 18:00-21:00 are taken as peak period and hours 1:00-4:00 are taken as off-peak period. The details of the formulations of this study are presented in Section II in **C5**.

In the second stage, optimal EV scheduling is integrated with the optimal electricity pricing to investigate a deep insight into the functionality of the proposed method. In particular, the optimally adjusted electricity price is used for making optimum EV schedules. The optimal EV scheduling is designed not only to support network for congestion management but also to exploit EV flexibility for peak

shaving and valley fillings. Since EV owners normally want to have minimum electricity bill, the proposed method is formulated as a minimization problem which minimizes total EV charging cost. The details of the optimal EV charging formulation are presented in Section III of **C5**.

The integration of optimal pricing and optimal EV scheduling is realized per procedure presented in Fig. 6 of **C5**. First, day-ahead electricity prices are optimally adjusted using the procedure presented in Section 4.6.1. The new price sets are then dispatched to every consumer to allow them to shift their loads in response to the price changes. Since EVs are fully flexible loads, optimum scheduling is proposed in this study to realize desired load shift.

4.6.2. Observations and Discussions

The performance of the proposed method is demonstrated through a 24 hour time-simulation considering average electricity price of a week in February 2014. Modified electricity price sets when different price modification percentages are allowed are illustrated in Fig. 4.12. It is observed that price during lower price periods has further reduced with consequent increment in price during peak periods, thereby creating higher price difference between peak and off-peak price to incentivize the consumers to shift their loads. In addition, Fig. 4.12b) illustrates aggregated demand profile under different pricing scenarios. It is observed that the higher the percentage change in electricity prices, the higher the load shifting from peak to off-peak periods is. Consequently, load during peak hours is lowered with corresponding increment in off-peak hours, which indeed forms a simple but effective load shifting approach to increase demand responsiveness.

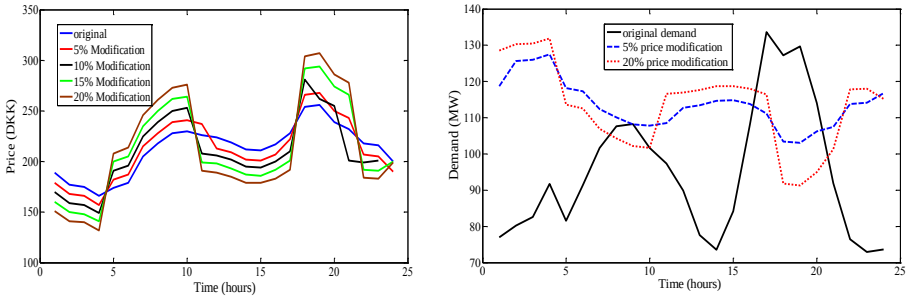

Fig. 4.12 Price modification mechanism. a) Optimal price and b) Corresponding load shift

To demonstrate the impacts of high EV penetration in the distribution system, an uncontrolled EV charging approach, where EVs start charging once they arrive at home and continue until fully charged, is implemented. In this case, most of the EVs are charged between 15:00 to 24:00 as shown in Fig. 8 of **C5**, thereby adding the EV charging demands to the feeder peak. This indeed creates network congestion. It can be observed from Fig. 9 of **C5** that the voltage profile of the far end node drops below allowable voltage limit during the peak periods (18:00 through 21:00). Therefore, technical as well as economic performance of the

proposed EV charging strategy is demonstrated with respect to i) *no change, ii) 5% change, and iii) 20% change, in day ahead electricity price are allowed.*

The EV charging profile for the aforementioned three cases is illustrated in Fig. 4.13. It can be observed from Fig. 4.13a) and Fig. 4.13b) that the EV charging profile is distributed more evenly when higher percentage of price change is allowed. For instance, compared to the base case, the EV charging profile is shifted more evenly when price change is allowed. It should be noted that EVs are considered as fully flexible loads such that the EV charging can be shifted to any periods provided the EV owner's requirements are fulfilled.

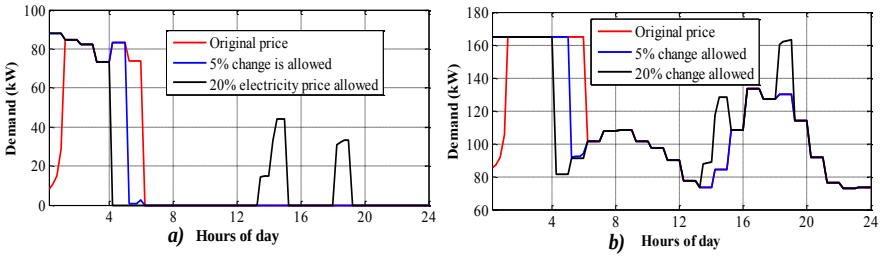

Fig. 4.13 Profiles of a) EV demand and b) Sum of EV and base load demand.

Fig. 12 of **C5** illustrates total EV charging cost for three different cases plus with the uncontrolled EV charging. It can be observed that the total EV charging cost gets significantly decreased for optimal pricing cases compared to the uncontrolled case, thereby providing additional incentives for end-users to shift their loads. Therefore, the proposed integrated EV charging optimization and electricity pricing approach is well suited to address the impact of future electrical loads in the network by properly shifting their demand to the off-peak periods.

4.7. Chapter Summary

This chapter summarized various DR control strategies developed for exploiting demand flexibility from residential consumer. A combination of centralized and decentralized control approach is presented in the first part of this chapter to manage constraints violations in LV distribution grids. The centralized control is executed hourly and acts proactively to distribute amount of flexibility among the consumers for alleviating expected grid violations. While, the decentralized control acts reactively in real-time once the voltage at the POC deviates beyond the pre-defined limits. As such, the centralized and decentralized controls can additionally be used to trade flexibility in balancing as well as regulating markets.

In addition, a novel voltage controlled dynamic DR strategy is developed in the second part of this chapter to avoid need of controlling individual loads/devices. In particular, a control strategy whereby voltage at MV/LV SS is regulated to realize up/down-regulation of the demand is implemented. The proposed method first calculates near real-time voltage dependency of the loads. Following the dispatch of demand regulation signal, required tap setting at intelligent MV/LV SS is computed using computed voltage dependency of the loads. A simplified adaptive voltage estimation technique is implemented to ensure network voltages are within limits.

A two stage control strategy, namely a central optimum scheduling and an adaptive local control has been implemented to exploit demand flexibility from EV/HP. The central scheduling extracts the major portion of the flexibility by optimally scheduling EV/HP operation. This indeed ensures economic benefits to the consumer by minimizing total electricity cost as well as technical requirements by satisfying consumer's and DSO's constraints. In addition, the adaptive control is implemented for real-time adjustment of EV/HP operation. Particularly, the adaptive control locally monitors local voltage and adjust EV/HP operation when voltage at its POC gets violated beyond the pre-specified limits.

Finally, in order to increase consumer's demand responsiveness, a novel optimal pricing algorithm is proposed, where a price difference is created between peak and off peak periods for incentivizing consumers to shift their loads from peak to off-peak periods. To realize the concept, a day ahead electricity price is optimally adjusted such that the price at off-peak or non-critical periods gets decreased and vice versa. Moreover, the effectiveness of the proposed method is demonstrated for a high penetration of flexible load to emulate the future scenario.

The control strategies presented in this chapter deal mainly with the active loads. As future SGs are anticipated to have significant penetration of generations, namely rooftop PV systems, the following chapter presents integrated control strategies for active loads and active generations.

Chapter 5. Control of Active Load and Local Generation

*This chapter presents integrated control of active loads and local generation for better exploitation of the demand flexibility from residential consumers/prosumers. In particular, the chapter contains a summary of control strategies documented in **C6** and **C7**. The effectiveness of the control strategies are demonstrated through integrated control of solar PV and DR considering EV and EWH as potential DRR.*

5.1. Introduction

Recently, attractive feed-in tariffs and declining costs of PV systems are causing rapid growth of rooftop solar PV in Denmark. Such increased integration of solar PV is introducing several power quality issues, such as overvoltage, reverse power flow, harmonic injections etc. in the distribution grids. On the contrary, increased penetration of sizable loads, such as EVs, HPs, EWHs etc., introduce grid congestion issues, particularly under-voltage and thermal overloading. As grid impacts of solar PV and active loads are often complementary to each other, control strategies are designed to neutralize their impacts. In particular, proper operation scheduling of flexible loads can absorb power generation from the solar PV, thereby increasing PV hosting capacity of the distribution networks. In turn, load hosting capacity of the grid also gets increased due to voltage support provided by PV for alleviating the under-voltage issues. Therefore, the key idea of this chapter is to design control strategies such that solar PV and active load becomes supportive to each other. In particular, this chapter summarizes integrated control of active loads and local generation documented in the publications **C6** and **C7**. In the first part, a coordinative control of DR (considering EV as potential DRR) and local generation (solar PV) is presented. The second part of the chapter contains an integrated LAC of active load, namely EWH, and solar PV to implement fully decentralized control for real-time grid support.

5.2. Control Strategies for Solar PV and EV

Since common methods to alleviate overvoltage problems, such as P and/or Q control of the PV system, normally create revenue loss and/or inverter cost increase, a coordinated control of DR and PV is proposed in this study not only to alleviate the overvoltage issues but also to avoid the aforementioned economic loss. A combination of centralized and decentralized control strategy is implemented. System modeling, proposed methodology and outcomes are presented as follows:

5.2.1. System Modeling

The LV test network, described in the Chapter 3, is used for the simulation studies. In particular, every cable branch is modeled by a short line model and loads are modeled as 3-phase loads. Similarly, EVs are modeled as three phase constant

power loads with unity PF, provided with an 11 kW charger and 25 kWh batteries. Solar PV is modeled as a static generator where the PV system operates as a constant power source at specified PQ set-point. Each PV system is rated with 6 kW peak. The PQ capability curve of the solar PV system is designed in compliance with VDE-AR-N 4105 standard [12]. As per the standard, the reactive power limits for the grid-tied inverters are set by limiting PF of the PV system within ±0.95. In addition, an auto regressive moving average model is used for forecasting consumer demand and PV production. The details of the modeling are presented in Section II of **C6**.

5.2.2. Proposed Methodology

As mentioned in the preceding section, a combination of centralized and decentralized control approach is implemented to realize the coordinative control of PV and EV. The centralized stage is executed by an aggregator or entity responsible for DR management and designed to control the EVs and PVs via optimal operational scheduling. Indeed, the optimal scheduling is formulated as an optimization problem where total electricity cost (difference of EV charging cost and revenue collected from PV production) is minimized.

In the first step, power injection from the PV is considered as non-controllable. So, the optimization is performed by taking the charging power of EV as control variables. However, if grid constraints still persist, rescheduling is done by considering both EV charging power as well as PV power injections as control variables. Such rescheduling lets the PVs to contribute prior to EV for the under-voltage violations and EVs to contribute prior to PV for the overvoltage violations. The EV and PV schedules after rescheduling correspond to final schedules to be dispatched as operating set-points to the corresponding EVs and PVs. The detailed formulation is presented in Section III.A of **C6**.

As the centralized control provides periodic inter-slot control with 15 minutes intervals, any intra-slot variations cannot be addressed by it. Therefore, the decentralized control is implemented at every EV and PV location to continuously monitor the voltage at the POC and adjusts the charging power of EVs or power injection from the PVs in real-time. The decentralized control for the PV is modeled as a piecewise linear droop such that the power injection by the PV varies with voltage at the POC. The key idea is that the power injection by the PV should be decreased for overvoltage and increased (if applicable) during under-voltage.

The decentralized controller for the EV is also designed as a piecewise-linear droop such that it adaptively adjusts the EV charging power according to the voltage at the POC. The key idea is to increase the EV charging power for overvoltage violations and decrease for the under-voltage violations as per the assigned droop. The PV and EV droops remains non-operational for the normal operating voltage range, however reacts to the under-voltage or overvoltage violations according to the assigned droop. The details of droop formulation, parameter assignment, and droop settings for different nodes are presented in Section III.B of **C6**. As such, both control stages runs in a coordinated manner as illustrated in Fig. 5.1. As can be seen, both controllers run successively with a

period of 15 minutes. Any deviations resulting from the decentralized control are taken care of by periodic optimization of the centralized control. Similarly, any uncertainties in load or generation during the actual operation are taken care of by the decentralized control, thereby supporting the decision making capability of the centralized control. The detail implementation of the centralized and decentralized control is done as illustrated in Fig. 5 of **C6**.

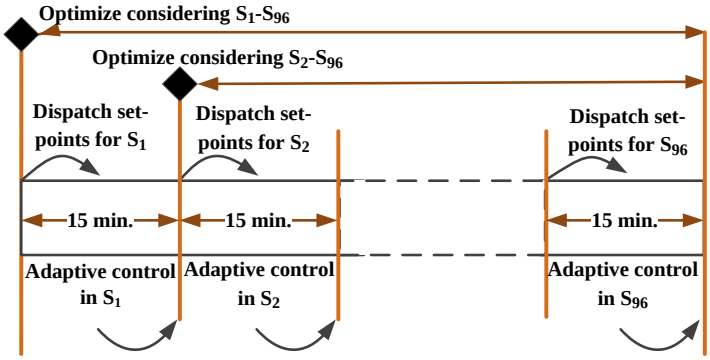

Fig. 5.1 Coordination between centralized and decentralized control.

5.2.3. Observations and Discussions

To demonstrate the performance of the proposed method, a 24 hour time-sweep simulation is performed in a LV test network with 80% PV and 60% EV penetration. A summer day characterized by maximum PV power generation is considered for the simulation to simulate the worst case scenario. The performance of the proposed method is compared to the commonly used P and PQ control methods. Fig. 8a) of **C6** illustrates profiles of available PV power generation, actual power injection using P-control, and injected power using PQ-control techniques. It is observed that available PV generation cannot be injected fully to the grid for several hours due to overvoltage limit violations as shown in Fig. 8b) of **C6**. So, power injection from the PVs has to be curtailed to alleviate the overvoltage.

To better utilize the PV power, optimal EV charging is integrated to the PV control. Fig. 9 of **C6** illustrates a PV power injection with and without integrating EV charging. Significant increment on the injected PV power is observed when optimal EV charging is integrated. In fact, the proposed method has resulted in 15.45% increment in PV power injection compared to the P-control and 7.51% compared to the PQ-control method. A small amount of PV power (about 4.7%) still needs to be curtailed due to presence of relatively less EVs during the day when overvoltage occurred.

In addition, to demonstrate the effectiveness of periodic optimization, original electricity prices and feeder demand are changed as shown in Fig. 10 of **C6**. The changes in demand are used to emulate forecasting uncertainties, whereas changes in electricity price are used to emulate a real-time pricing scenario. The impacts of those changes are investigated by simulations performed with and without periodic optimization. It can be observed from Fig. 5.2 that the changes in loads and

electricity prices significantly alter the charging profiles of the EVs and the total power injection from the PVs. Followed by the price change, several EVs which were initially scheduled for charging during midnight (3:00 through 5:00) are shifted to day (13:00 through 17:00), thereby contributing positively to increased PV power injection. The periodic optimization enables the EVs to adjust their charging according to the adjusted price. For the given configuration, the periodic optimization results in 25.73% decrement on EV charging cost with simultaneous 19.23% increment on the revenue to the PV owners.

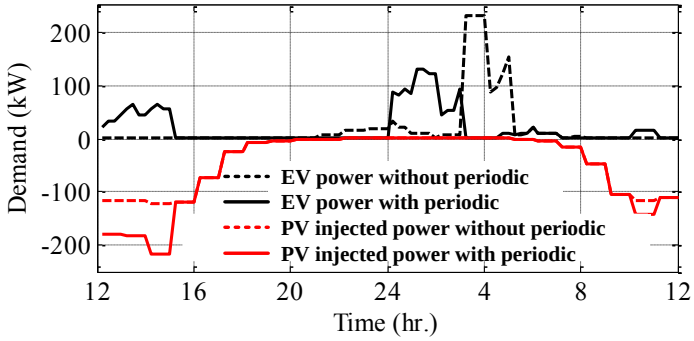

Fig. 5.2 PV power injection and EV charging power.

In order to investigate the real-time voltage support capability of the decentralized control, few load change events are created as shown in Fig. 5.3c) of **C6**. Indeed, the load change events emulate transient variability in PV production. It is observed form Fig. 5.3b) that load decrement at event 2 creates an overvoltage on the grid. In order to act over the overvoltage, some of the PVs whose voltage at the POC gets violated curtail their injected power to avoid the overvoltage. Fig. 13a) in **C6** illustrates an amplified view of Fig. 5.3 from 14:00 through 14:45. It is observed from Fig. 5.3a) of C6 that the injected power is reduced by approximately 14 kW to bring back the voltage to limit. Similarly, increase in load at event 4 in Fig. 5.3b) creates under-voltage violation as most of the EVs were charging during that event. Therefore, the EVs whose voltage at the POC get violated, adjust their charging power to support alleviating under-voltage. As illustrated in Fig. 13b) of **C6** (amplified view of event4), the EV charging power is decreased by approximately 12 kW to increase voltage above V_{min}.

As such, the proposed two-stage coordinated control of EV and PV effectively mitigate overvoltage issue under high PV penetration, particularly by efficient utilization of the PV generation for EV charging. Moreover, it provides real-time grid support by adapting EV charging power as well as PV power injection according to monitored voltage at the POC. Therefore, the proposed method demonstrates improvements in both technical and economic performance. From a technical perspective, it effectively mitigates the grid overvoltage, whereas from the economic perspective it efficiently utilizes the PV power, thereby providing increased PV power revenue and/or decreased EV charging cost.

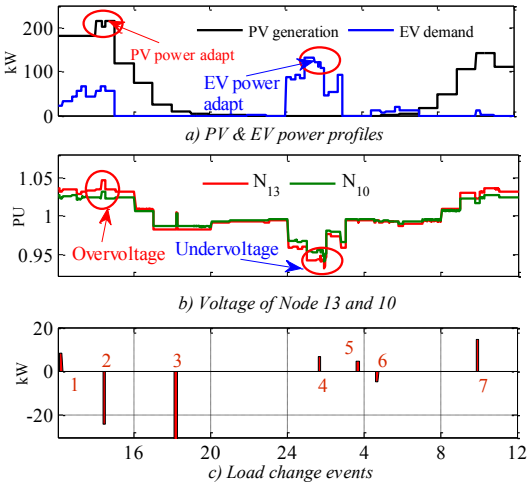

Fig. 5.3 Decentralized control results.

5.3. Integrated Adaptive Control of EWH and PV

In order to investigate deeper insights about local adaptive control, integrated adaptive control of solar PV and EWH is implemented. In particular, this section summarizes EWH and PV modeling, proposed adaptive control, and corresponding findings on the basis of publication **C7**.

5.3.1. Modeling of EWH and PV

The modeling of test network and solar PV system is similar to that in the preceding section and is presented in detail in Section II of **C7**. In addition, EWH is modeled as a constant power thermostatic load provided with a thermal storage tank. The proposed model is done such that the EWH provides flexibility in two ways. First, exploiting the constant power feature of the EWH, demand flexibility is realized by adjusting the power consumption of the EWH. In addition, the flexibility can be realized by adjusting temperature settings of the EWH such that the EWH consumes less power for lower temperature settings and vice versa. Thus, the flexibility is very dependent on size of the thermal storage tank and consumer's thermal demand. The modeling details are presented in Section II of **C7**.

5.3.2. Proposed Adaptive Control Strategies

The proposed adaptive control strategy is designed such that overvoltage resulting from solar PV gets compensated by EWH and under-voltage resulting from high EWH demands gets compensated by properly scheduling them to operate in the period of high PV generations. In particular, the control strategy for EWH and PV are designed separately so as to enable them to contribute differently in overvoltage and under-voltage violations.

As mentioned in preceding section, EWH adaptive control is designed to exploit flexibility in two ways. First, the flexibility is exploited by implementing power versus voltage droop. In particular, P-V and Q-V droops are assigned separately to every EWH such that the P-V droop decreases the active power consumption and

Q-V droop increases the reactive power injection whenever voltage at the POC drops below the predefined thresholds. Even though high R/X ratio of the LV distribution grids make active power control more effective in providing voltage support, the active power control incurred with deviations in electricity cost. For instance, active power curtailment of PV systems leads to revenue loss to the PV owner or decrease of active power consumption of the EWH may lead to consumer demand violations. The droops are designed such that the Q-V droop operates prior to the P-V for the under-voltage violations. This prevents adjustment of active power consumption by the EWH as long as the reactive power is sufficient to resolve the under-voltage. On the contrary, the P-V droop operates prior to the Q-V for the overvoltage violations, thereby letting the EWH to consume more power. The Q-V droop increases reactive power consumption only if the P-V droop is incapable to resolve the overvoltage issues. Such operational priorities are realized by introducing delays in the P-V and Q-V droops. Even though EWH provide lower demand flexibility compared to the EV, it is always available at home. So, it is effective to provide grid support during the day when PV has maximum generation.

An adjustable temperature band, expressed in terms of SOE, is implemented for exploiting additional flexibility when voltage violations occur. In particular, the allowable SOE limits (SOE_{min} and SOE_{max}) are increased in case of the overvoltage violations, thereby letting the EWH to operate for longer periods before its inherent thermostatic control turned it off. Similarly, for the under-voltage violation, the allowable temperature limits are decreased to let the EWH to operate for shorter periods. Particularly, SOE_{min} and SOE_{max} are increased by 0.1 pu for the overvoltage violations and decreased by the same amount for the under-voltage violations.

Similar to the EWH control, the adaptive control of the PV is designed with droops, namely P-V and Q-V. Both the droops are non-operational for the normal operating voltage. For the overvoltage violations, the Q-V droop operates prior to P-V to increase reactive power consumption. Such strategy prevents active power curtailment as long as reactive power is able to resolve the overvoltage issue. However, in the under-voltage violations, the P-V droops operates prior to Q-V to let the P-V droop to increase the active power injection to maximum possible value (if feasible). In addition to the operational priorities for P-V and Q-V droops, priorities are also set for EWH and PV operation as illustrated in Table I of **C7**. For instance, the EWH is allowed to operate prior to PV in the overvoltage violations whereas the PV operates first in the under-voltage violations. The detailed formulation of the proposed method is presented in Section III of **C7**.

5.3.3. Observations and Discussions

The effectiveness of the proposed adaptive control is demonstrated through a 24 hour time-sweep simulation performed in a LV distribution network. In particular, the performance is investigated for three scenarios, namely i) EWH penetration only, ii) PV penetration only, and iii) both EWH and PV penetration.

The first scenario is performed to investigate the performance of the EWH adaptive control. With and without adaptive control cases are simulated for maximum feeder loading (worst case scenario from loading perspective) condition

with high (50%) EWH penetration. It is observed from Fig. 5.4 that whenever voltage at the POC goes below the threshold voltage, the adpative control adjusts active and reactive powers consumption of the EWH. First, reactive power is injected to provide voltage support. The active power consumption of the EWH is also reduced according to the P-V droop since the reactive power is insufficient to alleviate the under-voltage problem. In addition, the power consumption of the EWH is reduced by adaptatively updating the SOE limits. As can be seen from Fig. 5.4, the SOE limits are decreased by 0.1 pu followed by the under-voltage violation, thereby providing additional flexibility. More importantly, EWHs at different nodes are contributing to voltage improvement as shown in Fig. 10 of **C7** unlike in the case of constant voltage settings. The detailed observation on EWH adaptive control capability is presented in Section IV of **C7**.

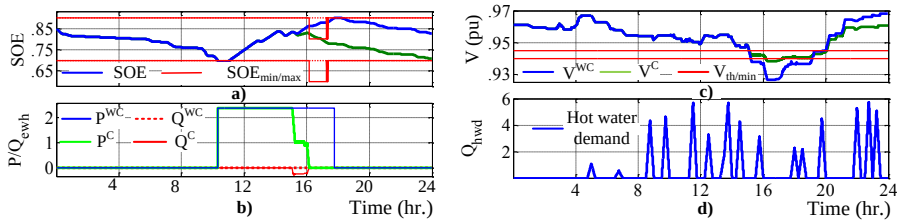

Fig. 5.4 Simulation results of EWH control. a) SOE, b) Active/reactive power consumption, c) POC Voltage, and d) Thermal demand, for a consumer. (WC: without & C: With control)

In the second scenario, the performance of the PV control is investigated for minimum feeder loading with high (80%) PV power penetration. As illustrated in Fig. 5.5, the PV power injection is adjusted according to voltage at the POC. It is observed that whenever the monitored voltage goes above threshold, the adaptive control consumes reactive power as shown in Fig. 5.5. Since reactive power is insufficient to solve the overvoltage issue for the given configuration, active power is curtailed to keep voltage at the POC above limit. Both active power curtailments as well as reactive power consumption contribute to bring the voltage below the maximum allowable voltage. It is clearly seen that voltage is improved significantly compared to the case without having control.

Scenario III is performed with both EWH and PV in order to investigate the interaction between EWH and PV in addressing voltage issues. To realize better investigation of the control approaches, simulations are performed for two cases, namely for light loading (worst case from PV penetration perspective) and high loading (worst case from EWH penetration perspective) conditions. Adaptive adjustment of EWHs power consumption as well as PVs power injection for light loading condition is illustrated in Fig. 13 of **C7**. It is observed that the active power consumption of the EWH is increased first to support the overvoltage. In addition, the reactive power consumption from the EWH is also increased as active power is insufficient to alleviate the overvoltage completely. However, as seen from Fig. 13c) of **C7**, there is no active power curtailment of the PV. Indeed, the power to be curtailed is compensated by adjustment of the EWHs consumptions.

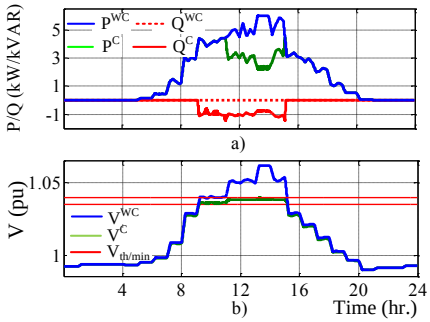

Fig. 5.5 PV results with/without control a) Active and reactive power b) POC Voltage.

Similarly, in order to demonstrate the solar PV support to the under-voltage problem, a simulation is performed for both EWH and PV with high loading conditions. It is observed from Fig. 14 of **C7** that the under-voltage violations are alleviated completely by active power injection from PVs. As such, it can be concluded that the integrated control of the solar PV and EWH provides better network support as well as results in better utilization of the available flexibility.

5.4. Chapter Summary

This chapter summarizes control strategies developed to realize integrated control of active loads and local generation. The key idea is to neutralize the impacts of solar PV and active loads (EV and EWH) by better operational scheduling of the loads and generation.

A two-level control strategy is implemented to demonstrate coordinative control of EV and solar PV. The first level control is a centralized control designed for optimum scheduling of the EVs and PVs. It considers electricity cost, network constraints (thermal and voltage), and consumer requirements to make the optimum schedules. The second level control is a decentralized real-time adaptive control which acts as an inner loop to provide real-time voltage support to the grid. A P-V is designed for every PV and EV to make their generation/demand adaptively adjusted per locally monitored voltage. The combined centralized and decentralized control demonstrates better technical as well as economic benefits.

In order to investigate deep insight of real-time network support capability of the adaptive control, an integrated EWH and PV control is developed. The proposed control is fully decentralized and works on the basis of locally measured voltage and power. In particular, P-V droops are designed for every EWH and PV to adjust active/reactive power consumption/injection by the EWH and/or solar PV. In addition to the droops, the energy bands, namely SOE_{min} and SOE_{max}, of the EWH are adaptively adjusted followed by the voltage violations. Particularly, energy band is increased by 0.1 pu following the overvoltage violations, while decreased by the same amount for the under-voltage violations.

As most of the current researches on SG are simulation based, practical demonstration and validation of DR control strategies is significantly lagging. To address this issue, a scaled-down SG testbed is developed in the following chapter.

Chapter 6. Development of Scaled Down SG Testbed

*This chapter demonstrates multi-disciplinary aspects of the SG by developing a scaled-down SGT, which is described as a part of manuscript **J3**. In particular, details on the SGT development and implementation of the proposed centralized-decentralized control schemes and ICT infrastructure for deploying DR in the physical testbed are presented. Moreover, the capability of the SGT is demonstrated from both power and communication perspectives through an optimized EV charging coordination over a heterogeneous network.*

6.1. Introduction

As mentioned in previous chapter, significant efforts have recently been invested by electric utilities, governments, and researchers to develop DR as a potential solution in the future grids integrating increased penetration of RESs and active loads. Nevertheless, very few attempts have investigated DR deployment capability from multi-disciplinary aspects. In particular, DR implementation not only involves power system but also comprises the ICT infrastructure. Therefore, the ICT plays a crucial role in the practical realization of the DR.

In addition, practical realization of the DR at residential consumer level is significantly lagging due to lack of testing and validation mechanism of the developed DR control strategies in real-world networks. Therefore, practical demonstration and validation of the DR techniques are key aspects to accelerate the DR deployment. However, several potential issues are being barriers to the practical demonstration and validation of the DR techniques. First, it is practically difficult to test and validate DR on the real distribution network due to consumers' concerns, namely power quality and reliability requirements. In addition, direct implementation of the DR on the real network might cause huge damage and economic loss to the utility. Second, it is practically and financially infeasible to setup utility scale networks for testing and validating the DR solutions due to huge investment, efforts, and time requirements.

Recently, pilot project is becoming a potential solution to deploy DR in a real-world network by extracting real-behavior of electricity consumers [111], [171]. However, developing a distribution network as a pilot project requires huge investments of money, time, and efforts. In addition, enabling the consumers to participate in DR programs is often the hardest part especially during the development phase due to their inherent restiveness to any changes and fear of losing operational flexibility, comforts, power quality, and reliability.

In this regard, a SGT is an effective approach to develop, analyze, and demonstrate various SG solutions, such as DR, congestion management etc. A novel method, whereby a larger electrical distribution network is scaled down into a low power and LV equivalent SGT, is developed. In particular, the SGT is

developed by scaling down a 250 kVA, 0.4 kV, LV distribution feeders down to 1 kVA, 0.22 kV. Next, anticipated DR controls and coordination are established by integrating a heterogeneous ICT infrastructure into the SGT. Therefore, a key intent of this study is to develop a cost-effective and efficient test platform for SG solutions. The SGT additionally provides an effective and riskless approach for deployment of the DR accounting the multi-disciplinary aspects of the SG. In particular, this chapter summarizes the SGT development presented in **J3**.

6.2. Development of Smart Grid Testbed

Similar to a real-world SG, the proposed SGT development comprises three major aspects, namely, power network, communication network, and integration of the power and communication network, as described in the following.

6.2.1. Electric Power Distribution Network

A 13-node LV distribution network fed by a 10/0.4 kV LV transformer substation is taken as a test network. In particular, the network is scaled down from 250 kVA, 0.4 kV LV to 1 kVA, 0.22 kV testbed and a single phase equivalent of the scaled-down SGT is implemented as an experimental SGT in a laboratory. The scaling parameters used to scale-down the LV network are summarized in Table 6.1. The voltage scaling factor is chosen to match the SGT with a nominal supply voltage at the site where the SGT was implemented. This is particularly done to avoid voltage conditioning equipment such as voltage converter and/or regulators. Additionally, the scaling factor for the power is chosen to enable the economy and readily availability of equipment on that range.

Table 6.1 Network parameters before and after scaling down.

Parameter	Before SD	After SD
Feeder Capacity	250 (kVA)	1 (kVA)
Feeder Voltage	0.4 kV	0.22 kV
Transformer R/X	4.64/18.64 (mΩ)	0.314/1.26 (Ω)
Cable R/X	207/78 (mΩ/km)	13.99/5.27(mΩ/km)

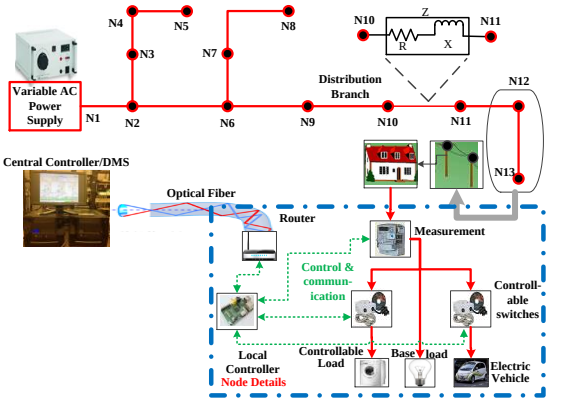

Fig. 6.1 Schematic diagram of 13-node scaled down network.

As illustrated in Fig. 6.1, the scaled down LV distribution feeder is configured such that every node consists of different load types (controllable loads, base load,

and EVs), smart meter, local controller, and smart controllable switches. Further, a variable AC supply with a capability to regulate supply voltage is implemented as a primary source of power to the SGT. This is intended to keep the input to SGT constant irrespective of supply voltage variations. Every feeder branch is modeled using an equivalent lumped series impedance as depicted in the Fig. 6.1. Similarly, the transformer is implemented with its corresponding scaled down series impedance. Scaled down values of line parameters and loads are computed on the basis of per unit techniques as presented in the Section II of **J3**. It should be noted that the load at each node of the SGT corresponds to an aggregated load of the consumers connected to that particular node. Based on the actual values of the scaled down load, small electrical loads (batteries, chargers, lamps, small motors, etc.) are connected at each node.

Fig. 6.2a) illustrates the experimental SGT implemented in the laboratory and Fig. 6.2b) illustrates an amplified view of a particular node. It can be seen that every node comprises a combination of controllable and non-controllable loads. In particular, each node consists of a local controller (Raspberry Pi model B), smart meter (TP4000ZC digital meter), electrical sensor (TP4000ZC digital meter), controllable load (TS5003, 0.21A, 115V), EV (12V, 4/7 Ah battery), an incandescent bulb, and two controllable switches (USB Net Power 8800 power controller). The two controllable switches are used to control flexible loads, namely the EV charger and motor (TS5003, 0.21A, 115V).

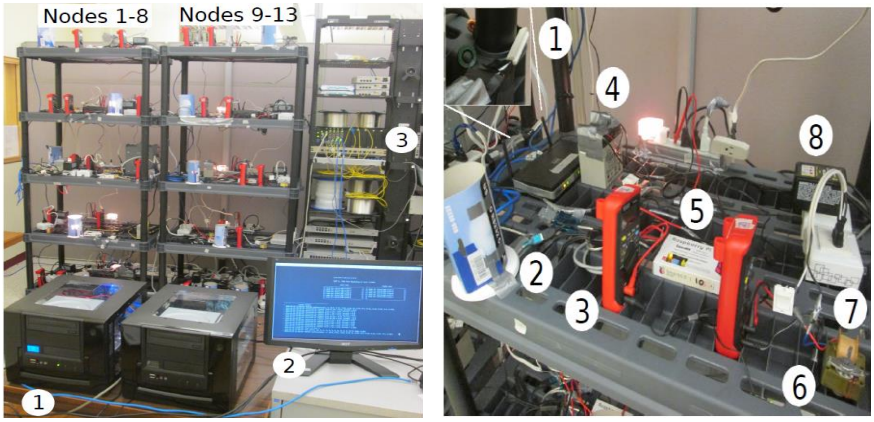

a) Scaled down SGT composed of DMS server (1), DMS (2), EPON (2), and Power network (nodes 1- 13)

b) Smart node composed of line (1), discharging load (2), seonsors/meters (3), battery (4), local controller (5), dynamic load (6), controllable switches (7), and charger (8)

Fig. 6.2 Laboratory implementation of the testbed.

In addition, each EV (emulated by 12 V 4/7 Ah capacity battery) are supplied with two types of chargers (2/4/8A and 0.9A) to simulate different charging schemes. In particular, EVs having 4 Ah capacities are provided with 0.9A chargers whereas EVs having 7 Ah capacities are provided with a 2/4/8A charger. The EV travel is emulated by discharging the battery through a 25 W incandescent bulb connected at every EV connected node. Power consumption by local controller, smart meter, sensor, and incandescent bulb constitute base loads at each node.

6.2.2. Communication Network

As depicted in Fig. 6.3, the ICT infrastructure primarily comprises a backhaul network based on an EPON and mesh NAN based on an IEEE 802.3 Ethernet. In particular, the EPON consists of 4 optical network units located 20 km from the optical load terminal, each having bidirectional data rate of 1 Gbps. Similarly, each link in the NAN is full duplex with 1 Gbps capacity. The optical network units aggregate the traffic from/to the Ethernet meshed network towards the nano-computers based on Raspberry Pi model B, hereafter called LAC. In particular, the DMS reaches every household or device via multiple routers namely the optical load terminal, EPON, and meshed NAN. Therefore, end-to-end delay between any source node to any destination node is computed by:

$$D_{s,d} = \sum_{i \in I_{s,d}} \varnothing_i + \frac{L}{c_i} + \frac{d_i}{200000}. \tag{6.1}$$

where $I_{s,d}$ is the set of network interfaces from s to d, $\varnothing_i$ is the queuing delay at interface i, L is the frame size, c_i is the capacity in bps at interface i, d_i is the distance in km at interface i through the adjacent node, and 200000 is the propagation speed in km at the speed of light through a wire (fiber). The queuing delay (first term) remains negligible as the traffic load is low. Whereas, the transmission delay (second term) remains significantly low since c_i equals 1 Gbps. The propagation delay component (third term) depends on the distance between nodes, for instance, communications between the optical load terminal and optical network units takes 0.1 *ms* for 20 km fiber length.

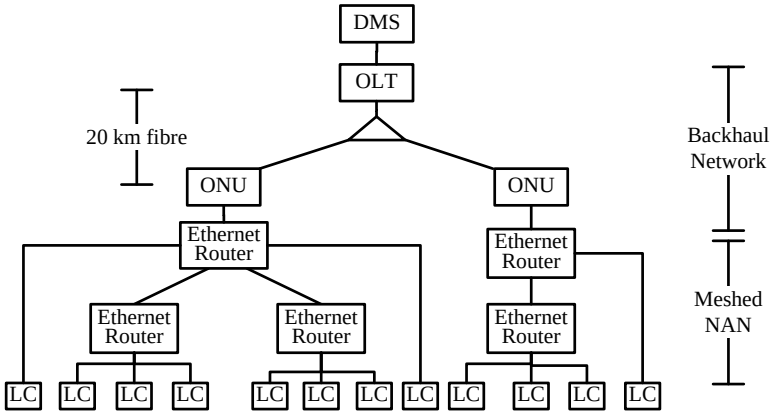

Fig. 6.3 Communication infrastructure implemented in the testbed.

6.2.3. Integration of Power and Communication Network

As mentioned in the preceding section, the LAC which is installed at each node provides a physical interface between the power and ICT network. It establishes bidirectional communication between the central DMS and the consumer in a pre-defined time interval and data format. In the proposed SGT, the communication frequency is limited to 15 minutes and the data format comprises a data matrix (e.g., power, current, voltage) encrypted with control data, as explained in detail in

Section II of **J3**. In addition to the interface functionality of the LAC, it serves as a controller and data hub to every consumer. In particular, the LAC at a particular node ensures measurement and control of every controllable devices connected to that node. Two separate meters are connected to the LAC to monitor battery SOC and node voltage. The LAC reads both meters twice per second. Based on the monitored data, the LAC executes the control of the load once the monitored voltage goes beyond the pre-set limits.

Whenever the central DMS need to execute any control on a particular load, it sends the control signal and the LAC of the particular node executes the actual control on the load as per the instruction contained in the signal. In fact, two controllable switches (USB Net Power 8800 power controller) are used to execute control (ON/OFF) of the controllable loads (EV charger and motor). In addition, in real-time, the LAC monitors the network conditions and performs the control action once the voltage at the POC deviates beyond the pre-specified limits. Therefore, the LAC plays a key role to bridge the power and communication in the testbed.

6.3. SGT Performance Demonstration

Optimized EV charging coordination realized through a combination of a centralized and a decentralized control algorithm is implemented for demonstrating the SGT performance. The details of each control are described in the following.

6.3.1. Centralized Control

The centralized control is implemented centrally at the DMS for determining optimum charging schedules for the entire EVs considering EV owners requirements, electricity price, and network conditions. In particular, the centralized control is implemented under the following framework:

- Every EV sends SOC_i, $T_{in,i}$, $T_{out,i}$, position in the network, battery capacity (BC_i), and minimum/maximum charger rating (P_{max}) to the DMS at plug-in. Any unusual travel requirement should also be specified at the plug-in.
- Unless specified any EV plug-in between k and k+1 time-slots is considered for optimization on the $(k + 1)^{th}$ slot.
- At the end of each slot, every EV sends updated SOC_i, charging power, charging current, and voltage to the DMS and the DMS re-compute the optimum charging schedules.

After receiving the aforementioned data from entire plugged-in EVs, the DMS first prepare optimum schedules for every EV considering their individual requirements and electricity prices. Mathematically, the problem is formulated as a minimization problem as:

$$Min. \sum_{k=T_{in,i}}^{T_{out,i}} P_{i,k}.x_{i,k}.t_k.C_K, \tag{6.2}$$

$$Subjected\ to: P_{min} \le P_{i,k} \le P_{max}$$

$$P_{i,avg} \le P_{max} \tag{6.3}$$

$$SOC_{i,T_{out}} = SOC_{max}.$$

where $P_{i,k}$, $x_{i,k}$, t_k, and C_k are the charging rate, operating state, slot duration, and electricity price for the k^{th} slot and i^{th} EV. $P_{i,min}$ and $P_{i,max}$ are the limiting values of EV charging rates, $P_{i,avg}$ is an average charging rate required to fully charge the EV by the plug-out time (i.e. $SOC_i = SOC_{i,max}$ by T_{out}), and $T_{in,i}$ and $T_{out,i}$ are the plug-in and expected plug-out time respectively. The first constraint is used to ensure the charging power is within the charger ratings, whereas, the second and third constraints are used to ensure that the EV should be fully charged by plug-out time. A binary integer programming is implemented for the optimization. The optimization gives a solution vector x_k comprising optimum charging states of EVs.

Nevertheless, as the network constraints are not included in this optimization, there remains a possibility that the optimum EV charging might not be supported due to network constraints. Therefore, following the optimization of the individual EVs, the feeder capacity is checked to make sure whether or not the feeder loading is within limit. If the feeder capacity gets violated, the optimization is done for all EVs considering the network limits as depicted in flow chart in Fig. 5 in **J3**. In this case, the optimization problem is formulated as follows:

$$Min. \sum_{k=1}^{N_{slt}} \sum_{i=1}^{N_{EV}} P_{i,k}.x_{i,k}.t_k.C_K, \tag{6.4}$$

$$Subjected\ to: \sum_{i=1}^{N_{EV}} P_{i,k} + FL_k \le FC, \tag{6.5}$$

where N_{EV} is the number of plug-in EVs, N_{slt} is the total number of time slots, FL_k is the feeder load at k^{th} slot, and FC is the maximum feeder capacity. A feeder capacity limit constraint (6.5) is additionally included together with the constraints (6.3) to respect the thermal limit. Consequently, the optimization problem is solved as a minimization problem using the objective function (6.4) and the constraints (6.3) & (6.5). It should be noted that such rescheduling may changes the charging schedules of some of the EVs, thereby increasing total EV charging cost. Fig. 5 of **J3** graphically illustrates major steps involved in the proposed EV charging.

6.3.2. Decentralized Control

The decentralized LAC is implemented locally at each EV to adapt their charging based on real-time monitored voltage at their POC. Irrespective of the scheduled operating states from the DMS, the LAC adjusts the EV states if monitored voltage deviates beyond pre-specified limits as follows:

$$EV_{i,N} = \begin{cases} ON & if\ V_N > 0.95 \\ OFF & Otherwise \end{cases}. \tag{6.6}$$

where $EV_{i,N}$, is the operating state of i^{th} EV connected to N^{th} node and V_N is the voltage at N^{th} node. If the V_N goes beyond the limits (0.95 pu), the LAC switches OFF the EV connected to that node to support the network. Thus, the LAC action may override the optimum OSs initially set by the DMS. In order to limit frequent switching (ON/OFF) of the EVs, the maximum number of switching within a slot is

limited to one. This will further help to prevent voltage oscillations that might result from frequent ON/OFF switching of the EVs.

Even though the proposed threshold based LAC provides real-time network support, two potential problems could arise. First, a large number of EVs could simultaneously switch ON/OFF, thereby leading to voltage oscillation. Second, EVs at the far end on the feeder suffer more compared to the EVs in the upstream. To solve the first problem, random response time (from 0 to 10 sec) is assigned to every LAC. Whereas, to address the second problem, SOC based prioritization is used during the optimization. Therefore, irrespective of the EV location in the network, the SOC based prioritization favor the EVs whose P_{avg} is lower than required to fully charged by its T_{out}.

6.3.3. Coordination of Decentralized and Centralized Control

As described previously, the centralized control periodically prepares optimum schedules and acts as inter slot control whereas the decentralized LAC acts as an intra-slot control to adapt to local voltage deviations in real-time. At the beginning of each slot, the optimized EV schedules are sent to every plugged-in EV centrally. Once the schedules are dispatched, the centralized control does not have any controllability to the EV. However, any voltage limits violation which might occur during actual operation gets compensated by the LAC action. Specifically, the LAC executes the control as per Eq. (6.6) to revert the voltage back once the monitored voltage goes beyond pre-defined thresholds. It should be noted that every EV is assigned with different response time to avoid the simultaneous switching.

As illustrated in Fig. 6 of **J3**, the LAC sends the updated SOC and charging state to the DMS at the end of each time slot and the DMS performs the optimization for the remaining slots. Therefore, any deviations on EV schedule resulting from the voltage based LAC are compensated while performing optimization by the next slot. Moreover, any uncertainties such as load variations, EV plugged-in/out which cannot be considered during centralized optimization are addressed by the LAC's real-time control. The key idea is to use the two controllers in coordinated manner as an intra- and inter-slot control.

6.4. Observations and Discussions

This section presents the SGT performance from power, communication, and computation perspectives by optimized EV charging coordination. As mentioned in the previous section, performance of the SGT is demonstrated through optimized EV charging coordination for 24 hours starting from noon until the noon of the next day. In particular, the 24 hours charging period is first discretized into 96 numbers of 15 minute slots. Each 15 minute slot is subsequently scaled down to 40 seconds. Therefore, all computation parameters are adjusted accordingly by time scale factor of 22.5 (*15*60/40 =22.5*). For performing experiment, T_{in} and T_{out} are assigned to each EV as illustrated in Fig. 7a) and a day-ahead electricity price as depicted in Fig 7b) of **J3** are considered. Further, daily load profile is created by controlling 5 motors in a pre-defined sequence as shown in Fig. 5 of **J3**. All parameters are kept constant throughout the experiment to facilitate comparison of various cases.

6.4.1. Power Performance

Three sets of experiments are performed to access the performance of the testbed from power perspectives. First, a price based optimization, whereby total charging cost of the EVs is minimized without considering the network condition is demonstrated. As the EV owner normally do not concern about the network conditions; they rather want to minimize their charging cost, the price based optimization forms a benchmark for rest of the cases. The charging profile of the EVs for the price based optimization is illustrated in Fig. 6.4. The time expressed on the x-axis corresponds to the scaled down time starting from 12 noon. It can be observed that the EV charging is closely following the electricity price (Fig. 7b of **J3**), thereby charging most of the EVs during the low price periods i.e. between 2000 to 3000 sec (1:00-5:00). Such simultaneous charging of EVs corresponds to approximately 200 W on top of the base load. In order to avoid testbed congestion, the experiment was performed using small base loads (LAC, sensors/meters, controllable switches, routers etc.) which correspond to approximately 12 W.

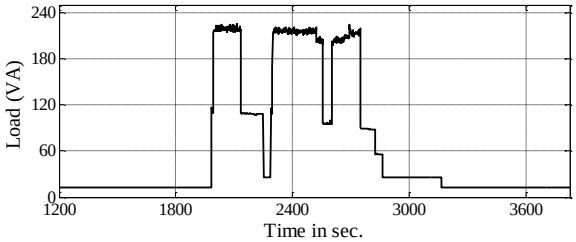

Fig. 6.4 Optimized EV charging power profile (price based optimization).

In order for the optimum EV schedules to be acceptable from DSO perspectives, the network constraints should be taken into account. For that reason, the network constraints are explicitly considered during optimization in the second case to respect the feeder capacity. Actually, a network limit of 300 W is considered to avoid feeder capacity violation due to simultaneous charging of EVs. Therefore, the experiment is performed with a predefined base load profile shown in Fig. 5 of **J3**.

The power profile comprising the EV charging power and feeder base load is depicted in Fig. 6.5a). It can be observed that the EV charging profile closely follows the electricity price as well as respect the feeder capacity limit. Indeed, the charging profile of the EVs in this case is very similar to the case without considering the network constraints. The minor differences are that some of the EVs which were initially scheduled for charging at low price periods get rescheduled to higher prices, thereby resulting in an increase in total EV charging cost. For the given configuration, the consideration of network limit results in increased charging cost by 27.8 % compared to without consideration of the network constraints. It should be noted that the feeder load slightly exceeds beyond the feeder limit of 300W (Fig. 6.5a)) due to feeder loss and operational variations on the efficiency of the EV charger, which were not considered while optimizing.

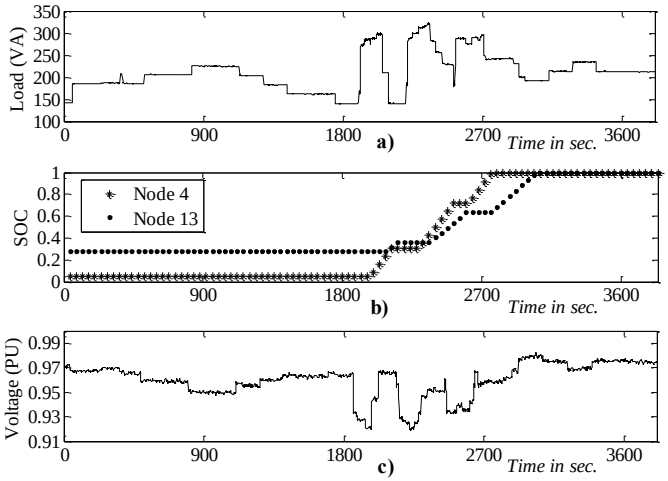

Fig. 6.5 EV charging optimization considering network constraints.

The charging profiles of two EVs connected at nodes 4 and 13 are illustrated in Fig. 6.5b). Even though the charging profiles of both the EVs are similar, their charging differs significantly in relation to slots at which the EV has charged and the charging rates. In fact, the EV at node 4 is charging faster compared to the EV at node 13 and gets fully charged prior to EV 13. Those differences arise due to the difference in charger ratings and plug-in time. Moreover, the difference in charging rates arises due to deviations on EV charging due to network limit violations. As illustrated in Fig. 6.5c), the voltage at node 13 has gone below the threshold (0.95 pu) during low price periods where most of the EVs are scheduled for charging. Even though the network constraint in terms of feeder capacity limit is included in the optimization, it cannot ensure that the voltage stays within the limits. Therefore, a technique adaptive to the real-time operation is anticipated to compensate any voltage deviations that might occur during actual operations.

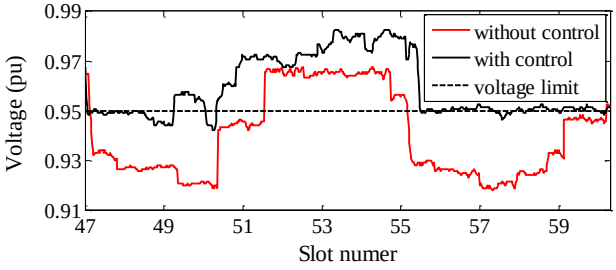

Fig. 6.6 Voltage profile of node 13 with local voltage control.

In the third case, a voltage based decentralized LAC is included to address the voltage issues, thereby adapting the network in real-time. An amplified view of the voltage profile at node 13 with and without LAC is illustrated in Fig. 6.6. It can be observed that the voltage, which is violating the limits quite significantly and

frequently without LAC, stays very close to the pre-defined limit of 0.95. Slight deviations in the voltage beyond the preset limits are due to discrete control (ON/OFF) and different response time of the EVs and controllable loads. It demonstrates that the proposed simple LAC (ON/OFF) helps significantly for real-time network support. Indeed, the proposed method provides an effective way to promptly react to the voltage violation in real-time and to provide substantial backup to the centralized scheduling.

The aforementioned experimental results demonstrate that the testbed is capable of implementing anticipated controls designed as per centralized-decentralized control schemes. Successful implementation of the centralized control for optimization and decentralized control for real-time local control demonstrates the effectiveness and applicability of the proposed method to in the future electrical grids maximizing the network support capability.

6.4.2. Computation Performance

Computation performance primarily depends on complexity of the algorithm, capabilities of the computing machines, and size of the problem. In particular, it plays a great role on the performance of the testbed as the higher computation time creates additional delays and consequently impact timely execution of control such as dispatch of optimum schedules to the EVs. In this study, the computation performance has been evaluated in terms of computation time required for the optimization. For a given slot s, the computation time is determined as:

$$C_T = |t_c - t_r| \tag{6.7}$$

where C_T is the computation time, t_c is the time when the optimization solver at MATLAB is called from Python, and t_r is the time when Python received back the optimized schedule. A lower value of C_T ensures better computation capability, thereby faster optimization.

Fig. 6.7 Computation time for optimization process.

The computation time as a function of time slot is depicted in Fig. 6.7 for a given configuration. It can be observed that the computation time decreases from a maximum of 0.3 sec to as low as 0.02 sec with increase in the slot number. Such low computation time demonstrates that the proposed algorithm and optimization works well for DR execution in the future SG.

6.4.3. Communication Performance

The communication is responsible not only for exchange of data but also for timely execution of the control actions. Therefore, reliable communication is essential for proper functioning of the testbed since the higher communication delay might cause undesired control and operation. In this study, the communication performance is demonstrated in terms of data traffic and synchronization methods. In particular, the synchronization performance of the two synchronization methods (time-based and coordinated sensor based) expressed in terms of average time interval between the received measurements (Δ_m) are depicted in the Fig. 6.8a). For both mechanisms, measurements are sent every second. It can be seen that the coordinated synchronization method performs better than the time-based one, with the Δ_m in the range of [1.5 - 4] ms, compared to up to 500 ms using time-based sensors. The time-based sensors Δ_m performance varies from 100 to 400 ms, since sensors get desynchronized over time due to local processing delays.

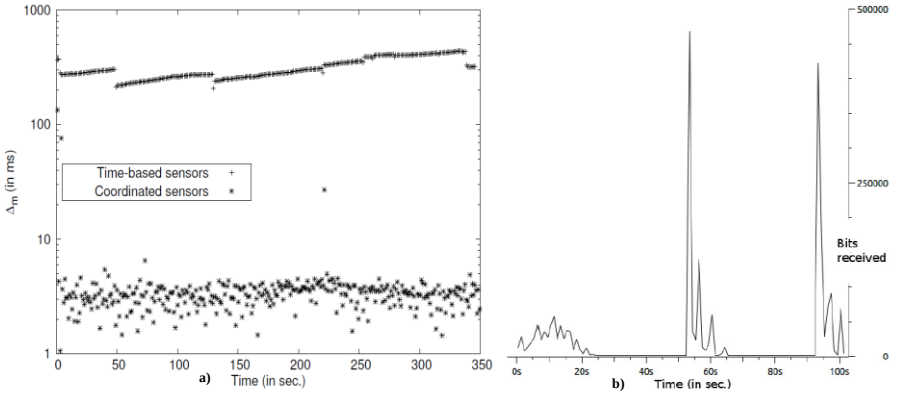

Fig. 6.8 Communication performance. a) Synchronization performance using time-based and coordinated sensors, and b) Captured traffic of the DMS port to/from optical load terminal

As mentioned in the section II-A4 of **J3**, the polling-based communications protocol generates low traffic. At low loads, the end-to-end delay remains low and stable. Fig. 6.8b) depicts the traffic profile (using the Wireshark packet analyzer4) at the beginning of the experiment. From 0 to 20 seconds, LACs connects to the DMS in order to register. Then, the DMS interrogates LACs at the beginning of each slot (50 - 60 and 90-100 sec. in Fig. 6.8b). During these interrogations a peak transmission of 450 Kbps is observed. To decrease this peak transmission, broadcast messages could be used instead of one TCP message per LAC.

6.5. Chapter Summary

The major contribution presented in this chapter can be categorized into three parts. First, unlike most of the current SG studies performed from either power or communication perspectives; this study has demonstrated the multidisciplinary aspects of the SG. As stated in the IEEE2030P standard about the SG requirement, this study considers power, communication, and information aspects. A key intent

of this consideration is to develop the SG solutions which better reflect the real-world problem and hence possess higher probability of acceptance.

Second, this study has proposed a new algorithm for development of a scaled down SGT to enable testing and validating key SG features. Specifically, a real-world 13 nodes, 250kVA, 0.4 kV LV distribution feeder is scaled down to 1 kVA, 0.22 kV and developed in the laboratory as an SGT. The ICT network based on EPON and meshed NAN is integrated in the scaled down power network to establish real-time monitoring and control. This novel scaled down based approach not only fosters faster and cost-effective testbed development but also provides an effective and riskless method for testing and validating various SG solutions.

Last, an effective centralized-decentralized control algorithm is designed and integrated in the SGT for exploiting DR. In particular, the performance of this two-stage algorithm is demonstrated through optimum EV charging coordination in the SGT. The testbed performance is evaluated by experimenting optimized EV charging coordination under three scenarios. It is shown that the proposed centralized and decentralized control approach for EV charging respect the charging cost, network congestion, and local voltage simultaneously. Furthermore, the real-time control and coordination among DMS, LAC and EVs is realized in the SGT through a synchronized exchange of power and control signals through a heterogeneous meshed network. More importantly, the SGT fosters SG research and development and facilitates researchers and utilities to analyze and compare various algorithm and protocols for the future SG.

Wide adaptation of ANM activities, such as DR, network reconfigurations, impacts protection of distribution system. As such, an adaptive protection algorithm is developed in the following chapter consideration high penetration of ANM and DERs in the MV networks.

Chapter 7. Proactive and Adaptive Protection Design

*This chapter first outlines key protection issues in distribution system and presents a detailed methodology to address those issues. In particular, a summary of the proactive and adaptive overcurrent protection algorithm developed in **C8** is presented to address the protection issues resulting from increased DERs penetration. Additionally, integration of ANM and adaptive protection is proposed for addressing protection challenges resulting from increased ANM activities.*

7.1. Introduction

The increased integration of DERs in a distribution system not only increase fault current magnitude but also alters the distribution of fault current over the network, thereby jeopardizing existing protection system. In addition, increased adaptations of ANM activities, such as network reconfiguration, DR etc., may changes network topologies which in turn impact the existing protection system. Therefore, conventional protection schemes, whereby the protective device settings are computed by decoupling protection from system operation, may render both ANM and protection system vulnerable which may lead to incorrect operation due to their interdependencies. As a result, single parameter settings of protective devices are insufficient to maintain selectivity and sensitivity to fault in a dynamic network environment and demand an effective adaptive protection.

Current practices to address the protection issues with high DER penetration include: limiting fault current [160]-[163], local adaptive protection [164]-[165], and communication assisted centralized protection [166]-[168]. A key idea of the first approach is to keep same protection settings with and without DERs connection. This is normally realized either by limiting the DER penetration [160], [161] or by limiting the fault current via fault current limiters [162], [163]. In the second approach, centralized communication assisted protection is established, whereby every protective device report measurements to a central protection unit for assisting fault identification. Consecutively, the central protection unit computes relay settings to adapt to post-fault network topology and send the updated settings to respective protective relays. On the contrary, local adaptive protection provides an adaptive update of the relay settings consistent with varying network topologies. In particular, faults are identified on the basis of locally measured current and/or voltages. Even though the local adaptive protection approaches effectively updates the relay settings for a particular network topology, they have limited network visibility. Therefore, any topological changes, such as addition of DERs or network reconfiguration, may easily lead the local adaptive protection to mal-operate.

Therefore, a two-stage protection strategy is designed in this study to address key protection issues. First, an offline fault analysis is performed to compute relay setting for every operating mode, such as grid-connected/islanded, with/without

DERs connection, with/without network reconfiguration etc., and then those settings are stored in respective relay memories. In the second stage, an online state detection algorithm is realized to detect the operating mode of the network and operating status of the DERs in real-time, thereby adapting proper relay settings consistent with the network topology and operating modes. A combination of local adaptive and communication assisted centralized protection scheme is implemented for online identification of the network status.

7.2. Key Issues to Protect Future Distribution Grids

Protection of a distribution grid is expected to be impacted due to increased integration of DERs as well as changes in control and operational practice of the existing networks. The following sections illustrate the key protection challenges resulting from wide adaptation of DERs and ANM activities at distribution level.

7.2.1. Impacts of DERs in Distribution Protection

Increased DERs penetration alters not only the fault currents magnitude but also their distribution in the network; thereby challenging the existing protection system. Nevertheless, the severity of the impact depends greatly on type, size, and location of the DERs as well as the strength of the grid (weak/strong). For instance, the fault current contribution from a rotating machine based DER is significantly large and sustained compared to a small fault current contribution from an inverter interfaced DER. Similarly, the higher the DER size, the greater the impact is. Nevertheless, protections blinding and false tripping are foreseen as two key challenges in relation to maintaining selectivity for permanent faults [164].

7.2.1.1 Protection Blinding

Protection blinding is a case in which the fault current seen by a relay get changed (increased or decreased) due to connection of DERs in a network, thereby leading to mal-operate the relay. For instance, a fault current seen by relay R_1 for a fault F_{P1} gets reduced because of connection of a DER at node 2 as in Fig. 7.1. So, relay R_1 see fault far from the actual location, thereby facing under-reach problem.

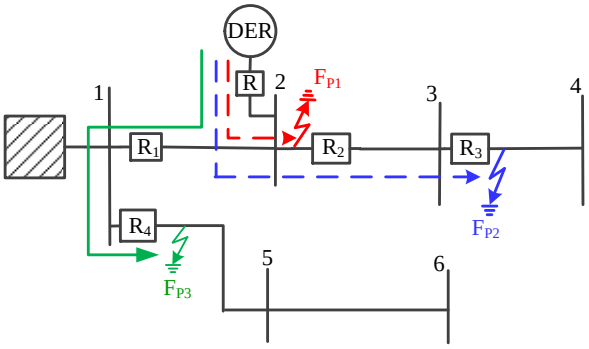

Fig. 7.1 Protection blinding and false tripping due to DER penetration.

As a result, relay R_1 is prevented to operate for the faults towards the ends of its protection zone. Similarly, the fault current seen by relay R_2 for the fault F_{P2} gets increased because of the DER connection. This causes overreach of the relay R_2,

thereby operating R_2 for out of zone fault F_{P2}. In either fault conditions (F_{P1} and F_{P2}), the relays are partially blinded to the fault; upstream relays face under-reach, whereas the downstream relays face overreach. An effective method to dynamically adjust the relay reach is adaptive update of relay pickup current on the basis of DER connection status. For a given operation time, the pickup current should be increased for upstream and decreased for downstream relays followed by DER connection.

7.2.1.2 False Tripping

False tripping is a case in which connection of a DER causes a relay connected to a feeder to operate for a fault in an adjacent feeder. If a fault contribution from the DER exceeds the pick-up current of the relay in healthy feeder, it can lead to a trip of a healthy feeder before the fault is cleared by the relays in the faulted feeder. For example, the fault current contribution from the DER for a fault F_{P3} in Fig. 7.1 might cause the relay R_1 to trip if the fault current seen by relay R_1 exceeds its pickup value. In this case, depending upon the fault current contribution from the DER and pickup settings of relays R_1 and R_4, the relay R_1 might get falsely tripped. The fault tripping is a major concern mainly in weak grids having long feeder length since the relay settings in this case have relatively small pick-up current, thereby leading to slow response time. The false tripping is commonly dealt by employing a directional protection integrated with an adaptive relay update per DER connection status.

7.2.2. Impacts of Network Operation in Protection

Wide adaption of the SG concept is leading to significant change in control and operation of the existing system, such as active network reconfiguration, changes in mode of network operation (grid-connected/islanded), DR activities etc. Such transformations in turn impact the network protection in the following ways:

7.2.2.1 Intentional/Unintentional Islanding

Islanding is basically a condition where DER continues to supply power for a particular area during loss of supply from the utility or for any economic reason. Typically, the short circuit current during islanded operation is very low compared to grid-connected mode. This lead to a condition that the relays provided with grid-connected settings may fail to discriminate fault during islanded operations and vice versa. As such, dynamic relay setting is desired to adapt the mode of operation. An approach, whereby the relay settings are changed based on the online identification of the network operating mode, is presented in this study.

7.2.2.2 Active Network Management

Exploiting controllability of SG, various ANM activities, such as DR, network reconfiguration etc., are foreseen to be widely integrated in the distribution system. Such anticipated changes may lead to changes in network topology, thereby causing mis-coordination of the protective devices. For instance, distribution feeder reconfiguration done for decongesting the network may change the fault current distribution and may demand to update settings of protective devices to maintain selectivity. Such issue is dealt with by integrating the ANM activities into the protection philosophy such that the protective device settings are updated to adapt to the dynamic network topology.

7.3. Implementation of Proposed Algorithm

The proposed protection methodology is realized in two stages. The first stage is proactive protection; whereby an offline fault analysis is performed to compute relay settings for various operation modes and the second stage is an adaptive protection, in which an online state detection algorithm is implemented to detect correct operating state of the network for activating proper relay settings. First, offline fault analysis as illustrated in Fig. 3 of **C8** is performed to compute relay settings, namely TMS and relay pickup current 'I_P', for the following modes.

- *Grid connected operation without DERs (base case)*
- *Grid connected operation with DERs*
- *Islanded operation with DERs*
- *Network reconfiguration*

It should be noted that some operating modes may have more than single settings, for instance, settings of the relays for grid connected operation with DERs could have multiple settings depending on (N-1) DERs contingencies. The relay settings for all operating modes are then assigned to respective relay memories and the proper setting get activated during actual operation per online identification of the network operating mode.

A modified zonal concept based state detection algorithm is implemented to facilitate online identification of the network operating states. The distribution network is decomposed into various zones, as shown in Fig. 2 of **C8**, such that fault current contributions from the DERs in a zone has minimal impact on fault discrimination of the relays in other zones. In particular, (N-1) DER contingency in a zone does not demand changes on the settings of the relays in the other zones. For example, if the fault current contribution from the DER, in Fig. 7.1 does not impact relay R_4, then the feeder $F_{1-2-3-4}$ is taken as a single zone and the rest as another zone. However, if the DER impact the setting of R_4, both the feeders, $F_{1-2-3-4}$ and F_{1-5-6}, should be a single zone. An extensive fault analysis considering (N-1) DER contingency for different fault types, fault locations, and fault impedance, forms a basis of the zone formulation.

A key idea of zone formation is to let the protective devices within a zone to operate independent of the DER status in the other zones. Particularly, each relay within a zone, called IZRs, is designed to detect ON/OFF states of the DERs within that zone and the relays at zone boundaries, called ZSRs, are designed to detect major topological changes, namely grid-connected/islanded, network reconfiguration etc. In fact, a central protection unit uses an event driven communication to ZSRs during major topological changes, and the ZSRs in turn transmit the event to every IZRs within their zone. Indeed, relays which are at zone boundaries act as IZR as well as ZSR. The proactive protection is followed by online fault identification as illustrated in Fig. 3 of **C8** and described as follows.

7.3.1. State Detection of Distributed Energy Resources

As zones are formed such that (N-1) contingency within a zone does not impact setting of the relays in other zones and vice versa, IZRs need to be updated based on the ON/OFF status of DERs within that zone only. Thus, every IZR is

configured with an event driven local communication for every change in operating status of DERs within the zone. Indeed, following any changes in DER status within a zone, IZRs communicates with adjacent relay(s) to adapt their setting, particularly the I_P and TMS accordingly. Unlike conventional communication assisted protection, where every relay talk back and forth with a central coordinating unit, the proposed algorithm use limited event driven communication where ON/OFF states of the DERs within the zone are communicated with the adjacent IZR(s). It should be noted that there is no need of inter-zone communication, thereby avoiding fault discrimination issues resulting from communication delays and jitters. Additionally, single point of failure in the centralized communication assisted protection approach is avoided since the protection failure is limited maximally to a zone.

7.3.2. Detection of Islanded/Grid-connected Modes

Switching of network operation from grid-connected to islanded mode and vice versa significantly alters the fault current seen by relays. Therefore, it is desirable to promptly identify the operating mode such that relays update their settings to the respective mode of operation. A simplified interlocking approach is implemented in this study for online detection of the operation mode, whereby grid connecting relay R_{12} identifies the operating state (grid-connected/islanded) of the network. Whenever relay R_{12} trips for any reason, such as an upstream fault, upstream network maintenance, or intentionally letting the downstream network to run in islanded mode, the switching status of R_{12} is communicated to all ZSRs, which enables the relays to switch their setting to islanded mode. Similarly, when grid switches back to the grid-connected mode, the R_{12} status is communicated to the every ZSRs so as to switch back the relay settings to grid-connected mode.

7.3.3. Detection of Changes in Network Topologies

As wide adaptation of ANM may lead to selectivity issues to the protection coordination, it is desirable to integrate network operation and network protection. Therefore, an approach, whereby the ANM is integrated to the protection, is proposed in this work such that any ANM activity requiring update of relay settings is taken care of by the protection unit. In particular, such integrated approach lets the relays to adapt their setting per ANM and provides increased operational flexibility to ANM activities. Following the ANM activity, the centralized protection unit communicates the reconfiguration status to the respective relays using centralized communication assisted protection and direct the relays to switch their settings. For instance, whenever a network reconfiguration is done as shown in Fig. 4 of **C8** (connect R_{64} & R_{46} and disconnect R_{23} & R_{32}), then respective relays (R_{12}, R_{23}, and R_{26}) gets information from the central protection unit and update their settings to ensure protection coordination during dynamic network topology.

7.4. Observations and Discussions

In order to demonstrate the performance of proposed method, MV (10 kV) distribution feeder as illustrated in Fig. 4 of **C8** is used. The details of the test network including loading, line parameters, and DER types and connections are presented in Section IV.A of **C8**.

Relay settings, namely pickup current (instantaneous pick-up, I_P^{Ins}, and time-overcurrent pickup, I_P^{TOC}) and TMS are first computed for all relays for every network configurations. A key idea of having I_P^{Ins} and I_P^{Ins} setting is to instantaneously clear the high fault-currents and provide time delay to maintain selectivity during lower fault-currents. The I_P^{Ins} for instantaneous trip is set such that any bolted fault within the relay's protection zone is cleared instantaneously. In this study, an instantaneous operating time of 35 milliseconds is taken for accounting operation delay of the physical relays as well as for avoiding relay trip for temporary faults. Additionally, the I_P^{TOC} for the time-over current protection is set as 1.5 times nominal load current. A key intent to set I_P^{TOC} equals 1.5 times nominal load current is for avoiding overload tripping as well as maintaining sensitivity to faults. Selectivity is established by assigning proper time of operation to each relay. In particular, TMS of each relay is calculated using IEC very inverse characteristics described in (7.1) such that every relay provides backup protection with a margin of 50 milliseconds or more [172].

$$T_r = TMS * \left(B + \frac{A}{\left(I/I_P\right)^{\rho} - 1} \right) \tag{7.1}$$

where T_r is operating time of relay; I_P and I are pickup current and actual fault current through the relay; and A, B, and ρ are constants whose values equals 13.5, 0, and 1 respectively. The parameters are selected based on IEC very inverse characteristics and are kept constant provided fault discrimination is realized by adjusting I_P and *TMS* settings. Fig. 7.2 illustrates relays settings and corresponding characteristics for a base case, where the network is connected to the main grid and has no DERs integration.

Relay	Pickup current (kA)		TMS
	I_P^{Ins}	I_P^{TOC}	
R_{12}	15.77	.345	.03
R_{23}	5.66	.259	.062
R_{34}	3.15	.195	.1043
R_{45}	1.786	.088	.1342
R_{26}	2.02	.093	.078
R_{67}	1.78	.044	.03

a)

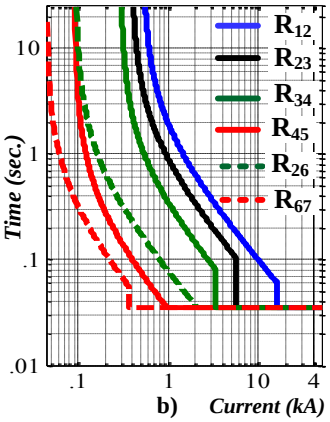

b)

Fig. 7.2 a) Relay settings and b) Time-overcurrent characteristics.

It is observed that each relay is properly coordinated with both upstream and downstream relays such that each upstream relay provides time delayed backup to the downstream relays. However, relays may lose selectivity during instantaneous modes of operation. For instance, if the fault current exceeds 3 kA, it forces the

relays R_{34} and R_{45} to enter to their instantaneous operation, thereby leading them to operate inappropriately. To avoid such problem, instantaneous as well as time overcurrent settings are adapted per the procedure described in the following. It should be noted that settings of relays R_{d1}, R_{d2} and R_{d3} is fully dependent on corresponding DER type and rating and does not get impacted due to connection/disconnection of DGs in other parts of the network. Therefore, their fault trip mechanism is simply set according to the low voltage ride through capability as presented in [164]. Explicit examination of DER relay (R_{d1}, R_{d2}, and R_{d3}) coordination with the other relays is not the focus of this study.

7.4.1. Adaptive Relay Update for Protection Blinding

The changes in fault current seen by relays due to DER(s) integration impact the relay reach and in turn cause relay mal-operation. In particular, fault current seen by various relays in the test feeder with and without having DER integration is illustrated in Fig. 7.3. Indeed, it is depicted that some relays are facing under-reach issues due to decrease in fault current flowing through them, whereas the others are facing overreach issues due to increase in fault current flowing through them. For instance, relay R_{12} face the under-reach problem as the fault current seen by it gets decreased due to fault current contribution from the DERs, whereas the other relays face overreach due to increased fault current seen by them. Particularly, every relay gets partially blinded to faults due to fault current contribution from the DERs. Nevertheless, the extent of blinding and hence the mal-operation of the relay depends greatly on relay settings, network strength, fault type, and location.

Fig. 7.4a) illustrates a fault current seen by relays R_{34} and R_{45} (as in Fig. 4 of **C8**), fault signal, and tripping signals for corresponding relays for a bolted fault F_1 as illustrated in Fig. 4 of **C8**. It can be observed that the fault current seen by R_{34} increases due to DER contribution. Such condition increase the relay reach and lead the relay to instantaneously trip for out of zone fault, F_1. In particular, the fault F_1 forced both the relays R_{34} and R_{45} into instantaneous operating modes, thereby undesirably tripping R_{34} as shown in Fig. 7.4a) for the out of zone fault.

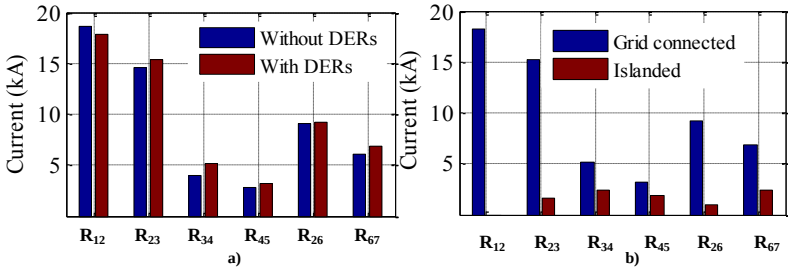

Fig. 7.3 Maximum fault current seen by relays for different cases.

To overcome the protection blinding issue, pickup settings of the relays are updated adaptively on the basis of the connection status of the DERs identified as per the online state detection algorithm presented in section 7.3. In fact, the pickup settings, I_P^{Ins} & I_P^{TOC}, of the relays R_{34} and R_{45} are increased followed by detection of DER connection to avoid their overreach, thereby discriminating out-of-zone

faults. The response of relays R_{34} and R_{45} for the same fault, F_1, after implementing the proposed adaptive algorithm is illustrated in Fig. 7.4b). It can be clearly observed that relay R_{45} gets tripped well before R_{45} to clear the fault F_1, thereby avoiding the overreach of R_{34}. This indeed clears the fault by isolating the section of the network downstream to R_{45}, thereby leaving the rest of the network, network upstream to R_{45}, to operate normally.

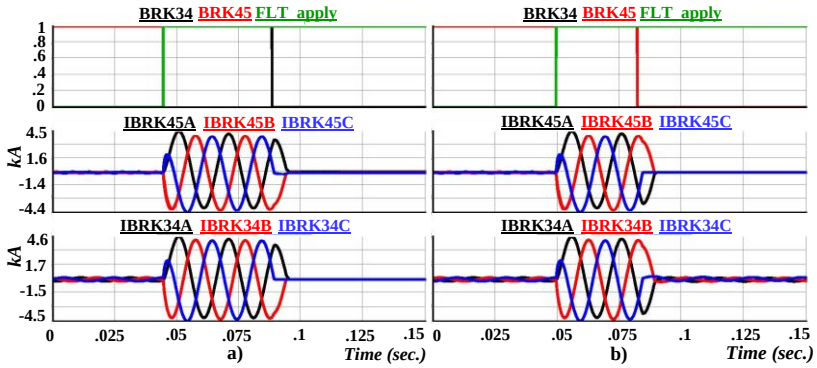

Fig. 7.4 a) Protection blinding of relay R_{34} and b) Solution by proposed adaptive method.

7.4.2. Adaptive Relay Update for False Tripping

False tripping of a relay occurs when fault current contribution from DER on a healthy feeder cause to trip it for fault in the adjacent feeder. Fault current contribution from DER3 for a bolted fault F_2 in the test network (Fig. 4 of **C8**) causes the relay R_{26} to operate before R_{23} since the pickup current of the R_{23} is significantly higher than that of the R_{26}. The 1st subfigure in Fig. 7.5a) depicts breaker status corresponding to relays R_{23} and R_{26}, whereas the 2nd and 3rd subfigures illustrates the fault current seen by the respective relays for the fault F_2. It is seen that both R_{23} and R_{26} enters into instantaneous tripping modes for the bolted fault F_2, thereby causing a false tripping of the healthy feeder $F_{2\text{-}6\text{-}7}$.

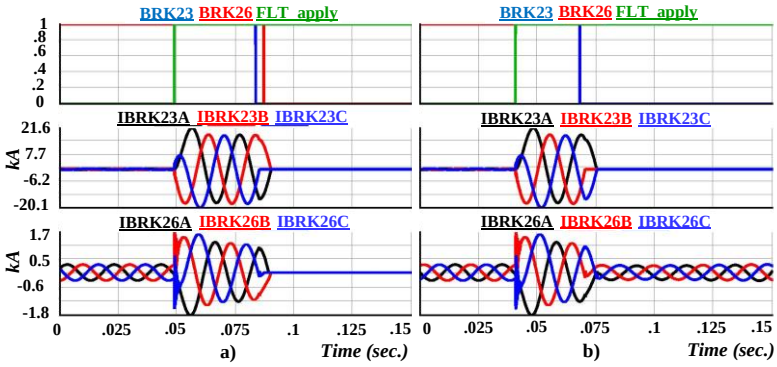

Fig. 7.5 a) False tripping of relay R_{26} and b) Solution by proposed adaptive method.

To overcome the false tripping problem, directional blocking mechanism

integrated with an adaptive update of the pickup current is implemented. Irrespective of the previous operating conditions, relay R_{26} and R_{62} are set to forward and reverse directional mode respectively and the setting of relay R_{62} is increased once the state detection algorithm detects DERs connection. In particular, I_P^{Ins} and I_P^{TOC} of the R_{62} are adaptively updated to 2.23 kA and 0.302 kA respectively to overcome the false tripping. The operation of the corresponding relays (R_{26} and R_{23}) after implementing proposed algorithm is presented in Fig. 7.5b). It is clearly seen from Fig. 7.5b) that the online state detection algorithm based adaptive relay updates avoid the false tripping of healthy feeder $F_{2\text{-}6\text{-}7}$.

7.4.3. Adaptive Updates for Grid-connected/Islanded Mode

As illustrated in Fig. 7.3b), fault currents seen by relays vary greatly while switching from grid-connected to island mode and vice versa. The fault current distribution in the network also varies significantly from grid-connected to islanded modes. For instance, fault current seen by the relay *R23* is significantly higher than the fault current seen by *R34* in grid connected mode, whereas it is significantly lower in islanded mode. In addition, the changes in fault current seen by relay R_{23} is significantly large compared to the changes seen by the R_{45}. It leads to a condition where the relays lost their coordination during islanded condition unless their settings are updated adaptively.

Relay	Pickup current (kA)		TMS
	I_P^{Ins}	I_P^{TOC}	
R_{23}	1.65	.251	.0702
R_{34}	1.05	.215	.0253
R_{45}	0.85	.0485	.05
R_{26}	1.86	.302	.1204
R_{67}	0.65	.044	.03

a)

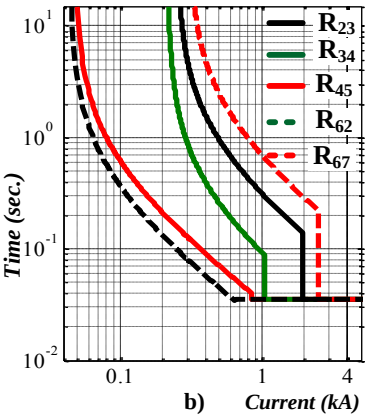

b)

Fig. 7.6 a) Relay settings for islanded operation and b) Time-current curve of relays.

A centralized interlocking mechanism described in Section 7.3 has been implemented to switch the relay settings once the islanded condition is detected. In particular, the feeder connecting relay detects the islanded/grid-connected modes and communicates that status to each relay. Each relay then update their settings based on the status received from the centralized protection unit. The relay settings for the islanded mode of operation are illustrated in Fig. 7.6a) and their corresponding characteristics are presented in Fig. 7.6b). It can be observed from the relay settings that they have changed significantly and are quite different. Therefore, both the TMS and I_P settings have adapted to establish coordination among the relays in islanded mode. The proposed centralized communication

assisted transfer-trip method adaptively switches the relay settings depending on the connection status of the grid, thereby ensuring fault selectivity. Unlike existing centralized communication assisted protection, whereby central protection unit talk back and forth to every protecting units, the proposed event driven transfer trip method demonstrates better performance.

7.5. Chapter Summary

Protection of future distribution system has been challenged not only due to increased DER integration but also due to wide adoption of ANM activities. In particular, increased DER penetration alters fault current magnitude as well as its distribution in the network, thereby changing the reach of the relays. In general, the upstream relays face under-reach, whereas the downstream relays face overreach problems. Moreover, ANM activities, namely network reconfigurations, DR, may lead to modification in network topology and jeopardize the protection. Therefore, conventional relay commissioning approach, whereby relays are assigned with a single setting for the entire operating scenarios, faces serious issues to discriminate fault in the future distribution system.

To address the issue, a two-stage protection approach is developed along the course of this study, whereby an offline fault analysis is firstly performed to compute relay settings for every possible operating mode which are then stored in respective relay memories. In second stage, an online state detection algorithm is implemented to detect the operating state of the network such as ON-OFF status of individual DERs and/or modes of operation of the network (grid-connected/islanded or reconfigured network). In particular, a local adaptive protection was implemented to detect small topological changes in the network, namely the ON/OFF states of a DER within a zone. This is done by establishing an event driven communication of the relay to the adjacent relays within the zone. For instance, whenever there is change in operating states of any DER, the state is transferred to the adjacent relays within that zone. Upon receipt of DER status, each relay activates proper settings to adapt to the changed network topology.

A centralized communication assisted protection is implemented to detect large topological changes, such as grid-connected/islanded or reconfiguration status of the network. The grid connecting relay is equipped with an islanding and grid-reconnection detection algorithm. Therefore, any changes in the network operation modes is detected by the grid connection relay and transferred to every ZSR for directing them to update their settings accordingly. Similarly, the central protecting unit, coordinated with the ANM activities, transfers the network status to respective ZSRs provided the ANM activity desire the relay updates. The simulation results demonstrate that the proposed method effectively eliminate major protection issues, namely the protection blinding and false tripping. Therefore, the proposed proactive and adaptive protection approach demonstrates better performance to establish selectivity and sensitivity in dynamic network topology, thereby providing a framework for protecting future SG.

Chapter 8. Conclusion

This chapter presents a summary and draws conclusions based on the outcomes of the entire PhD thesis. In particular, major scientific contributions with respect to novelty and applications are presented. Since this study opened a new research window on SG *area, perspectives for the future works are also presented.*

8.1. Summary and Conclusions

This dissertation has addressed various technical issues in relation to the utilization of flexible demand and local generation for supporting LV networks. Moreover, the study address issues related to the protection of MV networks in presence of DER and ANM activities. Therefore, the key objectives of this research is to develop suitable control architecture for exploiting DR, quantify impact of DR to the LV network, develop DR control methods and strategies for network support, demonstrate the developed DR methods in a physical testbed, and develop an adaptive protection algorithm for varied network topologies. In particular, those are the major issues to be resolved to make the DR deployment technically and economically viable.

In the first part of this study, an intelligent control architecture a so called the HCA is developed for coordinating the key SG actors, namely consumers, DSOs, aggregators, and market entities. On the one hand, the architecture exploits flexible demand for supporting the network, whereas, on the other hand, it facilitates market participation to enable commercial trading of the flexibility. Three DR control loops, primary, secondary, and tertiary, are developed for enabling the flexible loads to support the distribution network in various ways. The primary loop is capable of supporting the network in real-time, such as real-time voltage support and power balancing, due to its prompt response (range of fraction of seconds) capability. Similarly, the secondary loop is suitable for economic dispatch of flexible loads leading to its response in the ranges of few minutes, thereby acting as a potential resource for congestion management and intra-day balancing. Finally, the response time of the tertiary loop ranges from few minutes up to a day, thereby making it suitable for day ahead or intraday scheduling. As each control loop has different latency, time-coordination is established to enable each control loop to backup each other. For example, any deviations resulting from real-time primary control is backed-up by instant up/down regulation capability of the secondary control and so on.

In order to deploy demand flexibility, existing DR techniques are categorized into ADR, DLCDR, DDDR, and PDR, which are then assigned to respective control loop of the HCA. More specifically, the primary loop executes ADR, the secondary loop executes DLCDR, and the tertiary loop executes DDDR and PDRs. Moreover, a heterogeneous communication infrastructure is integrated to the HCA to realize the anticipated control and communication in the HCA. The performance

of the architecture is demonstrated in a power and communication co-simulation environment. The co-simulation results demonstrated that the proposed architecture is capable of effectively integrating responses from widely distributed loads and provide a technical and commercial framework for exploiting the flexibility.

Next, DR control strategies are developed to exploit flexibility from key flexible loads and local generation. In particular, EVs HPs, and EWHs are considered as potential flexible loads as they are anticipated new loads resulting from electrification of the heating and transportation sector, while solar PV is considered as local generation due to its wide penetration at residential consumer level. Impacts of high integration of those anticipated loads and generation is accessed in relation to a LV distribution network. Moreover, the performance of the developed models and DR control strategies are demonstrated in the LV network. Even though benefits and impacts of the proposed DR control strategies are quantified with reference to a particular LV network, the developed models, control strategies, and algorithms are generic which can be applied to any network. The outcome from this part of the study consists of algorithms to exploit the demand flexibility from the EVs, HPs, and EWH for supporting the LV network in various ways. Indeed, sizable rating together with storage capability of those loads demonstrated great potential for supporting the future grid. In order to present more realistic scenarios particularly in Denmark, integrated control of active loads and local generation are developed. The outcomes demonstrated that operation of the EVs and PVs can be made supportive to each other through the proposed DR control strategies.

Furthermore, despite having significant research on SG, the practical demonstration considering multi-disciplinary aspects of the SG is still lagging. In this regards, a novel approach is developed in this study to scale down a larger distribution network into a small scale testbed. In fact, a LV test case network is scaled down to a 1 kVA testbed and the scaled down testbed is built in a laboratory for practical demonstration of developed DR models and control strategies. An optical fiber and TCP/IP based communication is integrated in the testbed to enable control and communication of the data. The testbed performance is demonstrated by adapting combined centralized-decentralized control algorithms for EV charging coordination. In particular, the decentralized control is implemented at each consumer location and is realized by nano-computers capable of real-time monitoring and control. Similarly, the centralized control is implemented at central place and realized using DMS. The centralized control prepares and dispatches optimum charging schedules to every EV with 15 minutes latency and the decentralized control adaptively adjust the charging power on real-time based on locally monitored voltage. At the end of each time slot, the decentralized control sends actual data (charging power, current, and POC voltage) back to the centralized control using ‘TCP/IP – optical fiber’ to facilitate the centralized control to update EV charging schedules. The centralized and decentralized control work as inter-slot and intra-slot control respectively for realizing the proposed algorithm.

Finally, an adaptive overcurrent protection is designed for a MV distribution system having high share of RESs. In the future grid, the protection is affected not only by bidirectional power flow due to RESs but also due to the ANM activities, such as demand response, network reconfigurations etc. Therefore, unlike the conventional protection methodology where protective settings are made static, an approach to adapt relay settings based on dynamic network topologies is desired. In particular, an integrated local and central communication assisted protection strategy is developed for dynamically setting the protective devices based on the ON/OFF status of the DGs and changes in network topologies. The developed methodology integrates the protection and ANM such that the protection settings are investigated and ensured for every network operating mode and topology. The performance of the developed method is demonstrated in a MV distribution network using RTDS. The proposed protection algorithm provides a new dimension on protection as the protection of the future grid is expected to be impacted by various ANM and DERs integrations.

In summary, the outcomes from this research provide a framework for exploiting demand flexibility from widely distributed consumers/prosumers, which in turn are potential solutions for DSOs to deal with network technical issues. In addition, the outcomes provide economic incentives to the consumers to trade their flexibility to electricity markets. Therefore, this study provides a framework to integrate heating, gas, and transportation sectors into the electrical system, thereby supporting Danish government's 100% renewable energy goal by 2050. Furthermore, this study serves as a reference for future researches on DR control and utilizations for various network support activities.

8.2. Major Contributions

The major contributions of this dissertation are as follows:

- HCA to provide a framework for exploiting demand flexibility from the residential consumers and enable their participation in the electricity marketsis developed. A primary, secondary, and tertiary control loop are designed to activate various DRs and establish their time-coordination. Those control loops exploit demand flexibility to support the network in several ways, such as local voltage support, congestion management, peak saving, economic optimizations, and so forth.
- Detailed models of the key flexible loads, local generation, and distribution network are developed. Potential impacts of the integration of the electrical, heating, and transport sectors in relation to the LV distribution network are accessed.
- Various DR control strategies for exploiting the demand flexibility from different load types are developed. In particular, voltage controlled dynamic DR, ADRs, DDDRs, PDRs, and DLCDRs are realized to support the network.
- An optimization algorithm to control key residential loads, namely EV, HP, and EWH, and local generation, namely solar PV is developed. Both the technical

and economic aspects are addressed by accounting consumer comfort, network constraints, and electricity cost.

- A novel two-stage control algorithm is developed, whereby the central stage activates a control using optimum set-points resulting from the optimizations and the local stage adaptively perform real-time control using predefined control logic based on local voltage variations.
- An algorithm to integrate multi-disciplinary aspects of the DR by performing power and communication co-simulation is developed. As the DR performance in the future grid depends on the performance of power and communication aspects, the developed solutions from the co-simulation environment hold higher probability of acceptance for real-world applications.
- Demonstration of the developed DR control strategies in smart grid testbed is performed. A scaled-down smart grid testbed is developed, whereby a centralized and decentralized control algorithm is demonstrated. A heterogeneous communication infrastructure is integrated to the testbed to enable the control of the physical loads and exchange of data between local and central controllers.
- Adaptive protection algorithm for ensuring protection coordination in dynamic network topologies is developed. The protection algorithm also integrates ANM such that the protection is ensured following the activation of ANM activities.

8.3. Future Work

Even though various aspects of DR control and coordination in the future grids have been covered in this study, further investigation of some of the other aspects is interesting. Some aspects that are deemed potential for future work are as follows:

- Additions of new loads, namely HPs, Evs, and EWHs, and local generation, namely PVs, have several consequences on power quality. Frequent control of inverter interfaced EV and PV might inject harmonics, whereas the high starting currents of the HPs might contribute to the voltage flicker. In addition to the steady state voltage deviations considered in this study, detailed investigation on impacts of those loads and generation on the power quality would be interesting.
- The electricity consumption behavior of the consumers is stochastic; their demand varies randomly over time. It would be interesting to implement probabilistic models to quantify their flexibility and impacts to the grids.
- The application of active demand control is demonstrated in relation to its capability for supporting the network for voltage control and congestion management. It would be interesting to investigate the application of the developed architecture and DR control methodologies for frequency support.
- The future smart grid will be a multi-disciplinary field comprising power, information, and communications. The communication performance in this

study is demonstrated in terms of the latency and delay. However, detailed investigation of the communication performance including latency, delay, throughput, jitter, and error rates would be interesting to better access the practical viability of the developed DR control methods.

- As various storage technologies are becoming competitive for grid supports, it would be interesting to develop a hybrid control algorithm considering DR and storage technologies.
- An adaptive overcurrent protection for the MV network is developed in this study. An integration of the LV network protection with the ANM activities would be an interesting study that could support the DR deployment better.
- Detail investigation on the need of actual control instrumentation to realize the proposed control strategies as well as observability and controllability of the grid would be an interesting study.

BIBLIOGRAPHY

[1]. European Commission, “2030 framework for climate and energy policies,” [Online]. Available: http://ec.europa.eu/clima/policies/2030/index_en.htm, 2014.

[2]. European Commission, “European 20-20-20 Targets,” [Online]. Available: http://ec.europa.eu/clima/policies/package/index_en.htm, 2013.

[3]. Eurostat, “Renewable energy statistics,” [Online]. Available: http://ec.europa.eu/eurostat/statistics-explained/index.php/Renewable_energy_statistics.

[4]. International Energy Agency, “World energy outlook 2014,” [Online]. Available: http://www.worldenergyoutlook.org/publications/weo-2014/, 2014.

[5]. The Danish government, “Our future energy,” Technical Report, Nov. 2011.

[6]. The European Wind Energy Association, “Wind in power,” Technical Report, Feb. 2014.

[7]. The Danish Ministry of Climate, Energy, and Building, “Smart grid strategy: The intelligent energy system of the future,” Technical report, May 2013.

[8]. P. Sorknæs, H. Mæng, T. Weiss, and A. N. Andersen, “Overview of the Danish power system and RES integration,” Technical report, Jul. 2013.

[9]. I. D. D. C. Mendaza, “An interactive energy system with grid, heating, and transportation systems”, PhD Dissertation, Aug. 2014.

[10]. Global wind energy council, “Global wind statistics 2014,” Technical report, Feb. 2015.

[11]. Energinet.dk, “Wind turbines reached record level in 2014,” [Online]. Available:http://www.energinet.dk/EN/El/Nyheder/Sider/Vindmoeller-slog-rekord-i-2014.aspx , Jan. 2015.

[12]. Energinet.dk, “Energinet.dk’s analysis assumptions 2013-2035,” Technical report, Apr. 2013.

[13]. J. R. Kristoffersen, “The horns rev wind farm and the operational experience with the wind farm main controller,” in *Proc. Copenhagen Offshore Wind 2005*, pp. 1-9, Oct. 2005.

[14]. D. V. Vittal and T. Harbour, “Impact of increased penetration of DFIG-based wind turbine generators on transient and small signal stability of power systems,” *IEEE Trans. Power System*, vol. 24, no. 3, pp. 1426-1434, Aug. 2009.

[15]. E. Muljadi, N. Samaan, V. Gevorgain, J. Li, and S. Pasupulati, "Short circuit current contribution for different wind turbine generator," in *Proc. IEEE PES General Meeting*, pp. 1-8, Jul., 2010.
[16]. Danish Energy Agency and Danish Board of District Heating, "District heating - Danish and Chinese experience," Technical Report, 2012.
[17]. Danish Ministry of Climate, Energy, and Building, "DK Energy Agreement," Technical document, March, 2012.
[18]. Energinet.dk, "Natural gas transmission and distribution system," [Online] Available: http://www.energinet.dk/EN/GAS/, 2014.
[19]. Energinet.dk, "Gas consumption and supplies 2015-2050," [Online] Available: http://www.energinet.dk/EN/GAS/ , Dec., 2015.
[20]. Energitnet.dk, "Natural gas and Biogas consumption trend," [Online]. Available: http://www.energinet.dk/EN/GAS/ , 2014.
[21]. Energinet.dk, "Hydrogen injection in the natural gas network," [Online]. Available: http://www.energinet.dk/EN/GAS/ , 2014.
[22]. Ministry of Transport and Statistics Denmark, "Key figures for transport 2011," Statistical Survey, Jun. 2012.
[23]. North Sea Region Electric Mobility Network, e-mobility NSR, "Danish experiences in setting up charging infrastructure for electric vehicles with special focus on battery swap stations," Technical report, Mar. 2013.
[24]. Energinet.dk, "Strategy plan 2010," Technical report, 2010.
[25]. X. Xiu and B. Li, "Study on energy storage system investment decision based on real option theory," in *Proc. IET Sustainable Power Generation and Supply*, pp. 1- 4, Sep. 2012.
[26]. F. M. Andersen et al., "Analysis of demand response in Denmark," Risø-R-1565(EN), Risø National Laboratory, Oct. 2006.
[27]. NordPool Spot, "Trade at the Nordic Spot Market (NordPool Spot AS) - The world's first international spot power exchange," Technical report, Apr. 2004.
[28]. NordPool Spot, "Annual report 2013," Technical report, 2013.
[29]. NordPool spot, "Intraday Market Elbas," [Online]. Available: http://www.nordpoolspot.com/TAS/Intraday-market-Elbas/.
[30]. Energinet.dk, "Regulation C2: The balancing market and balance settlement," Technical regulation, Dec. 2008.
[31]. Energinet.dk, "Smart grid in Denmark 2.0," Technical report, [Online]. Available:http://energinet.dk/SiteCollectionDocuments/Engelske%20dokumenter/Forskning/Smart%20Grid%20in%20Denmark%202.0.pdf
[32]. International Energy Agency, "Demand-side management," [Online]. Available: https://www.iea.org/techinitiatives/end-use-electricity/demand-sidemanagement/.

[33]. I. Lampropoulos, W. Kling, P. Ribeiro, and J. van den Berg, "History of demand side management and classification of demand response control schemes," in *Proc. IEEE PES General Meeting 2013*, pp. 1-5, Jul. 2013.

[34]. P. Rowles, "Demand response and demand side management" [Online]. Available: http://www.energyadvantage.com/blog/2010/02/demand-response-demand-side-management-what%E2%80%99s-difference/.

[35]. B. Davito, H. Tai, and R. Uhlaner, "The smart grid and the promise of demand-side management," *Technical report*, 2010.

[36]. US Department of Energy, "Demand Response." [Online] Available: http://energy.gov/oe/technology-development/smart-grid/demand-response

[37]. V. S. K. M. Balijepalli, V. Pradhan, S. A. Khaparde, and R. M. Shereef, "Review of Demand Response under Smart Grid Paradigm," in *Proc. IEEE PES Innovative Smart Grid Technologies*, pp. 236 – 243, Dec. 2011.

[38]. M. H. Albadi and E. F. El-Saadany, "Demand response in electricity markets: An overview," in *Proc. IEEE PES General Meeting 2007*, pp. 1-5, Jun. 2007.

[39]. F. Boshell and O. P. Veloza, "Review of developed demand side management programs including different concepts and their results," in *Proc. IEEE/PES Transmission and Distribution Conference and Exposition: Latin America*, pp. 1-7, Aug. 2008.

[40]. P. V. Dievel, K. D. Vos, R. Belmans, and K. D Vos, "Demand response in electricity distribution grids: regulatory framework and barriers," in *Proc. International Conference on the European Energy Market*, pp. 1-5, May 2014.

[41]. O. Erdinc, N. G. Paterakis, T. D. P. Mendes, A. G. Bakirtzis, and J. P. S. Catalao, "Smart household operation considering bi-directional EV and ESS utilization by real-time pricing based DR," *IEEE Trans. Smart Grid*, vol. 6, no. 3, pp. 1281-1291, Sep. 2014.

[42]. C. P. S. Gill, Y. S. Brar, and K. Singh, "Incentive based demand response program: An effective way to tackle peaking electricity crisis," in *Proc. IEEE Canadian Conference on Electrical and Computer Engineering*, pp. 1-6, 2012.

[43]. P. Khajavi, H. Abniki, and A. B. Arani, "The role of incentive based demand response programs in smart grid," in *Proc. 10th international Conference on Environment and Electrical Engineering*, pp. 1-4, May 2011.

[44]. L. Ying-chen, C. Lu, and C. Xing-ying, "Economic benefit analysis of incentive-based demand response," in *Proc. International Conference on E-product, E-service and E-Entertainment*, pp. 1-4, Nov. 2010.

[45]. M. A. A. Pedrasa, M. M. Oro, N. C. R. Reyes, and J. R. I. Pedrasa, "Demonstration of direct load control of air conditioners in high density residential buildings," in *Proc. Innovative Smart Grid Technology-Asia*, pp. 400-405, May 2014.

[46]. S. R. Mattix, M. K. Donnelly, D. J. Trudnowski, and J. E. Dagle, "Autonomous demand response for frequency regulation on a large-scale model of an interconnected grid," in *Proc. IEEE PES General Meeting*, pp. 1-8, Jul. 2012.

[47]. N. Forouzandehmehr, M. Esmalifalak, H. Mohsenian-Rad, and Z. Han, "Autonomous demand response using stochastic differential games," *IEEE Trans. Smart Grid*, vol. 6, no. 1, pp. 291-300, Sep. 2014.

[48]. J. Hansen, J. V. Knudsen, and A. M. Annaswamy, "Demand repsonse in smart grids: Parcitipants, challenges, and a taxonomy," in *Proc. IEEE 53rd Annual conference on Decision and Control*, pp. 4045-4052, Dec. 2014.

[49]. N. Zhu, X. Bai, and J. Meng, "Benefits analysis of all parties participating in demand response," in *Proc. IEEE PES Asia Pacific Power and Energy Engineering Conference*, pp. 1-4, Mar. 2011.

[50]. L. Chang-Chien, L. N. An, T. Lin, and W. Lee, "Incorporating demand response with spinning reserve to realize an adaptive frequency restoration plan for system contingencies," *IEEE Trans. on Smart Grid*, vol. 3, no. 3, pp. 1145-1153, Sep. 2012.

[51]. C. Sahin, M. Shahidehpour, and I. Erkmen, "Allocation of hourly reserve versus demand response for security constrained scheduling of stochastic wind energy," *IEEE Trans. Sustainable Energy*, vol. 4, no. 1, pp. 219-228, Sept. 2012.

[52]. W. Liu, Q. Wu, F. Wen, and J. Østergaard, "Day-ahead congestion management in distribution system through household demand response and distribution congestion prices," *IEEE Trans. Smart Grid*, vol. 5, no. 6, pp. 2739-2747, Jul. 2014.

[53]. H. Johal, K. Anaparthi, and J. Black, "Demand response as a strategy to support grid operation in different time scales," in *Proc. IEEE Energy Conversion Congress and Exposition*, pp. 1461-1467, Sept. 2012.

[54]. S. N. Singh and J. Østergaard, "Use of Demand Response in Electricity Markets: An overview and key issues," in *Proc. International Conference on the European Energy Market*, pp. 1-6, Jun. 2010.

[55]. Z. Baharlouei and M. Hashemi, "Demand side management challenges in smart grid: A review," in *Proc. Smart Grid Conference*, pp. 96-101, Dec. 2013.

[56]. P. Kundur, "Power system stability and control", McGraw-Hill Inc., 1994.

[57]. K. M. Muttaqi, A. D. T. Le, M. Negnevitsky, and G. Ledwich, "A coordinated voltage control approach for coordination of OLTC, voltage regulator, and DG to regulate voltage in a distribution feeder," *IEEE Trans. Industry Applications*, Vol. 51, no. 2, pp. 1239 - 1248, Mar.-Apr. 2015.

[58]. M. Nick, R. Cherkaoui, and M. Paolone, "Optimal allocation of dispersed energy storage systems in active distribution networks for energy balance and grid support," *IEEE Trans. Power Systems*, vol. 29, no. 5, pp. 2300-2310, Feb. 2014.

[59]. N. S. Lu et al., "Centralized and decentralized control for demand response," in *Proc. IEEE PES Innovative Smart Grid Technologies*, pp. 1-8, Jan. 2011.

[60]. C. L. Siebert et al., "Centralized and decentralized approaches to demand response using smart plugs," in *Proc. IEEE PES Transmission and Distribution Conference and Exposition*, pp. 1-5, Apr. 2014.

[61]. E. K. Akuacom, and M. A. Piette, "Direct versus facility centric load control for automated demand response" in *Grid-Interop Forum*, Nov. 2009.

[62]. I. D. D. C. Mendaza, I. G. Szczesny, J. R. Pillai, and B. Bak-Jensen, "Flexible demand control to enhance the dynamic operation of low voltage networks," *IEEE Trans. Smart Grids*, vol. 6, no. 2, pp. 705-715, Dec. 2014.

[63]. C. A. Canizares et al, "Trends in microgrid control," *IEEE Trans. Smart Grid*, vol, 5, no. 4, pp. 1905-1919, Jul. 2014.

[64]. P. B. Andersen, J. Hu, and K. Heussen, "Coordination strategies for distribution grid congestion management in a multi-actor, multi-objective setting," in *Proc 3rd IEEE PES Innovative Smart Grid Technologies (ISGT)*, pp. 1-8, Oct. 2012.

[65]. OpenADR alliance, "OpenADR 2.0 specification," [Online]. Available: http://www.openadr.org.

[66]. IEEE P2030, "Guide for smart grid interoperability of energy Technology and information technology operation with the electric power system (EPS), and end-Use applications and loads," *IEEE Standards Association*, Sep. 2011.

[67]. K. Mets, J. A. Ojea, and C. Develder, "Combining power and communication network simulation for cost-effective smart grid analysis," *IEEE Communications Surveys & Tutorials*, vol. 16, no. 3, pp. 1771-1796, Mar. 2014.

[68]. D. Q. Xu, G. Jo´os, M. L´evesque, and M. Maier, "Integrated V2G, G2V, and renewable energy sources coordination over a converged fiber-wireless broadband access network," *IEEE Transactions Smart Grid*, vol. 4, no. 3, pp. 1381–1390, Sep. 2013.

[69]. X. Wang et al., "Interfacing Issues in multiagent simulation for smart grid applications," *IEEE Transactions Power Delivery*, vol. 28, no. 3, pp. 1918–1927, Jul. 2013.

[70]. X. Sun, Y. Chen, J. Liu, and S. Huang, "A co-simulation platform for smart grid considering interaction between information and power systems," in *Proc., IEEE Innovative Smart Grid Technologies (ISGT)*, pp. 1-6, Feb. 2014.

[71]. W. Song, D. De, S. Tan, S. K. Das, and L. Tong, "A wireless smart grid testbed in lab," *IEEE Wireless Communications*, vol. 19, no. 3, pp. 58–64, Jun. 2012.

[72]. I. Georgievski, V. Degeler, G. A. Pagani, T. A. Nguyen, A. Lazovik, and M. Aiello, "Optimizing energy costs for offices connected to the smart grid," *IEEE Trans. Smart Grid*, vol. 3, no. 4, pp. 2273–2285, Dec. 2012.

[73]. R. C. Qiu et al., "Cognitive radio network for the smart grid: experimental system architecture, control algorithms, security, and microgrid testbed," *IEEE Trans. Smart Grid*, vol. 2, no. 4, pp. 724–740, Dec. 2011.
[74]. Aalborg University, "Smart grid laboratory," [Online]. Available: (http://www.et.aau.dk/research-programmes/intelligent-energy-systems-and-active-networks/).
[75]. Technical university of Denmark, "PowerLabDK," [Online]. Available: http://www.powerlab.dk/
[76]. Royal Institute of Technology, "SmartTS Lab," [Online]. Available: https://www.kth.se/en/ees/omskolan/
[77]. F. W. Fuchs et al., "Research laboratory for grid integration of distributed renewable energy resources - design and realization," in *Proc. IEEE Energy Conversion Congress and Exposition*, pp. 1974-1981, Sept. 2012.
[78]. F. W. Fuchs et al., "Research laboratory for grid-integration of distributed renewable energy resources - integration analysis of DERs," in *Proc. 15th International Conference on Power Electronics and Motion Control (EPE/PEMC)*, pp. LS7a.4-1 – LS7a.4-8, Sep. 2012.
[79]. J. Soares, H. Morais, T. Sousa, Z. Vale, and P. Faria, "Day-ahead resource scheduling including demand response for electric vehicles," *IEEE Trans. Smart Grid*, vol. 4, no. 1, pp. 596-605, Mar. 2013.
[80]. M. Chen and G. Rincon-Mora, "Accurate electrical battery model capable of predicting runtime and I-V performance," *IEEE Trans. Energy Conversion*, vol. 21, no. 2, pp. 504 – 511, Jun. 2006.
[81]. D. W. Dees, V. S. Battaglia, and A. Bélanger, "Electrochemical modeling of lithium polymer batteries," *Journal of Power Sources*, vol. 110, no. 2, pp. 310 – 320, 2002.
[82]. J. Newman, K. E. Thomas, H. Hafezi, and D. R. Wheeler, "Modeling of lithium-ion batteries," *Journal of Power Sources*, vol. 119, pp. 838–843, 2003.
[83]. P. Rong and M. Pedram, "An analytical model for predicting the remaining battery capacity of lithium-ion batteries," *IEEE Trans. on Very Large Scale Integration Systems*, vol. 14, no. 5, pp. 441–451, May 2006.
[84]. S. Vazquez, S. Lukic, E. Galvan, L. Franquelo, and J. Carrasco, "Energy storage systems for transport and grid applications," *IEEE Trans. Industrial Electronics*, vol. 57, no. 12, pp. 3881 – 3895, Dec. 2010.
[85]. R. C. Kroeze and P. T. Krein, "Electrical battery model for use in dynamic electric vehicle simulations," in *Proc. IEEE Power Electronics Specialists Conference*, pp. 1336–1342, Jun. 2008.
[86]. O. Tremblay, L. A. Dessaint, and A. I. Dekkiche, "A generic battery model for the dynamic simulation of hybrid electric vehicles," *in Proc. IEEE Vehicle Power and Propulsion Conference*, pp. 284–289, Sept. 2007.
[87]. K. Qian, C. Zhou, M. Allan, and Y. Yuan, "Modeling of load demand due to EV battery charging in distribution systems," *IEEE Trans. Power Systems*, vol. 26, no. 2, pp. 802-810, Aug. 2010.

[88]. S. Yang, M. Wu, X. Yao, and J. Jiang, "Load modeling and identification based on ant colony algortihms for EV charging stations," *IEEE Trans. Power Systems*, vol. 30, no. 4, pp. 1997–2003, Sept. 2014.

[89]. S. Wang, N. Chang, Z. Li, and M. Sahidehpour, "Modeling and impact analysis of large scale V2G electric vehicles on the power grid," in *Proc. IEEE PES Innovative Smart Grid Technologies - Asia*, pp. 1-6, May 2012.

[90]. A. H. Foosnæs, J. Rasmussen, C. A. Andersen, O. Gehrke, and G. Isbrandt, "Grid codes and regulation related to EVs," Technical report, Oct. 2011.

[91]. A. Briones et al., "Vehicle-to-grid (V2G) power flow regulations and building codes review by AVTA," Technical report, Sept. 2012.

[92]. Z. Yang, G. Pedersen, L. Larsen, and H. Thybo, "Modeling and control of indoor climate using a heat pump based floor heating system," in Proc. 33rd Annual Conference on IECON, pp. 2985–2990, Nov 2007.

[93]. P. Andersen, T. Pedersen, and K. Nielsen, "Observer based model identification of heat pumps in a smart grid," in *Proc. IEEE International Conference on Control Applications*, pp. 569–574, 2012, Oct 2012.

[94]. J. M. Nyers and A. J. Nyers, "COP of heating-cooling system with heat pump," in *Proc. IEEE 3rd international Symposium on Exploitation of Renewable Energy Sources (EXPRES)*, pp. 17-21, Mar. 2011.

[95]. L. Totu, J. Leth, and R. Wisniewski, "Control for large scale demand response of thermostatic loads," in *Proc. American Control Conference (ACC)*, pp. 5023–5028, Jun. 2013.

[96]. E. Veldman, M. Gibescu, H. Slootweg, and W. Kling, "Impact of electrification of residential heating on loading of distribution networks," in *Proc.* IEEE Trondheim *PowerTech*, pp. 1–7, Jun. 2011.

[97]. S. Koch, M. Zima, and G. Andersson, "Potentials and applications of coordinated groups of thermal household appliances for power system control purposes," in *Proc. IEEE PES/IAS Conference on Sustainable Alternative Energy (SAE)*, pp. 1–8, Sept. 2009.

[98]. R. Yokoyama, S. Okagaki, T. Wakui, and K. Takemura, "Performance Analysis of a CO2 heat pump water heating system by numerical simulation with a simplified model," in *Proc. 19th International Conference on Efficiency, Cost, Optimization, Simulation and Environmental Impact of Energy Systems*, pp. 1–6, May 2012.

[99]. C. Verhelst, D. Degrauwe, F. Logist, J. Van Impe, and L. Helsen, "Multi-objective optimal control of an air-to-water heat pump for residential heating," *Building Simulation*, vol. 5, no. 3. pp. 281–291, Apr. 2012.

[100]. E. Vrettos, K. Lai, F. Oldewurtel, and G. Andersson, "Predictive control of buildings for demand response with dynamic day-ahead and real-time prices," in *Proc. 2013 European Control Conference (ECC)*, pp. 2527–2534, Jul. 2013.

[101]. ESS Model, "CO2 air source heat pump," [Online]. Available: http://www.esru.strath.ac.uk/EandE/Web_sites/10-11/ASHP_CO2/modelling_EESmodel.html.

[102]. N. Mohammad, M. Quamruzzaman, M. R. T. Hossain, and M. R. Alam, "Parasitic effects on the performance of DC-DC SEPIC in photovoltaic maximum power point tracking applications," *Smart Grid and Renewable Energy*, vol. 4, no. 1, pp. 113-121, Apr. 2013.
[103]. R. W. Wimmer, "Regelung einer Wärmepumpenanlage mit Model Predictive Control," *PhD Dissertation*, ETH Zürich, 2004.
[104]. M. A. Bianchi, "Adaptive modellbasierte prädiktive regelung einer kleinw armepumpenanlage," *PhD Dissertation*, ETH Zürich, 2006.
[105]. K. Rapolu, P. Singh, S. P. Shea, and D. L. Meier, "Numerical two dimensional modeling of silicon solar cells with experiment validation," in *Proc. 10th International Conference on Numerical Simulation of Optoelectronic Devices*, pp. 75-76, Sept. 2010.
[106]. P. Mathiesen, J. M. Brown, and J. Kleissl, "Geostrophic wind dependent probabilistic irradiance forecasts for coastal California," *IEEE Trans. Sustainable Energy*, vol. 4, no. 2, pp. 510-518, Jul. 2012.
[107]. V. P. Singh, V. Vijay, M. S. Bhatt, and D. K. Chaturvedi, "Generalized neural network methodology for short term solar power forecasting," in *Proc. 13th International Conference on Environment and Electrical Engineering*, pp. 58-62, Nov. 2013.
[108]. X. Su, M. A. S. Masoum, and P. Wolfs, "Comprehensive optimal photovoltaic inverter control strategy in unbalanced three-phase four wire low voltage distribution networks," *IET Generation, Transmission and Distribution*, vol. 8, no. 11, pp. 1848-1859, Nov. 2014.
[109]. A. Samadi, R. Eriksson, L. Soder, and B. G. Rawn, "Coordinated active power-dependent voltage regulation in distribution grids with PV systems," *IEEE Trans. Power Delivery*, vol. 29, no. 3, pp. 1454-1464, Jan. 2014.
[110]. M. J J. E. Alam, K. M. Muttaqi, and D. Sutanto, "Mitigation of rooftop solar PV impacts and evening peak support by managing available capacity of distributed energy storage systems," *IEEE Trans. Power Systems*, vol. 28, no. 4, pp. 3874-3884, May 2013.
[111]. Energinet.dk, "Cell Controller Overview and Future Perspectives," Technical Report, Doc. ID 20735/12, Sep. 2012.
[112]. P. Kadurek, J. Cobben, and W. Kling, "Overloading protection of future low voltage distribution networks," in *Proc. IEEE Trondheim PowerTech*, pp. 1–6, Jun. 2011.
[113]. M. Arnold, W. Friede, and J. Myrzik, "Investigations in low voltage distribution grids with a high penetration of distributed generation and heat pumps," in *Proc. 48th International Universities Power Engineering Conference (UPEC)*, pp. 1–6, Sept. 2013.
[114]. R. A. Verzijlbergh, Z. Lukszo, J. G. Slootweg, and M. D. Ilic, "The impact of controlled electric vehicle charging on residential low voltage networks," in *Proc. IEEE International Conference on Networking, Sensing and Control (ICNSC)*, pp. 14–19, Apr. 2011.
[115]. A. Masoum, S. Deilami, P. Moses, and A. Abu-Siada, "Impact of plug-in electrical vehicles on voltage profile and losses of residential system,"

in *Proc. 20th Australasian Universities Power Engineering Conference (AUPEC)*, pp. 1–6, Dec. 2010.

[116]. M. A. S. Masoum, P. Moses, and K. Smedley, "Distribution transformer losses and performance in smart grids with residential plug-In electric vehicles," in *Proc. IEEE PES Innovative Smart Grid Technologies (ISGT)*, pp. 1–7, Jan. 2011.

[117]. F. Marra, M. Jensen, R. Garcia-Valle, C. Traholt, and E. Larsen, "Power quality issues into a Danish low-voltage grid with electric vehicles," in *Proc. 11th International Conference on Electrical Power Quality and Utilisation (EPQU)*, pp. 1 – 6, Oct. 2011.

[118]. M. Brandao, A. Panosyan, and R. Walling, "Potential strategies to increase rooftop solar PV penetration in LV networks in Australia," *in Proc. IEEE PES Innovative Smart Grid Technology-Asia*, pp. 1-7, Nov. 2011.

[119]. E. Demirok, "Control of grid interactive PV inverters for high penetration in low voltage distribution networks," *Ph.D. Dissertation*, Department of Energy Technology, Aalborg University, Aalborg, 2012.

[120]. K. A. Joshi and N. M. Prndoriya, "Impact investigation of rooftop solar PV system: A case study in India," in *Proc. IEEE PES Innovative Smart Grid Technology-Europe*, pp. 1-8, Oct. 2012.

[121]. P. Richardson, D. Flynn, and A. Keane, "Impact assessment of varying penetrations of electric vehicles on low voltage distribution systems," in *Proc. IEEE PES General Meeting*, pp. 1–6, Jul. 2010.

[122]. P. Mancarella, C. K. Gan, and G. Strbac, "Evaluation of the impact of electric heat pumps and distributed CHP on LV networks," in Proc. IEEE PES Trondheim PowerTech, pp. 1–7, Jun. 2011.

[123]. T. A. Short, "Electric Power Distribution Handbook," *Taylor and Francis Group*, CRC Press, 2014.

[124]. A. Kulmala, S. Repo, and P. Jarventausta, "Coordinated voltage control in distribution networks including several distributed energy resources," *IEEE Trans. Smart Grid*, vol. 5, no. 4, pp. 2010-2020, Jul. 2014.

[125]. P. Mahat, M. Handl, K. R. Kanstrup, A. P. Lozano, and A. Sleimovits, "Price based electric vehicle charging" in *Proc. IEEE PES Society General Meeting*, pp. 1 – 8, Jul. 2012.

[126]. P. Richardsen, D. Flynn and A. Keane,"Optimal charging of electric vehicle in low voltage distribution grid", *IEEE Trans. Power System*, vol. 27, no. 1, pp. 268-279, Feb. 2012.

[127]. C. Wen, J. Chen, J. Teng, and P. Ting, "Decentralized plug-in electric vehicle charging selection algorithm in power systems," *IEEE Trans. Smart Grid*, vol. 3, no. 4, pp. 1779–1789, Dec. 2012.

[128]. C. Jin, J. Tang, and P. Ghosh, "Optimizing electric vehicle charging: A customer's perspective," *IEEE Trans. Vehicular Technology*, vol. 62, no. 7, pp. 2919–2927, Sep. 2013.

[129]. B. Geng, J. K. Mills and D. Sun, "Two-stage charging strategy for plug-in electric vehicles at the residential transformer level," *IEEE Trans. Smart Grid*, vol. 4, no. 3, pp. 1442–1452, Sep. 2013.

[130]. P. Richardson, D. Flynn, and A. Keane, "Local versus centralized charging strategies for electric vehicles in low voltage distribution systems," *IEEE Trans. Smart Grid*, vol. 3, no. 2, pp. 1020–1028, Apr. 2012.
[131]. O. Sundstrom and C. Binding, "Flexible charging optimization for Electric Vehicles Considering Distribution Grid Constraints," *IEEE Trans. Smart Grid*, vol. 3, no. 1, pp. 26-37, Mar. 2012.
[132]. J. Hu, S. You, M. Lind, and J. Østergaard, "Coordinated charging of electric vehicles for congestion prevention in the distribution grid," *IEEE Trans. Smart Grid*, vol. 5, no. 2, pp. 703-711, Mar. 2014.
[133]. K. M. Nielsen, T.S. Pedersen and P. Andersen, "Heat pumps in private residences used for grid balancing by demand response methods", in *Proc. IEEE PES Transmission and Distribution Conference and Exposition*, pp. 1–6, May 2012.
[134]. M. Diekerhof, S. Vorkampf, and A. Monti, "Distributed optimization algorithm for heat pump," in *Proc. IEEE PES innovative smart grid technologies Europe (ISGT-Europe),* pp. 1-6, Oct. 2014.
[135]. T. Masuta and A. Yokoyama, "Supplementary load frequency control by use of a number of both electric vehicles and heat pump water heaters", *IEEE Trans. Smart Grid*, vol. 3, no. 3, pp. 1253–1262, Sept. 2012.
[136]. P. T. Bjerregaard, I. G. Szczesny, I. D. C. Mendaza, and J. R. Pillai, "Intelligent control of flexible loads for improving low voltage grids utilization" in *Proc. IEEE PES Innovative Smart Grid Technologies - Europe*, pp. 1-5, Oct. 2013.
[137]. T. Buber, S. V. Roon, A. Gruber, and J. Conard, "Demand response potential of electrical heat pumps and electric storage heaters," in *Proc. IEEE IES IECON*, pp. 8028-8032, Nov. 2013.
[138]. B. Biegel et al., "Smart grid dispatch strategy for ON/OFF demand-side devices", in *Proc. European Control Conference (ECC)*, pp. 2541–2548, Jul. 2013.
[139]. R. Jia, M. H. Nehrir, and D. A. Pierre, "Voltage control of aggregate electric water heater load for distribution system peak load shaving using field data", in *Proc. 39th North American Power Symposium*, pp. 492–497, Sept. 2007.
[140]. M. Brandao, A. Panosyan, and R. Walling, "Potential strategies to increase rooftop solar PV penetration in LV networks in Australia," in *Proc. IEEE PES Innovative Smart Grid Technologies – Asia*, pp. 1-6, Nov. 2011.
[141]. E. Demirok et al., "Local reactive power control methods for overvoltage prevention of distributed solar inverters in low-voltage grids," *IEEE Journal of Photovoltaics*, vol. 1, no. 2, pp. 174 - 182, Dec. 2011.
[142]. R. Tonkoski, L. A. C. Lopes, and T. H. M. El-Fouly, "Coordinated active power curtailment of grid connected PV inverters for overvoltage prevention," *IEEE Trans. Sustainable Energy*, vol. 2, pp. 139-147, Apr. 2011.

[143]. M. J. E. Alam, K. M. Muttaqi, and D. Sutanto, “Mitigation of rooftop solar PV impacts and evening peak support by managing available capacity of distributed energy storage systems,” *IEEE Trans. Power System*, vol. 29, pp. 3874-3884, Nov. 2013.

[144]. X. Liu, A. Aichhorn, L. Liu, and H. Li, “Coordinated control of distributed energy storage system with tap changer transformers for voltage rise mitigation under high photovoltaic penetration,” *IEEE Trans. Smart Grid*, vol. 3, pp. 879-906, Jun. 2012.

[145]. A. Mustapha, O. Takashi, T. Yumiko, and J. G. S. Fonseca, “Reduction of PV reverse power flow through the usage of EV’s battery with consideration of the demand and solar radiation forecast,” in *Proc. IEEE International Electric Vehicle Conference*, pp. 1-3, Oct. 2013.

[146]. J. Traube et al., “Mitigation of solar irradiance intermittency in photovoltaic power systems with integrated electric-vehicle charging functionality,” *IEEE Trans. Power Electronics*, vol. 28, pp. 3058-3067, Jun. 2013.

[147]. J. M. Foster, G. Trevino, M. Kuss, and M. C. Caramanis, “Plug-In electric vehicle and voltage support for distributed solar: theory and application,” *IEEE System Journal*, vol. 7, pp. 881-888, Dec. 2013.

[148]. B. W. Kennedy and R. H. Fletcher, "Conservation voltage reduction (CVR) at Snohomish County PUD," *IEEE Trans. Power Systems*, vol. 6, no. 3, pp. 986 - 998, Aug. 1991.

[149]. M. E. Baran and M.Y Hsu, “Volt/Var control at distribution substation,” *IEEE Trans. Power System*, vol. 14, no. 1, pp. 312–318, Feb. 1999.

[150]. R. Liang and Y. Wang, “Fuzzy-based reactive power and voltage control in a distribution system,” *IEEE Trans. Power Delivery*, vol. 18, no. 2, pp. 610–618, Apr. 2003.

[151]. J. C. Erickson and S. R. Gilligan, "The effects of voltage reduction on distribution circuit loads," *IEEE Trans. Power Apparatus and Systems*, vol. PAS-101, no. 7, pp. 0018-2018, Jul. 1982.

[152]. T. L. Wilson, "Energy conservation with voltage reduction - fact or fantasy," in *Proc. IEEE Rural Electric Power Conference*, pp. C3_1 – C3_6, May 2002.

[153]. M. Khurmy and B. Alshahrani, “Measurement & verifications of voltage optimization for conserving energy,” in *Proc. 10th International Conference on Environment and Electrical Engineering*, pp. 1-5, May 2011.

[154]. R. Singh, F. Tuffner, J. Fuller, and K. Schneider, “Effects of distributed energy resources on conservation voltage reduction (CVR)” in *Proc. IEEE PES General Meeting*, pp. 1–7, Jul. 2011.

[155]. J. Solanki, N. Venkatesan, S. K. Solanki, “Coordination of demand response and volt/var control algorithm using multi agent system,” in *Proc. IEEE PES Transmission and Distribution Conference and Exposition*, pp. 1–4, May 2012.

[156]. N. Markushevich and E. Chan, "Integrated voltage, var control and demand response in distribution systems," in *Proc. IEEE PES Power System Conference and Exposition (PSCE)*, pp. 1-4, Mar. 2009.
[157]. P. Kadurek, M. M. Sarab, J. F. G. Cobben, and W. L. Kling, "Assessment of demand response possibilities by means of voltage control with intelligent MV/LV distribution substation," in *Proc. IEEE PES General Meeting*, pp. 1–6, Jul. 2012.
[158]. H. Lee Willis, "Electric Transmission and Distribution Reference Book", ABB, p. 787, 1997.
[159]. I. Xyngi and M. Popov, "An Intelligent Algorithm for the Protection of Smart Power Systems," *IEEE Trans. Smart Grid*, vol. 4, no. 3, pp. 1541-1548, Aug. 2013.
[160]. V. R. Pandi, H. H. Zeineldin, and X. Weidong, "Determining optimal location and size of distributed generation resources considering Harmonic and protection coordination limits," *IEEE Trans. Power Systems*, vol. 28, no. 2, pp. 1245-1254, Apr. 2013.
[161]. J. Chen, R. Fan, X. Duan, and J. Cao, "Penetration level optimization for DG considering reliable action of relay protection device constrains," in *Proc. International Conference on Sustainable Power Generation and Supply*, pp. 1-5, Apr. 2009.
[162]. B. Li, C. Li, F. Guo, and Y. Xin, "Overcurrent protection coordination in a power distribution network with the active superconductive fault current limiter," *IEEE Trans. Applied Superconductivity*, vol. 24, no. 5, pp. 1051-5223, Oct. 2014.
[163]. H. Yazdanpanahi, Y. W. Li, and W. Xu, "A new control strategy to mitigate the impact of inverter based DGs on protection system," *IEEE Trans. Smart Grid*, vol. 3, pp. 1427-1436, Sept. 2012.
[164]. P. Mahat, Z. Chen, B. Bak-Jensen, and C. L. Bak, "A simple adaptive overcurrent protection of distribution system with distributed generation," *IEEE Trans. Smart Grid*, vol. 2, pp. 428-437, Sept. 2011.
[165]. J. Ma, W. Ma, X. Wang, and Z Wang, "A new adaptive voltage protection scheme for distribution network with distributed generations," *Canadian Journal of Electrical and Computer Engineering*, vol. 36, no. 4, pp. 142-151, Fall 2013.
[166]. F. Coffel, C. Booth, and A. Dysko, "An adaptive overcurrent protection scheme for distribution networks," *IEEE Trans. Power Delivery*, vol. 30, no. 2, pp. 0885–8977, Feb. 2014.
[167]. M. Khederzadeh, "Adaptive setting of protective relays in micro-grids in grid-connected and autonomous operation," in *Proc. IET International Conference on Developments in Power System Protection*, pp. 1- 4, Apr. 2012.
[168]. M. A. Zamani, A. Yazdani, and T. S. Sindhu, "A communication-assisted protection strategy for inverter based medium voltage micro-grids," *IEEE Trans. Smart Grid*, vol. 3, no. 4, pp. 2088-2099, Dec. 2012.
[169]. F. A. Ituzaro, R. H. Douglin, and K. L. Butler-purry, "Zonal overcurrent protection for smart radial distribution systems with distributed

generation," in *Proc. 2013 IEEE PES Innovative Smart Grid Technologies*, pp. 1-6, Feb. 2013.

[170]. M. Brahma and A. A. Girgis, "Development of adaptive protection scheme for distribution system with high penetration of distributed generation," *IEEE Trans. Power Delivery*, vol. 19, no. 1, pp. 56-63, Dec. 2004.

[171]. Y. Ding, S. Pineda, P. Nyeng, J. Østergaard, E. M. Larsen, and Q. Wu, "Real-time market concept architecture for EcoGrid EU - A prototype for European smart grids," *IEEE Trans. Smart Grid*, vol. 4, pp. 2006–2016, Jul. 2013.

[172]. RTDS Technologies, "Power System User Manual", Dec. 2012.